JMU

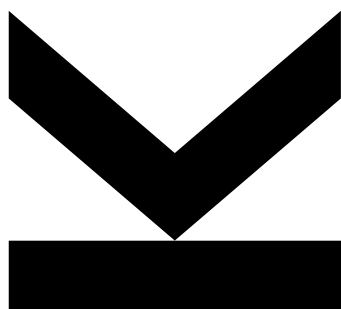## JOHANNES KEPLER
UNIVERSITÄT LINZ

DEVELOPMENTS TOWARDS BIOCOMPATIBLE DEGRADABLE MOLECULARLY IMPRINTED POLYMERS BASED ON POLYPHOSPHAZENES

Submitted by
Bc. Paul Strasser BSc.

Submitted at
Institute of Polymer Chemistry

Supervisors
Univ.-Prof. Dr. Oliver Brüggemann
Assoc. Univ.-Prof. Dr. Ian Teasdale

Co-Supervisor
Dr. Helena Henke

November 2018

Master's Thesis

To confer the joint academic degrees of

Master of Science

In the Master's Program

Biological Chemistry Joint Master Program

STATUTORY DECLARATION

I hereby declare that the thesis submitted is my own unaided work, that I have not used other than the sources indicated, and that all direct and indirect sources are acknowledged as references. This printed thesis is identical with the electronic version submitted.

Place, Date

Signature

ACKNOWLEDGMENTS

This master thesis would not have worked out the way it did without the contribution of many people. First of all, I want to thank my supervisors, Univ.-Prof. Dr. Oliver Brüggemann for enabling me to work on this thesis and sharing his experience on the topic of molecular imprinting, Assoz. Univ.-Prof. Dr. Ian Teasdale for his insights into the chemistry of polyphosphazene, and of course Dr.^{in} Helena Henke for countless, invaluable hours of support in the lab as well as during writing this thesis. Furthermore, I want to thank Dr.^{in} Aitziber Iturmendi for various helping hints and advices, my office colleagues, and then fellow master students, Doris and Vanessa for the great time, also aside of the laboratory work, and their good spirit, as well as Wolfi, Sabrina, Andi, Antonia, Renate, Gudrun and all the other members of the ICP for their help and the wonderful time I had at the institute.

I also want to thank my study colleagues, and more importantly, my friends, Helmut, Kathi, Lisa and Nora, for every time they helped me out, either work related or personally, and in general, for the time we spent together working towards our master's degree.

Last, but not least, I thank my family and friends at home, Mum, Dad and Hannah, Max and Lilli for their support and also their understanding when I am at my worst, and my friends, Moe, Lukas, Georg, and all the others, who will forgive me for not naming everyone, for being there and getting me back up if needed and reminding me that there are also other things to worry about.

ABSTRACT

Despite several different approaches describing degradable and biodegradable molecularly imprinted polymers (MIPs), the extent of their application and further research in this area remains scarce. In this thesis the preparation of molecularly imprinted polymers based on poly(organo)phosphazenes and their potential use as a modular construction kit for biocompatible, degradable molecularly imprinted polymers is reported.

Molecularly imprinted polymers in general are to a great extent based on polyacrylates, additionally, in more recent approaches, their synthesis in form of nanoparticles have become more apparent. Due to the research focus on those approaches, the degradability of these materials has not been investigated. To the best of my knowledge, only a few reports of (bio)degradable MIPs based on poly(3-hydroxybutyrate), poly(lactic acid)/poly(ethylene glycol) or degradable cross-linkers look specifically into these characteristics, despite their potential use in biomedical applications.

Poly(organo)phosphazenes, a group of inorganic-organic hybrid polymers with a backbone of alternating phosphorus and nitrogen atoms, offer unique and highly tunable characteristics due to the vast range of applicable organic substituents, enabling precise controlled degradability and degradation to benign small molecules. This, as well as the use of various functional groups for imprinting, makes these polymers serve as potential candidates as basis for biocompatible and degradable MIPs. Poly(organo)phosphazenes have been investigated for biomedical applications, specifically for controlled drug release, be it polymer therapeutics or vaccine adjuvants, or tissue engineering.

The synthesis of polyphosphazenes via a novel phosphine mediated one pot method is presented, with glycine substituents for the wanted degradability and functionalized with thioglycolic acid operating as a functional monomer, to imprint propranolol, a widely established template allowing comparison with recent literature, furthermore, the influence of different porogens and cross-linkers on the selectivity of the imprinted polymers over non-imprinted ones is determined.

ZUSAMMENFASSUNG

Trotz unterschiedlichster Herangehensweisen an bioabbaubare und abbaubare molekular geprägte Polymere (molecularly imprinted polymers, MIPs) verbleibt deren praktische Anwendung und weiterführende Forschung in diesem Bereich begrenzt. In dieser Arbeit wird die Herstellung von molekular geprägten Polymeren auf der Basis von Poly(organo)phosphazenen und deren potentieller Nutzen als modular konzipierter Baukasten für biokompatible, abbaubare molekular geprägte Polymere erläutert.

Molekular geprägte Polymere basieren zu einem großen Teil auf Polyacrylaten, aber auch deren Nutzung in Form von Nanopartikeln gewinnt mehr und mehr an Bedeutung und durch den Forschungsschwerpunkt auf diesen Anwendungen wurde die Abbaubarkeit dieser Materialen nicht untersucht. Nach meinem besten Wissen wird nur wenig im speziellen über diese Eigenschaften berichtet, beispielsweise MIPs auf der Basis von Poly(3-hydroxybutyrat), Polymilchsäure/Polyethylenglycol oder abbaubaren Vernetzern, trotz deren Potential im Bereich von biomedizinischen Anwendungen.

Poly(organo)phosphazene, eine Gruppe anorganischer-organischer Hybridpolymere mit einem Polymerrückgrat aus sich abwechselnden Phosphor- und Stickstoffatomen, bieten einzigartige und höchst abstimmbare Eigenschaften auf Grund der verschiedensten nutzbaren organischen Substituenten, welche eine präzise kontrollierbare Abbaubarkeit und weiteres einen Abbau hin zu kleinen gutartigen Molekülen erlauben. Sowohl dadurch, als auch durch die Verwendung unterschiedlicher funktioneller Gruppen beim molekularen Prägen, dienen diese Polymere als potentielle Kandidaten für biokompatible und abbaubare MIPs. Poly(organo)phosphazene wurden für den Gebrauch im Bereich von biomedizinischen Anwendungen bereits untersucht, genauer, für gezielte Wirkstofffreisetzung, seien es Polymertherapeutika oder Impfstoffadjuvanzien, oder Gewebetechnologie.

In dieser Arbeit wird einerseits die Synthese von Polyphosphazene anhand einer neuartigen Phosphan-moderierten Eintopfreaktion präsentiert, adaptiert mit Glycin-Substituenten für die gewünschte Abbaubarkeit und funktionalisiert mit Thioglycolsäure als funktionelles Monomer zur Prägung von Propranolol, ein weitgehend etabliertes Templat, welches einen Vergleich mit aktueller Literatur erlaubt, und andererseits der Einfluss verschiedener Porenbildner und Vernetzer auf die Selektivität geprägter Polymer im Vergleich zu nicht geprägten Polymeren aufgezeigt.

LIST OF CONTENT

1. Introduction

1.1. Polyphosphazenes

1.1.1. Molecular structure

Polyphosphazenes are a unique type of polymer, consisting of a backbone of alternating phosphorus and nitrogen atoms linked via alternating single and double bonds. The character of the -P=N- bond is still under investigation, nevertheless, in silico experiments propose partly different and somehow interacting theories, namely the zwitterion model and the model of negative hyperconjugation, both explaining the special properties of the polyphosphazenes backbone to some degree.[1] Noteworthy are the contributions of negative hyperconjugations building up a multiple bond character of the P=N bond with a minimal hindrance to bond rotations, allowing for an unexpected flexibility of the polyphosphazenes backbone.[1–9] Nevertheless, the substituents of the final poly(organo)phosphazene influence the flexibility to a great extent, as holds true for the other properties of the polymer described below. These substituents are linked to the backbone via nucleophilic attack on the phosphorus atom. Organic nucleophiles can be readily attached to the inorganic backbone resulting in an inorganic-organic hybrid polymer. These hybrid polymers offer a broad band of varying properties depending on the interplay of the organic substituents and the inorganic backbone. Furthermore, the possibility to produce mixed substitutions increases the accessibility of desired properties. This enables the creation of vast libraries of polymers with specific attributes, positioning polyphosphazenes of increasing academic interest in various of research fields.[10–13]

1.1.2. Synthesis

Polyphosphazenes are commonly synthesized following one of two methods, either ring-opening or living cationic polymerization. Ring-opening polymerization results in high molecular weight polymers with broad polydispersities, whereas living cationic polymerization allows for controlled molecular weight polymers with narrow polydispersities, in exchange for a lower molecular weight.[2,14] Both methods follow the same scheme, depicted in Figure 1, by first synthesizing poly(dichloro)phosphazene, which is subsequently reacted with organic nucleophiles to poly(organo)phosphazenes during a postpolymerization substitution reaction.[2]
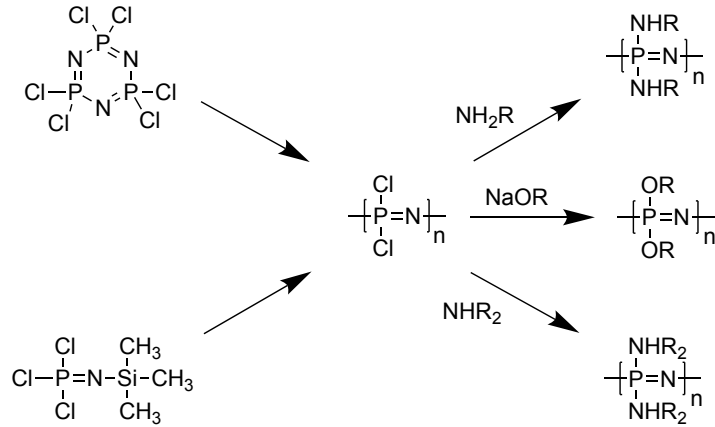
Figure 1: Schematic representation of the common synthesis pathways towards poly(organo)phosphazenes with varying substituents (R).

1.1.2.1. Ring-opening polymerization

Ring-opening polymerization is the classical route to prepare linear, high molecular weight poly(dichloro)phosphazenes from hexachlorocyclotriphosphazene in large amounts. The cyclic trimer is heated to 250 °C in vacuum in a sealed class tube for several hours leading to cleavage of the chlorine atoms and formation of a cationic phosphazenium species, propagating the polymerization by reacting with another cyclic trimer by the eponymous ring opening, Figure 2.[15,16] While allowing for poly(dichloro)phosphazenes of high molecular weight, this synthesis is limited to broad polydispersities and no control over the molecular weight. This is due to the initiation mechanism itself, proceeding by cleaving Cl from the cyclic trimer, which can happen throughout the whole polymerization process and can initiate a new chain over the whole course of the reaction. Furthermore, a tight temperature control is necessary to enable a reasonable polymerization rate while keeping side reactions and branching at bay.[2]
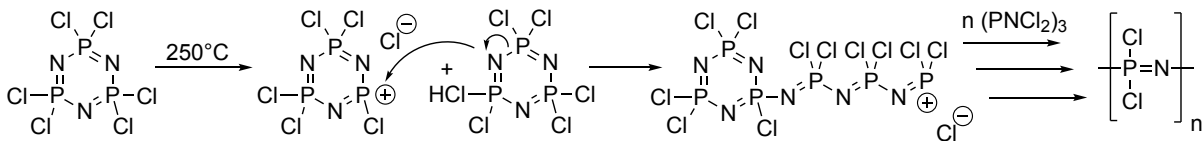

Figure 2: Commonly accepted mechanism of the ring-opening polymerization of hexachlorocyclotriphosphazene to poly(dichloro)phoshazene.

1.1.2.2. Living cationic polymerization

The living cationic polymerization route allows for a controlled polymerization at room temperature,[2,17] using phosphoranimines, such as P-chloro-P-methyl-phenyl(N-trimethylsilyl)phosphoranimine (ClPhMePNSiMe$_3$) and trichloro(N-trimethylsilyl)phosphoranimine (Cl$_3$PNSiMe$_3$) as monomers, with the latter being the monomer of choice for the work presented in this thesis.[18] In general, the polymerization of trichlorophosphoranimine can be regarded as a polycondensation, where Cl$_3$PNSiMe$_3$ forms the cationic species [Cl$_3$PNPCl$_3$]$^+$ and the counter ion PCl$_6^-$ via reaction with two equivalents of PCl$_5$. The polymer chain is propagated by the residual Cl$_3$PNSiMe$_3$ in the reaction solution, as can be viewed in Figure 3, producing an equivalent of ClSiMe$_3$ for each repeating unit attached to the growing chain.[17]

One living cationic end group stemming from one cationic initiator per growing polymer chain enables narrow polydispersities, as well as, controlled molecular weight by controlling the monomer initiator ratio, as, in contrast to the ring-opening polymerization mechanism, the initiator is formed just at the beginning of the polymerization reaction, and each chain is propagated by just one cationic initiator during living cationic polymerization. Furthermore, the whole polymerization reaction can easily be observed in ^{31}P NMR spectroscopy via the disappearance of the monomer signal, a single, sharp peak at -54 ppm, and a shift of the signal to the characteristic signal for poly(dichloro)phosphazenes, a single, sharp peak at -18 ppm.[2,14,19]

With PCl$_5$ used to form the cationic initiator, a certain degree of bidirectionality regarding the chain growth can be observed, due to the migrating propagating site from one chain end to the other.[20] To allow only monodirectional growth to occur, R$_3$PNSiMe$_3$ type substrates can be used, R being either an alkyl or aryl residue, but typically phenyl groups. Analogous to the procedure described above, R$_3$PNSiMe$_3$ is reacted with two equivalents of PCl$_5$ to form the cationic initiator enabling polymerization of Cl$_3$PNSiMe$_3$ via an identical mechanism but with the R-groups blocking one end of the initiator forcing monodirectional chain growth and resulting in different and defined chain ends, depicted in Figure 3.[2,21]

In addition, R$_3$PCl$_2$, chlorinated tertiary phosphines with R being again either an alkyl or aryl residue, may be used in polar solvents, in which they are present completely in an ionized form [R$_3$PCl]$^+$Cl$^-$,[22] to initiate the living cationic polymerization of Cl$_3$PNSiMe$_3$ enabling monodirectional growth as well, the reaction can be seen again in Figure 3.[23,24] A significant advantage is also the possibility to use monofunctionalized tertiary phosphines which are not only commercially available but allow synthesis of polyphosphazenes with a functionalized α-chain end, opening the way to higher architectures and macromolecular engineering.[2,23]

Again, the course of the reaction can be followed by NMR spectroscopy, and additionally the end groups of the chain can be distinguished. Even more, after a suitable macrosubstitution, the ratio of the intensities of signals stemming from protons from the end group and the substituents can be used as a fast and facile method to determine the average chain length of the synthesized

polymer, hitherto, only determinable by the monomer to initiator ratio without a suitable control after the polymerization.

The monomer, $Cl_3PNSi(CH_3)_3$, itself is required in large amounts of high purity, and is synthesized in a two-step process by reacting PCl_3 with $LiN(Si(CH_3)_3)_2$ and oxidizing the formed $Cl_2PN(Si(CH_3)_3)_2$ with SO_2Cl_2 to give $Cl_3PNSi(CH_3)_3$ leading to high yield prior to purification. However, significant loss during purification via vacuum distillation still occurs, and, additionally, scaling up the process is limited due to the limitations of the purification step.[2,25]

In anticipation of these problems a one-pot synthesis directly polymerizing $Cl_3PNSi(CH_3)_3$ following its formation has been described by Wang,[26] omitting the purification step and producing $[NPCl_2]_n$ directly without an intermediate step at the monomer. This allows for an easier scale up and higher overall yields, both at the cost of control over the polymerization. Nevertheless, this special approach has also been followed for parts of this work and adapted throughout it.
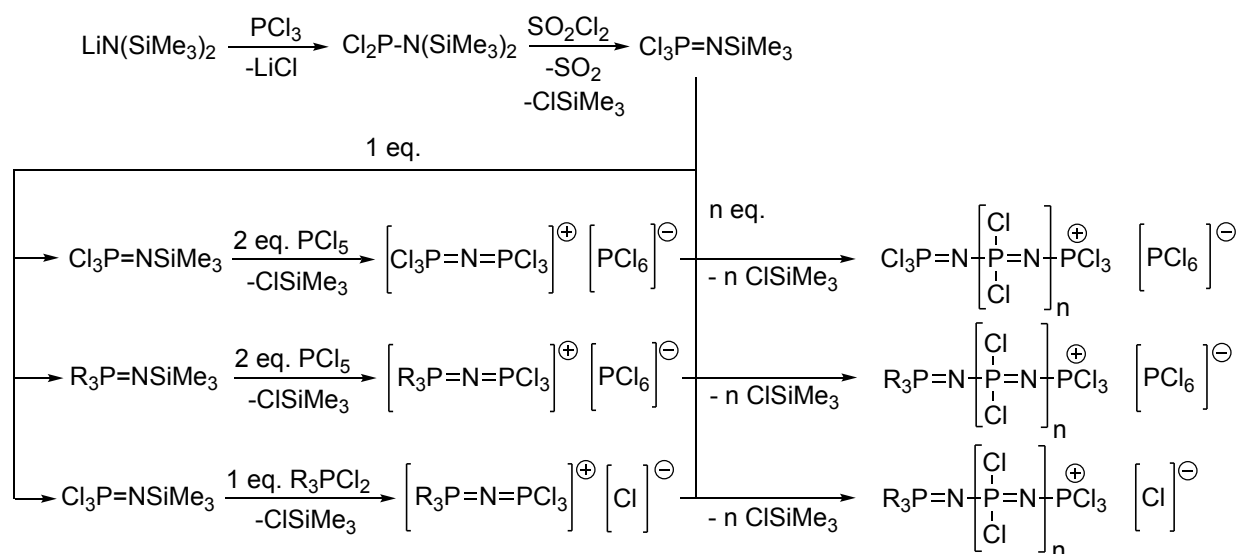
Figure 3: Schematic representation of the living cation polymerization with different cationic initiators and including monomer synthesis. R being either an alkyl or aryl residues with a preferred use of phenyl groups.

1.1.2.3. Macrosubstitution

As described above, and depicted in Figure 1, following the synthesis of the poly(dichloro)phosphazenes a postpolymerization substitution, termed macromolecular substitution by Allcock[16], is performed to synthesize poly(organo)phosphazenes. This allows for not only the synthesis of the various polymers with their own unique features, as already mentioned, but is also necessary to stabilize the polymer, which would otherwise degrade upon hydrolysis, due to the high reactivity of the poly(dichloro)phosphazene. Moreover, storage times of several years have been reported for poly(dichloro)phosphazenes upon storing the polymer in diglyme, without substituents to stabilize the polymer.[2,15]

4

The macrosubstitution itself may pose some difficulties, requiring a large number of simultaneous reactions, as well as different reaction conditions and times, greatly depending on the character of the desired substituent, namely its nucleophilicity and steric hindrance.[27] Moreover, a complete macrosubstitution has to be ensured to avoid the aforementioned degradation of the polymer, as well as a possible cross-linking due to the labile P-Cl bonds.[2] As for the poly(dichloro)phosphazene synthesis, the progress of the macromolecular substitution can easily be followed via NMR spectroscopy.[16] Either in the shift of the ^{31}P NMR signal from the sharp, single peak at -18 ppm for [NPCl$_2$]$_n$ to a broader peak at 0 ppm, due to the larger side groups, or in the ^{1}H NMR spectrum by the increase in intensity of the substituents signals from which also the average chain length can be estimated as mentioned above, as well as a broadening of the signals.

Special utilization of the macromolecular substitution are, for example, mixed substitutions where two different substituents are used, offering an additional possibility to modify the properties of the polymer in various ways. Nevertheless, it has to be kept in mind that two or more different substituents complicate the macrosubstitution significantly. Although all phosphorus atoms react once first before a second substituent is attached to any of them, the process is random and, subsequently, can lead to exchange of the used substituents, disturbing the wanted ratios and influencing the properties in an unforeseen way, as well as prolonging the reaction time.[28]

1.1.3. Degradation

A key feature of polyphosphazenes, especially for many biomedical applications, is their degradability.[2,13,29,30] The degradation of poly(organo)phosphazenes occurs via hydrolysis of the backbone, substitution of the organic substituents with water, resulting in the formation of hydroxyphosphazene and subsequently phosphazane species. These instable derivatives finally lead to chain cleavage and, overall, result in a degradation of the polymer into a mixture of phosphates and ammonia alongside the organic side group, which can be altered by desire to be benign and biocompatible, depending on the substituent.[2,29,30] The complete pathway can be seen in Figure 4.

Effects on the stability of the polymer, as well as on the degradation rate, depend highly on the character of the side group and its functionality which can interplay to a certain degree, complicating the development of guidelines regarding the influence of the side group on the degradation. Nevertheless, P-NH-R compounds are observed to degrade faster than their P-O-R counterparts accounting for the higher stability of the P-O bond. The same holds true for bulky or hydrophobic residues, which protect the backbone from attack of H$_2$O. In addition, the pH influences the degradation rate in a way that lower pH values have a positive effect on the degradation time, whereas slightly basic pHs show just little effect.[2,10,29,30]

With this set of findings, a controllable degradation behavior of polyphosphazenes in a chosen range can be achieved and tuned to the needs of a specific application.[29]
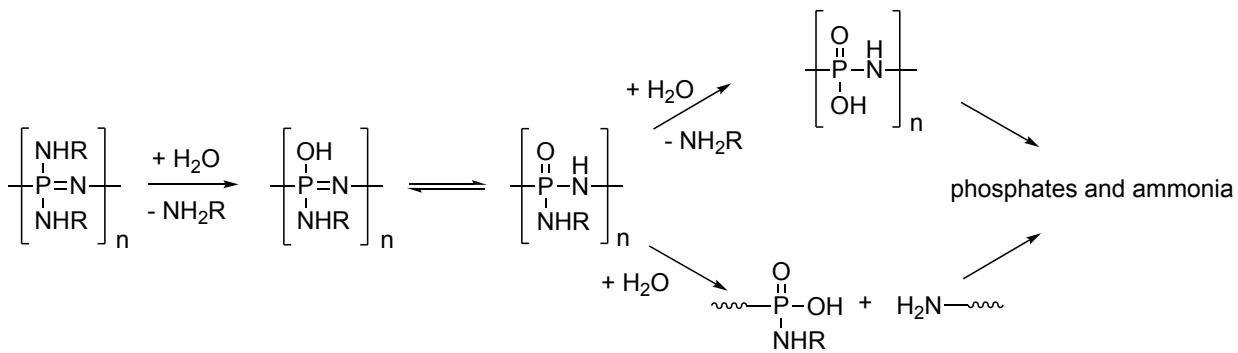
Figure 4: Scheme of the degradation mechanism of poly(organo)phosphazenes upon hydrolysis.

1.1.4. Applications

As is highlighted in this chapter, polyphosphazenes enable the alteration of their properties to cover a broad range, via the macromolecular substitution and the perfect coordination of substituents. As a consequence, their applications are as broadly distributed over various research fields as are their attributes. Focusing on their degradability and biocompatibility, they come to use in different fields of biomedical applications[13] be it tissue engineering[12], drug[31,32] or gene delivery[33] or vaccine delivery.[10] On the other hand they have also found applications in areas like in fuel cells, as membranes, as high performance supercapacitor electrodes or more general as high performance elastomers for various uses, polyphosphazenes have established themselves as valuable and useful materials.[11,34,35]

Despite being used as a basis for molecularly imprinted polymers in the past,[36] polyphosphazenes are not established as suitable polymers for molecularly imprinted polymers, even though they offer a great versatility of properties and functionalities, as well as desirable properties like biocompatibility and degradability for areas with growing interest for molecular imprinting.

1.2. Molecular imprinting

1.2.1. Basic principle

Molecular imprinting is a process greatly based on the "Lock and Key" theory for enzymes, and can be defined in short as following: The synthesis of polymers, containing selective binding sites for a ligand, formed upon covalent assembly of the bulk phase in presence of a template (atom, ion, complex, microorganisms, and molecular, ionic or macromolecular assemblies) with subsequent removal of the employed template to allow for selective recognition in the emptied cavities.[37–40]

Different methods can be utilized for the formation of a molecularly imprinted polymer, nevertheless, the basic principles are identical and depicted in Figure 5.
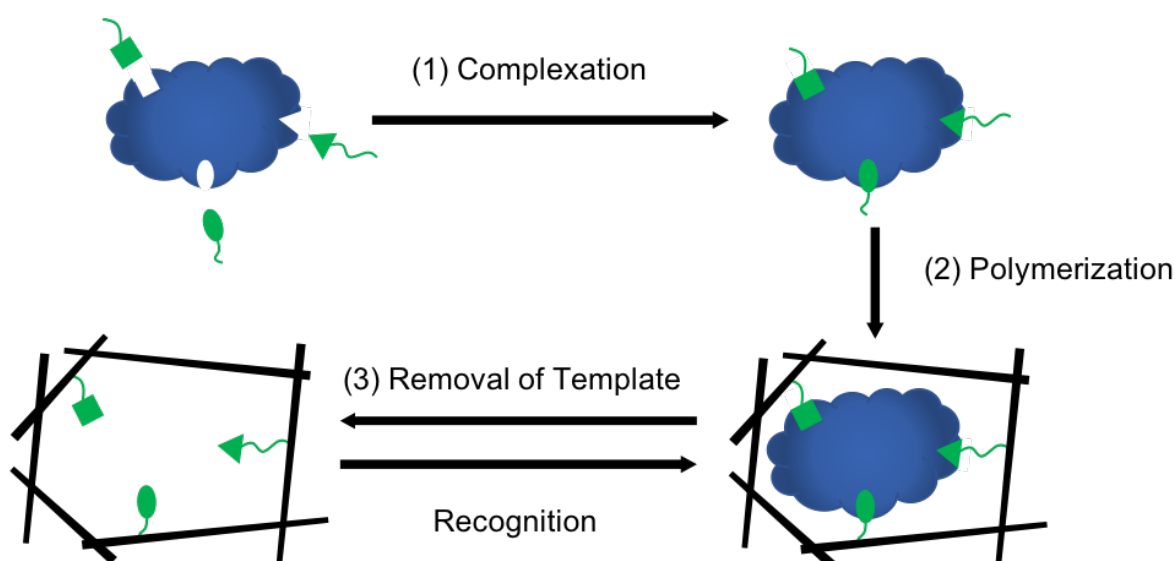

Figure 5: Schematic illustration of the molecular imprinting process, adapted from the literature.[41]

A functional monomer is mixed with the template and they interact either covalently or non-covalently to form a pre-polymerization complex, Figure 5(1). This complex is subsequently enclosed in a 3D-network upon polymerization, using suitable cross-linkers forming a cavity occupied by the template, Figure 5(2). Finally, the template is removed, either washed out or, for example, chemically cleaved, leaving a free cavity, ideally, remembering size, structure and other properties of the template, such as chemical functionality, allowing for a successful and specific rebinding of the template, Figure 5(3).[41–43]

For the characterization of molecularly imprinted polymers, different methods can be applied, depending on the characters, morphology, chemical properties, recognition behavior and the specific properties of interest. Morphological characteristics are traditionally investigated by microscopic methods, light microscopy or electron microscopy, as well as scanning probe microscopy, namely atomic force microscopy (AFM). Beside these, also Brunauer-Emmett-Teller (BET) analysis can be applied to determine specific areas and pore sizes. Chemically, the characterization of MIPs is more complex due to their insolubility, therefore, solid-state nuclear magnetic resonance (ss-NMR) and Fourier-transform infrared spectroscopy (FT-IR) are methods

of choice. The recognition behavior, probably the most important characteristic, can be evaluated in various forms and methods, for example, one way to test the binding capacity is a batch rebinding experiment. In addition, chromatographic methods are of good use, where the MIP is packed in a column as the stationary phase, and the retention time of the template is determined. Structurally related molecules can be tested easily this way, and thus the specificity of the MIP towards its template.[37,41,42] More recent literature also reports the use of force spectroscopy utilizing AFM to evaluate recognition specificity.[44] For this work, FT-IR has been used to ensure the chemical characteristics of the molecularly imprinted polymer, BET-analysis has been performed, and batch-rebinding with comparison to a non-imprinted polymer has been carried out to determine the recognition behavior.

1.2.2. Imprinting - covalent, non-covalent

The imprinting process, Figure 5, is described further in a more detailed way for which two different methods can be distinguished, covalent and non-covalent imprinting, referring to the interaction between the template and the functional monomer, a comparison can be seen in Figure 6.
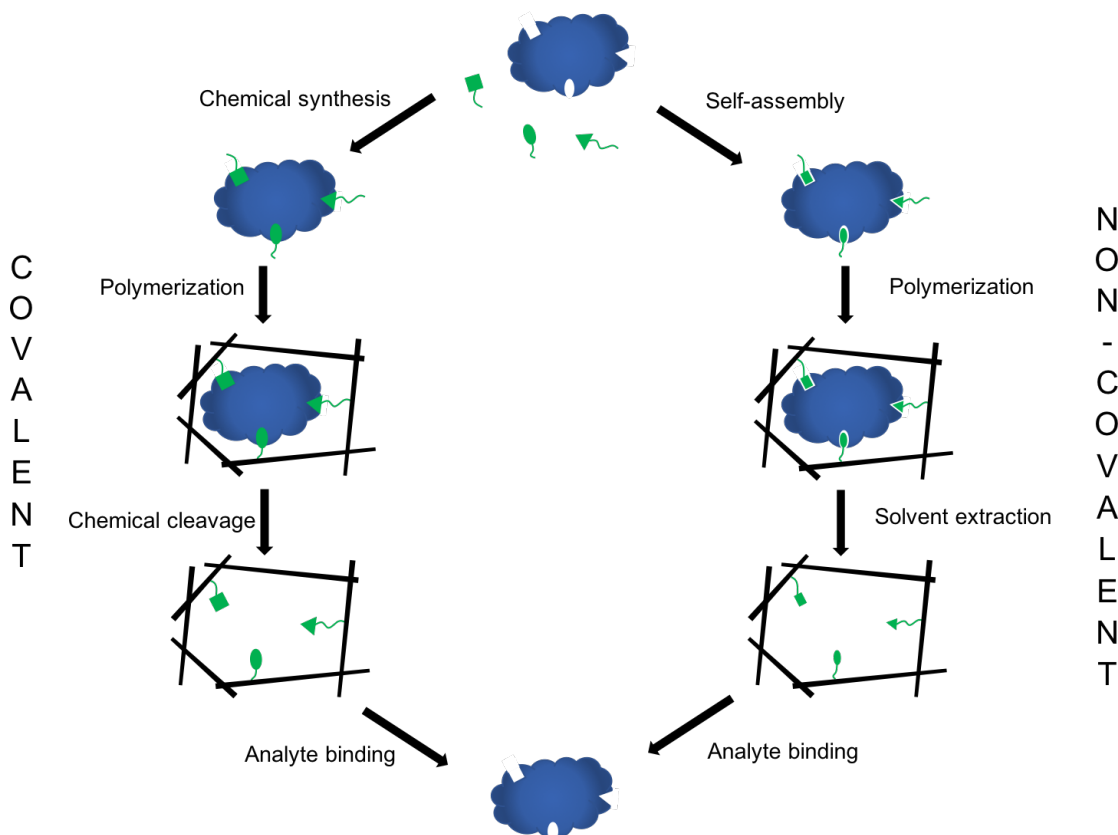
Figure 6: Schematic comparison of covalent and non-covalent molecular imprinting, adapted from Yan and Row.[43]

1.2.2.1. Covalent imprinting

As described above, during covalent imprinting the template and the functional monomer are linked to each other covalently and remain so during the polymerization step. The covalent bond is subsequently cleaved, and the template is removed allowing for rebinding. A schematic of the principle can be seen in Figure 7 by the example of a mannopyranoside.[41]
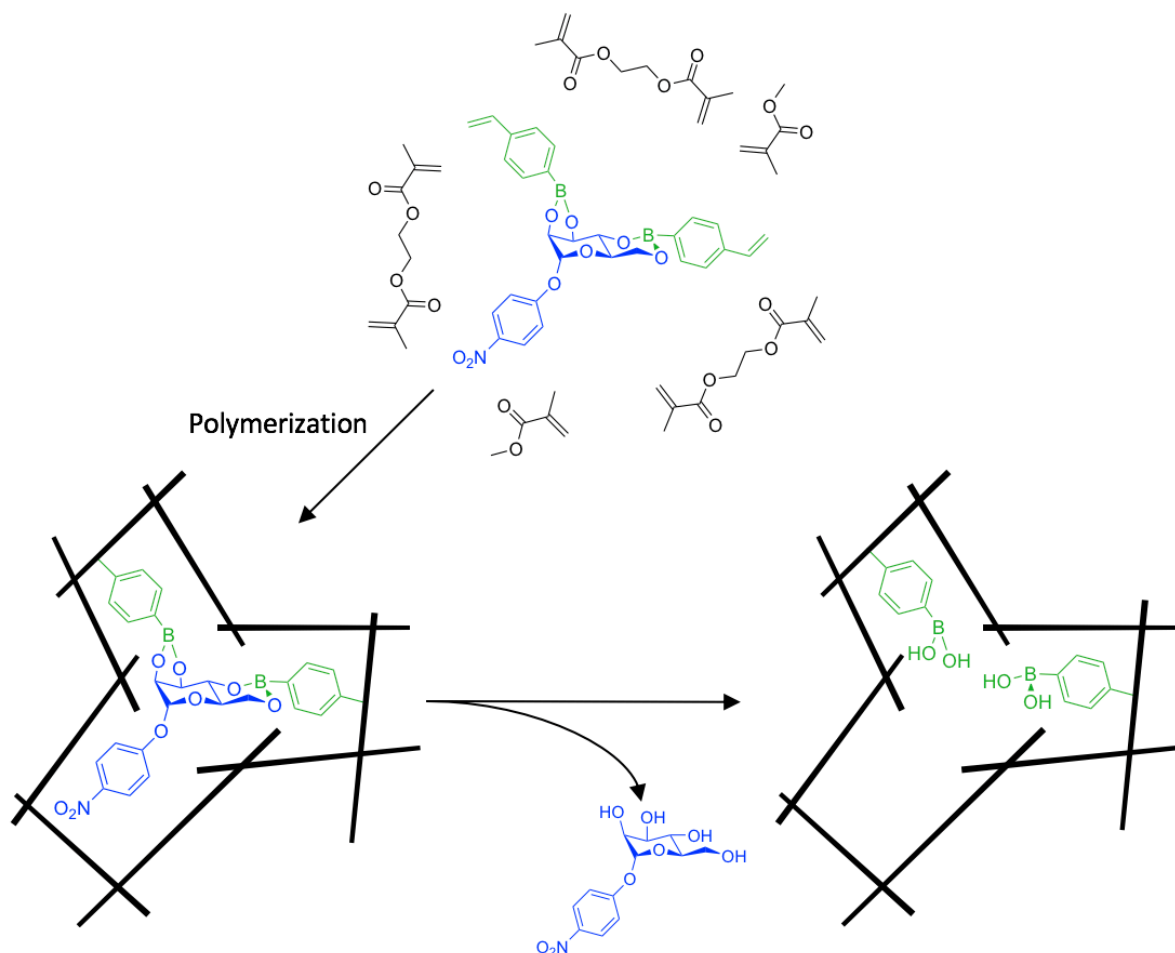
Figure 7: Covalent molecular imprinting of a mannopyranoside via its 4-vinylphenylboronic acid ester, adapted from the literature.[41]

While allowing for a variety of polymerization conditions and a clear template-functional monomer relation, covalent imprinting bears certain drawbacks. For one, it is limited by the necessity for reversible covalent linkages between the template and the monomer, and is also vulnerable during the removal of the template due to the potential of certain reaction conditions which can harm the imprint.[41,43,45]

1.2.2.2. Non-covalent imprinting

For non-covalent imprinting, the template and the functional monomer interact only by non-covalent interactions such as hydrogen bonds, van der Waals interactions, or electrostatic/ionic interactions during imprinting, as well as rebinding.[37] A schematic representation of the principle can be seen in Figure 8 by the example of theophylline.[41]
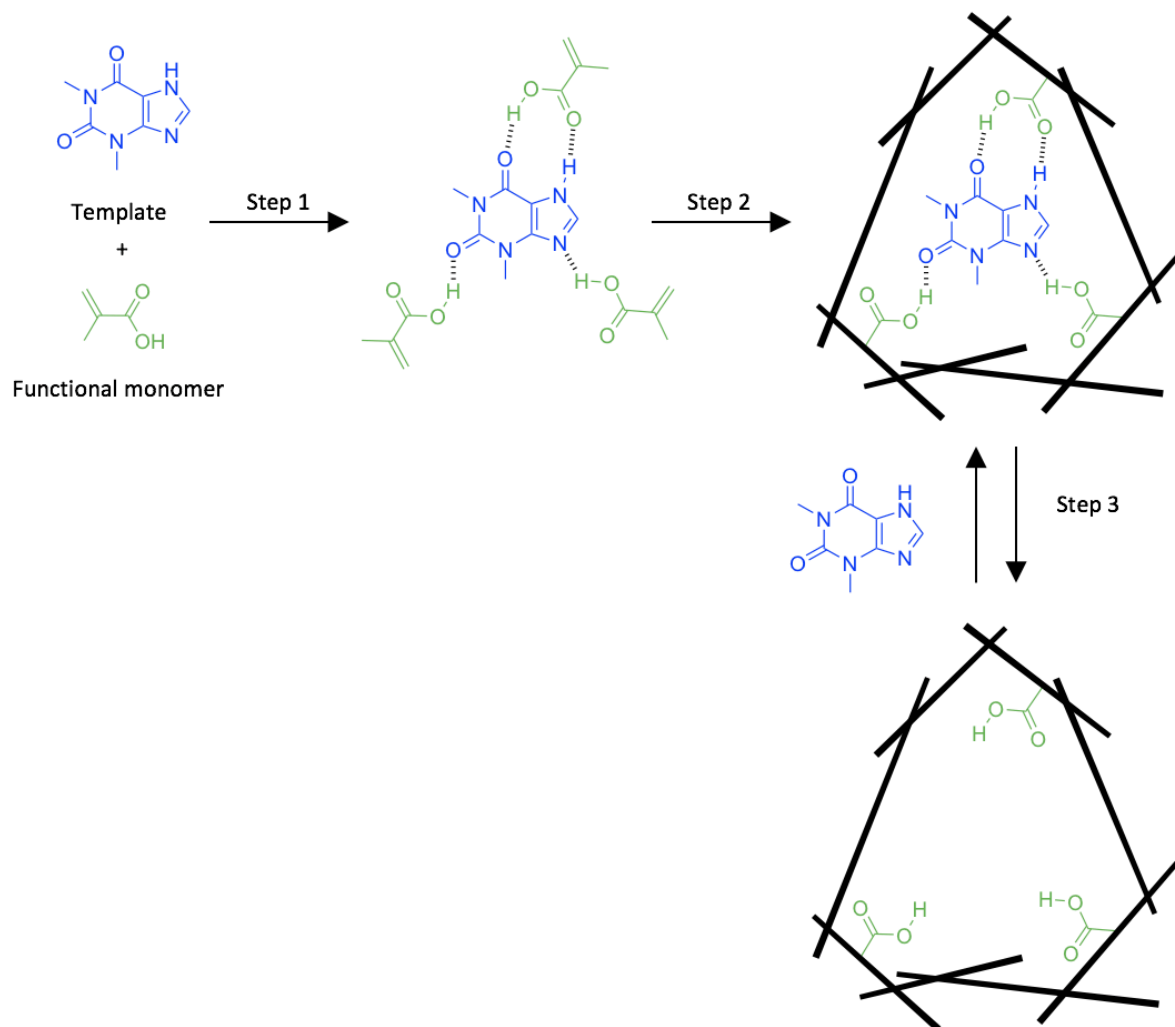
Figure 8: Non-covalent molecular imprinting of theophylline via methacrylic acid; Step 1: self-assembly, Step 2: polymerization, Step 3: template removal. Taken from Komiyama et al.[41]

Non-covalent imprinting is the most frequently used method, as it is simpler and can be more widely applied without the limitation of applicable reversible covalent linkages. Nevertheless, the interaction between the template and the functional monomer is less clear and the polymerization conditions have to be monitored rigorously to prevent disturbance of the non-covalent interactions.[41,43,45]

For the work presented in this thesis, non-covalent imprinting has been used.

1.2.3. Functional monomers

The choice of a suitable functional monomer may pose the most important question during the design of a molecularly imprinted polymer, significantly influencing its functionality. The role of the monomer is to form a stable pre-polymerization complex and enable successful polymerization and cavitation. In this sense, the monomer consists of two units, the recognition unit and the polymerizable unit. The polymerizable unit can be comprised of vinyl double bonds or silicon hydroxyl residues for example, depending in the polymerization process, chosen in a way to not interfere with the imprinting. The recognition unit has to be chosen in a way that allows a specific interaction with the template. Utilization of more functionalities or even multiple functional monomers interacting with the template can improve the specificity of the MIP. Regarding the aforementioned methods of imprinting, covalent and non-covalent, different functional monomers are used, and a short excerpt of different monomers can be seen in Table 1 and Table 2. Furthermore, the method of choice for the imprinting process also influences the ratio between template and functional monomer. Whereas for covalent imprinting a clear stoichiometry is known, non-covalent imprinting utilizes Le Chatelier's principle, using an excess of the monomer to increase the concentration of the pre-polymerization complex, routinely ratios of 1:4 or higher, determined empirically.[37,41–43,45]

Outstanding in the ranks of functional monomers is methacrylic acid (MAA), with it being both a hydrogen bond donor and acceptor, it is used as a somewhat universal functional monomer.[37] Additionally, the capability of MAA to dimerize[46], in this way increasing selectivity, as well as its pore forming properties in higher molar fractions[47] leading to an enhanced binding capacity, account for its broad use.[37]

Table 1: Common functional monomers used for covalent molecular imprinting.[37]
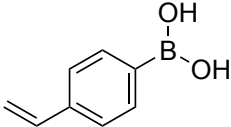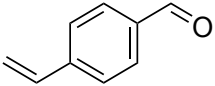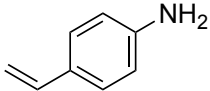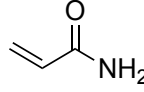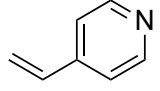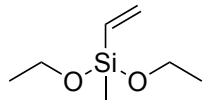
Name	Chemical Structure
(4-vinylphenyl) boronic acid	
4-vinyl benzaldehyde	
4-vinyl aniline	

Table 2: Common functional monomers used for non-covalent molecular imprinting.[37,42,43]

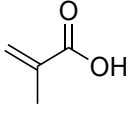| Name	Chemical Structure
methacrylic acid	
acrylamide	
4-vinylpyridine	
methylvinyldiethoxysilane	

1.2.4. Polymerization methods

Overall, two general polymerization methods are used for the production of molecularly imprinted polymers, free-radical polymerization and the sol-gel process.[37,41–43]

With radical polymerization being the most common one, an overview of the mechanism is depicted in Figure 9, different techniques have been established and compared, and the respective advantages and disadvantages are summarized in Table 3, adapted from the literature.[37,43]
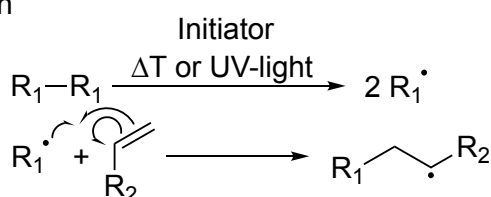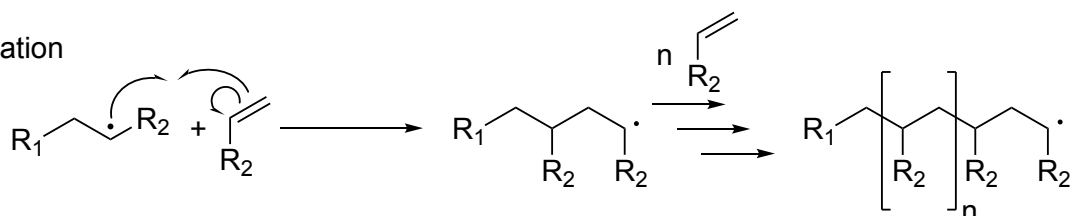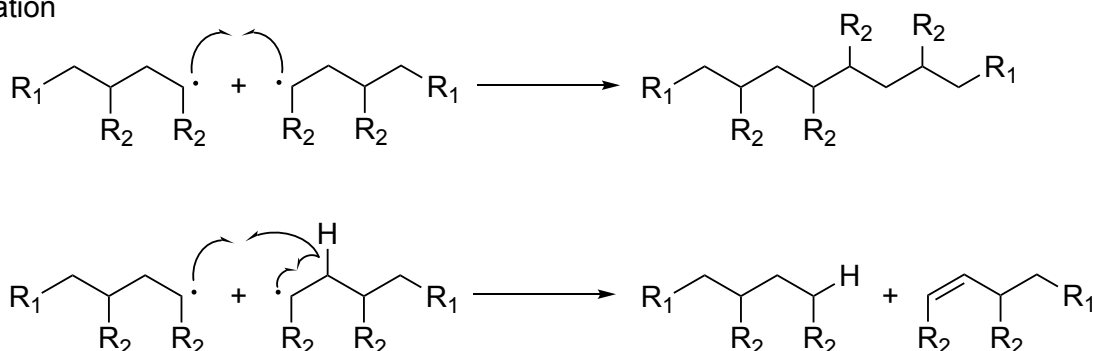
Figure 9: General depiction of the mechanism of free-radical polymerization.

Briefly, whereas bulk polymerization is the most widely used free-radical polymerization and allows for an easy preparation of MIPs, the necessary post-polymerization steps pose significant drawbacks of this technique. More sophisticated methods for molecular imprinting were therefore established, covering a broad range of approaches. Suspension polymerization is still simple in procedure but problematic in its use of solvents. Multi-step swelling allows for MIPs of controlled diameters, ideally suited for chromatographic applications, but is time consuming. Also, the use of water as a solvent is inconvenient as it can disturb non-covalent interactions. On the other hand, precipitation polymerization for example gives an even higher control over the size than multi-step swelling and works in organic solvents, but requires a large amount of solvent and a tight control of reaction conditions.[37,43]

Table 3: Summary of different polymerization methods for molecular imprinting.[37,43]

Polymerization method		Advantages	Disadvantages	Literature examples
Free-radical polymerization	Bulk polymerization	• simple and universal • no particular instrumentation necessary	• post-polymerization processing (grinding, sieving, packing) • no size/shape control • low performance	48–50
	Suspension polymerization	• spherical particles • reproducible • possible scale-up	• big particle size • special solvents needed	51–57
	Multi-step swelling polymerization	• spherical particles • controlled size • ideal for HPLC	• aqueous emulsion troublesome • complicate procedure	58–64
	Precipitation polymerization	• high yield • high quality • controlled size and shape	• large amount of template • large amount of solvent	65–72
	Emulsion polymerization	• high yield • water soluble polymers • monodispersed particles	• remnants of surfactant • low performance	73,74
Sol-gel process		• at room temperature • eco-friendly solvents	• lack of polymerization method and functional monomer	40

Less common polymerization methods include electrochemical polymerization and electrodeposition, as well as direct grafting on monolithic columns and photografting, and the aforementioned sol-gel process.[37,43]

For the work presented in this thesis, a different approach has been followed, synthesizing the polymer with the functional monomer attached beforehand and imprinting in a separate step during cross-linking.

1.2.5. Current perspective and future objectives

Molecular imprinting is used in a broad range of different fields, spanning from chromatographic functions to sensory applications to drug delivery systems or even catalysis.[42] Each of them with different demands of properties of the imprinted system and challenges in their production.

A short and selected overview of different areas of applicability and research interest can be seen in Figure 10. A more detailed discussion of the applications and distinct examples can be found in several extensive reviews on these matters, as for an overall discussion of MIP applications[42], for sample pretreatment, chromatographic or sensory applications[37], catalysis[75], as well as drug delivery systems[45].
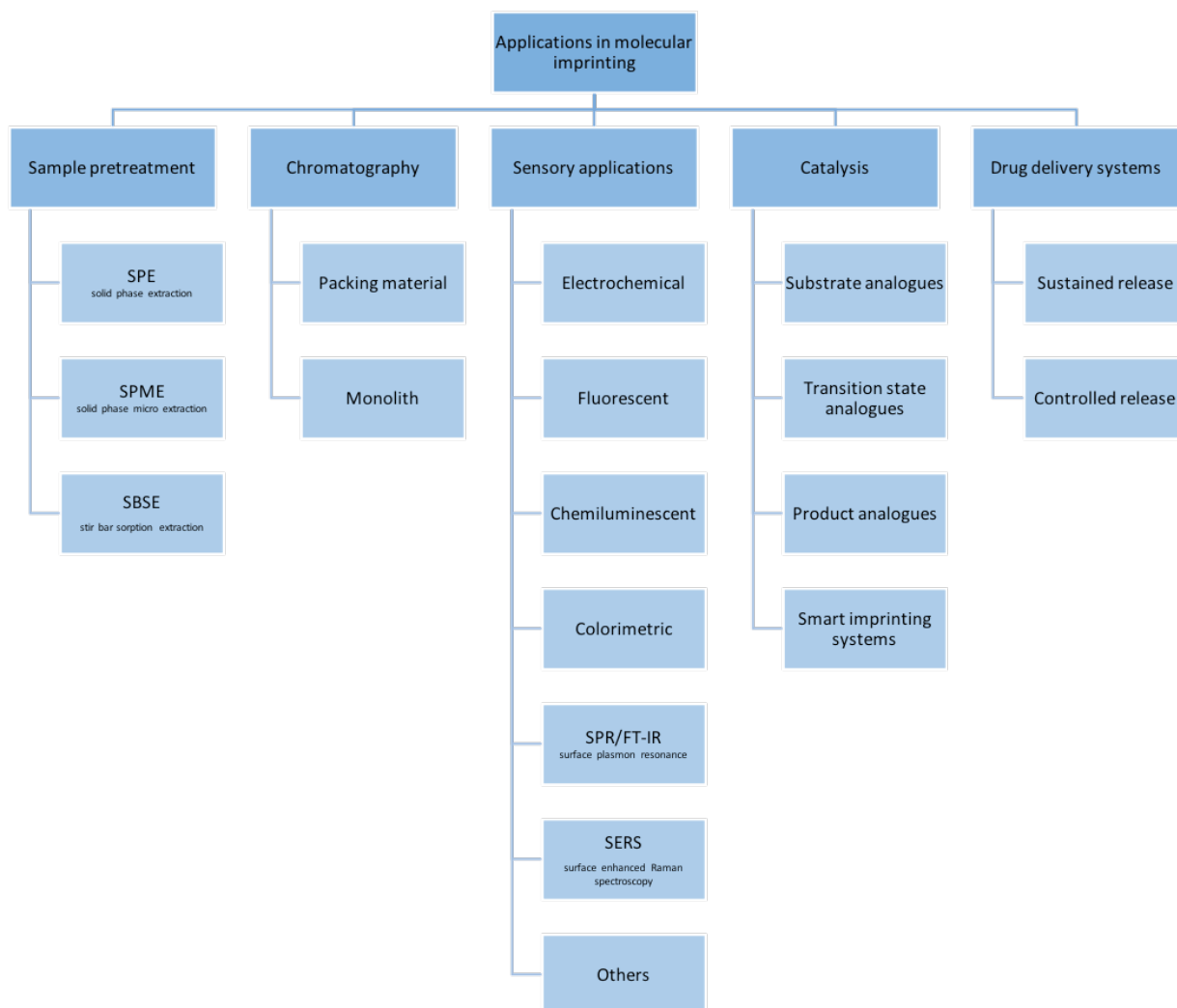
Figure 10: Selected overview of applications and research interests of molecularly imprinted polymers, adapted from the literature.[37,42,45,75]

Besides the advances in the various fields of interests, certain problems and challenges still remain. One of these problems, and probably the most severe one, since it interferes essentially with every other aspect in development, synthesis and optimization, is the laborious and time consuming work necessary to design an optimal MIP system.[42] Nevertheless, different approaches towards simultaneous work flows have been carried out and are promising shorter time scales for molecular imprinting.[76–78]

Another problem, especially for biological applications, arises in the water-compatibility of molecular imprinting, especially for non-covalent approaches water molecules can interfere with the binding capabilities of the polymer.[42] Also, the limited size of possible imprints is a problem which needs to be tackled to advance molecular imprinting in the fields of biological sensors or drug delivery even further.[45,79]

To focus more on problems regarding drug delivery applications and emphasize the opportunity and novelty of the work presented within this thesis, another drawback of some of the currently reported MIP systems are safety and toxicological concerns regarding the base polymers.[42] Some molecularly imprinted polymers based on degradable and/or biocompatible polymers have already been reported, for example on the basis of poly(3-hydroxybutyrate)[80] and poly(lactic acid)/poly(ethylene glycol)[81] or even polyphosphazenes[36], even though without the priority on degradability and biocompatibility. Nevertheless, to the best of my knowledge, the herein presented work opens up a new way of tackling the demands on polymers for molecular imprinting, especially in regard to biocompatibility, degradability, and, furthermore, permits a unique adaptability of the system.

1.3. Thiol-ene chemistry

Historically, and also most widely applied, thiol-ene chemistry is based on a free-radical reaction mechanism, nevertheless also other mechanistic pathways may apply.[82,83] In principle, an initiator, most often a photoinitiator, is used to induce the formation of a thiyl radical upon irradiation. The reaction proceeds by the direct attack, and addition to a C=C double bond resulting in a carbon radical. Finally, the chain transfer to a second thiol molecule occurs, resulting in the thiol-ene addition product, as well as a new thiyl radical for further propagation. The mechanism is summarized in Figure 11.[82]
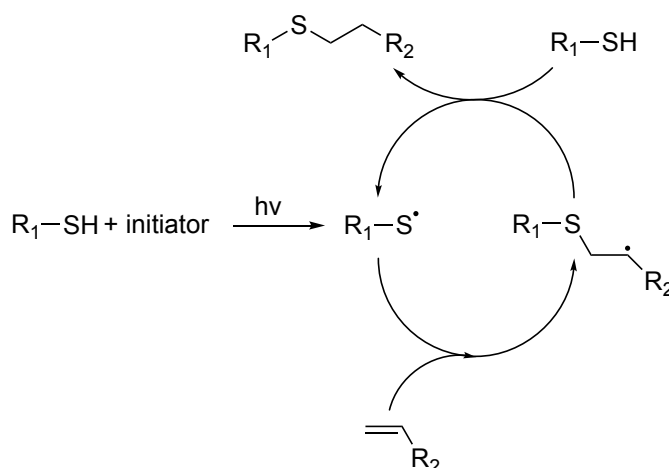
Figure 11: Mechanism for thiol-ene chemistry upon photoinitiation, adapted from the literature.[82]

Advantages of the thiol-ene chemistry include a rapid reaction process, tolerance towards the presence of air/oxygen or moisture, and quantitative, regioselective product formation. Furthermore, in regard to molecular imprinting, thiol-ene chemistry is extremely versatile allowing for a wide range of enes and basically any thiol.[82] This may simplify the design of a molecular imprinting system regarding the selection of the functional monomer, and the imprinting process itself.

Moreover, thiol-ene photochemistry has been widely applied with polyphosphazenes. Not only can substrates containing multiple thiol functionalities be used to cross-link poly(organo)phosphazenes containing substituents with a double bond without any interference with the -P=N- polymer backbone.[82,84] But thiol-ene chemistry has also proven itself exceptionally useful for different macrosubstitution applications in a way of a two-step post-polymerization reaction. By reacting the poly(dichloro)phosphazene first with a simple, double bond containing substrate and subsequent modification via a thiol-ene reaction, an easier way to controllably react multifunctional nucleophiles with poly(dichloro)phosphazenes without the necessity of laborious protection/deprotection reactions or the risk of unwanted cross-linking is provided. Plus, it simplifies the use of bulky molecules, where steric hindrance could lead to incomplete substitution and resulting degradation due to remaining chlorine atoms and chain cleavage, again by first reacting the poly(dichloro)phosphazene with a simple double bond containing entity and subsequent thiol-ene reaction with the desired, bulky side group.[85–88]

1.4. Propranolol

1.4.1. Development

At the beginning of the 20th century the receptor theory for the mode of action of drugs and other transmitting agents became apparent. One of the hallmarks in acceptance of this theory was the description of adrenergic receptors by Raymond P. Ahlquist, namely α- and ß-adrenergic receptors, which in return lead to the synthesize of respective antagonistic medications with propranolol being one of the first of them.[89–91]

ß-Adrenergic receptors, all members of the G-protein coupled receptor superfamily, can be further divided in three subclasses, ß1, ß2 and ß3, differing in their predominant location and sensitivity towards catecholamines like adrenalin and noradrenalin. Nevertheless, they all have in common their primary principle of operation through activation of adenylyl cyclases which catalyze the conversion of adenosine triphosphate (ATP) to the secondary messenger cyclic adenosine monophosphate (cAMP), binding and activating protein kinase A in return and affecting a broad range of cellular processes in this sense.[89,92]

Propranolol, actually a replacement of the preexisting ß-blocker medication pronethalol, which was found to cause thymic tumors in mice, is a non-specific ß-blocker binding to all three sub-types, and historically used against angina pectoris, a condition in which areas of the heart muscle are insufficiently supplied with oxygen rich blood.[91,93,94]

The structure of propranolol, as depicted in Figure 12, resembles epinephrine and norepinephrine, being composed of an aromatic group as well as an amine and alcohol functional group. However, propranolol, or 1-(isopropylamino)-3-(1-naphthyloxy)-2-propanol, is built from a naphthyloxy residue rather than a phenyl group, also missing the hydroxy residues on the aromatic rings, accounting for the water insolubility in contrast to epinephrine and norepinephrine. Furthermore, despite the occurrence of the active R enantiomer of epinephrine and norepinephrine in the body, S(-)-propranolol is about 100 times as potent as its R(+) counterpart.[95] This may be related to the naphthyloxy group inverting the order of the substituents on the chiral center resulting in the same relative orientation of the amino group to the alcohol group and to the aromatic group, both in S(-)-Propranolol and epinephrine/norepinephrine.
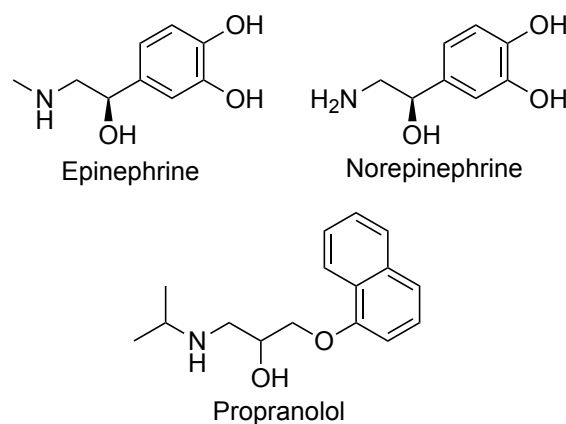
Figure 12: Molecular structures of epinephrine, norepinephrine and propranolol.

1.4.2. Use in medicine

Propranolol is a ß-receptor antagonist competing with classical agonists like catecholamines, and blocking the binding site of the receptor leading to a proportional decrease in chronotropic, inotropic and vasodilator response, affecting the heart rate, contractility and blood vessel relaxation, respectively, due to ß-adrenergic stimulation.[95–97]

1.4.2.1. Cardiovascular diseases

As described above, propranolol was initially designed against cardiovascular problems, angina pectoris in particular, referring to chest pain stemming from an insufficient supply of oxygen.[94]

By decreasing the blood pressure as well as keeping the heart rate low, a combination of propranolol's inotropic and chronotropic effect, the ß-blocker reduces myocardial oxygen consumption, counteracting the symptoms of angina pectoris. Furthermore, it is suggested that propranolol exerts vasodilation despite blocking ß-receptor response, which normally leads to smooth muscle relaxation to a small extend in coronary arteries.[98–100]

In this sense, propranolol is also used as a medication against hypertension and other cardiovascular disease.

1.4.2.2. Cancer

In recent years, propranolol evolved from being an exclusive cardio vascular drug to a broader field of application. Cancer is one of these application with reports of propranolol acting against prostate cancer, as well as breast cancer, leukemia and many others. The ß-blocker has shown effects in various ways, including the immune system, cell proliferation and increasing sensitivity of tumor cells to existing treatments.[101,102]

In addition, propranolol was reported as an adjuvant in a tumor vaccine model of breast tumor-bearing mice.[103]

1.4.2.3. Anxiety disorder

The fight-or-flight response is a primordial instinctive response to fear, anxiety, or other forms of stress.[104,105]

The systems behind this response are multilayered and complex, and chronic dysregulation of these can lead to sever functional impairments often associated with people constantly exposed to activating stimuli. This condition, named post-traumatic stress disorder (PTSD), leaves the patients with persistently re-experience of the trauma, a numbing to certain stimuli related to the trauma or their avoidance, negative mood/cognition and also physiological arousal. Catecholamines are one kind of factors affecting PTSD, adrenalin in particular influences arousal, pulse and blood pressure but also the encoding of fear memories and the response to such.[106–108]

In general, norepinephrine is associated with memory consolidation as well as extinction. Investigations into the mechanisms, in which these processes proceed, are currently ongoing, where the mitogen-activated protein kinase (MAPK) and Janus kinases (JAKs), Signaling Transducer and Activator of Transcription proteins (JAK/STAT) pathways, among others, may be included. Propranolol as a ß-blocker with the ability to cross the blood brain barrier poses as a potent medication for PTSD. It supposedly prevents memory reconsolidation, meaning a continuous erasure of the memory during reactivation, or it might also enhance extinction learning.[109,110]

Propranolol stays, despite a not yet fully understood mode of action, an interesting and effective substance against PTSD and keeps further room for investigations.

1.4.3. Application in molecular imprinting

Propranolol serves as a well-suited substrate for research in molecular imprinting, since, despite its relatively small size, it is chiral and enables different methods of functionalization either by hydrogen bonds, pi-stacking or hydrophobic interactions, and, due to its well-established use in different fields of medicine and biochemistry, it also serves a practical use as mentioned in detail above. Therefore, in means of research regarding new molecularly imprinted polymers, propranolol presents itself as a valuable template for simplicity, comparability, and practical applicability.

2. Experimental

2.1. Materials and characterization

The chemicals were purchased from different commercial providers. Anhydrous dichloromethane and potassium dihydrogen phosphate were purchased from Alfa Aesar, propranolol as a racemic mixture from Fluorochem, triethylamine and ethanol were purchased from Merck and N-(tert-butoxycarbonyl)glycine (Boc-Gly-OH) from Novabiochem. Lithium bromide, $LiN[Si(CH_3)_3]_2$, phosphorus trichloride, sulfuryl chloride, triphenyl phosphine dichloride, 4-diphenylphosphanyl benzoic acid-2-(trimethylsilyl) ethyl ester, hexachloroethane, trimethylolpropane tris(3-mercaptopropionate), pentaerythritol tetrakis (3-mercaptopropionate), pentaerythritol tetraacrylate, 2,2-dimethoxy-2-phenylacetophenone (DMPA), chloroform-d and potassium carbonate were purchased from Sigma Aldrich and allyl bromide from Aldrich. Trifluoracetic acid and adipic acid divinyl ester were purchased from TCI and diethyl ether, dichloromethane, dimethylformamide, tetrahydrofuran, chloroform, toluene, methanol, magnesium sulfate, sodium chloride, DMSO-d6 as well as HPLC grade methanol, acetonitrile and *ortho*-phosphoric acid from VWR. Jeffamine-1000 was received from Huntsman.

Et_3N was distilled and stored over molecular sieves. PCl_5 was sublimated and stored in the glove box.

All NMR experiments were measured on a Bruker® Advance 300 spectrometer. ^1H NMR spectra were recorded at 300 MHz and $^{31}P\{^1H\}$ NMR spectra at 121 MHz, the shifts of the proton spectra were referenced to residual solvent signals. FT-IR spectroscopy was performed on a Perkin Elmer Spectrum 100 FTIR spectrometer.

HPLC measurements were performed on an Agilent RRLC equipped with a Rapid Resolution HD Eclipse Plus C18 column (2.1 mm x 50 mm, particle size 1.8 µm). Dynamic light scattering (DLS) was measured on a Malvern Zetasizer Nano ZSP® in ethanol. A Micromeritics TriStar 3000 was used for BET measurements.

Photochemical reactions were carried in a Rayonet Chamber Reactor, with an UV lamp from Camag centered at 254 nm, in glass vials.

2.2. Synthesis

2.2.1. Monomer synthesis

The monomer $Cl_3PNSi(CH_3)_3$ was synthesized according to slightly adapted literature procedures.[25] Briefly, $LiN[Si(CH_3)_3]_2$ (25.08 g, 0.15 mol) was dissolved in anhydrous diethylether under Argon (Ar) and cooled to 0°C. PCl_3 (20.58 g, 0.15 mol) was added dropwise over the courses of 15 min and stirred at 0 °C for 1 h. Afterwards, SO_2Cl_2 (20.23 g, 0.15 mol) was added dropwise and stirred again for 1 h at 0 °C.

The reaction mixture was allowed to warm to room temperature (r.t.), subsequently filtered through dry Celite, and the solvent was removed under reduced pressure in a water bath at r.t.. Vacuum distillation at 1-5 mbar and 40 °C gave $Cl_3PNSiMe_3$ as a clear and colorless liquid.

Yield: 22.01 g (65 %); ^1H NMR (300 MHz, $CDCl_3$, δ): 0.17 ppm (d, 9H); ^{31}P NMR (121 MHz, $CDCl_3$, δ): -54.56 ppm.

2.2.2. Synthesis of poly(dichloro)phosphazene from $Cl_3PNSi(CH_3)_3$

The synthesis of the polymer, acting as a precursor for post polymerization functionalization, was performed in a glove box at r.t. adapted from the literature.[23,24] Briefly, the phosphine mediator Ph_3PCl_2 (100 mg, 0.29 mol) and the monomer $Cl_3PNSi(CH_3)_3$ (1.6 g, 7.13 mmol) were dissolved separately in ~5 mL CH_2Cl_2. Subsequently, the Ph_3PCl_2 solution was added dropwise to the monomer solution and stirred overnight. The resulting polymer was used without further purification for the macrosubstitution.

Yield: quantitative; ^{31}P NMR (121 MHz, $CDCl_3$, δ): -18.17 ppm, 20.02 ppm.

2.2.3. Synthesis of poly(dichloro)phosphazenes from $LiN[Si(CH_3)_3]_2$ by a one pot approach

The synthesis of the polymer starting from $LiN[Si(CH_3)_3]_2$ without a monomer interim stage was performed according to literature.[26] $LiN[Si(CH_3)_3]_2$ (1.67 g, 10 mmol) and PCl_5 (0.104 g, 0.5 mmol) were weighed in the glove box, sealed with a septum and transferred out. In the fume hood, $LiN[Si(CH_3)_3]_2$ and PCl_5, both under Ar, were dissolved separately in 40 mL and 10 mL anhydrous toluene, respectively. The $LiN[Si(CH_3)_3]_2$ solution was cooled to 0 °C in an ice bath, PCl_3 (1.37 g, 10 mmol) was added dropwise via a syringe over the course of 10 min and stirred for 30 min starting from the first drop of PCl_3 at 0 °C, followed by stirring at r.t. for 1 h. Next, the solution was cooled again to 0 °C and SO_2Cl_2 (1.35 g, 1 mmol) was added via a syringe over the course of 10 min followed by stirring for 1 h at 0 °C starting from the first drop SO_2Cl_2. Finally, the PCl_5 solution was added to the reaction mixture at r.t. and stirred overnight.

Yield: quantitative; ^{31}P NMR (121 MHz, $CDCl_3$, δ): -18.19 ppm, 20.04 ppm.

A phosphine mediated one pot synthesis was developed adapting previously described methods.[23,111] To begin with, the phosphine mediator 4-diphenylphosphanyl benzoic acid-2-(trimethylsilyl) ethyl ester (TMSE-triphenylphosphine) was chlorinated with hexachloroethane (C_2Cl_6). In the glove box, C_2Cl_6 (0.065 g, 0.275 mmol) was dissolved in 0.5 mL CH_2Cl_2, mixed with TMSE-triphenylphosphine (0.5 ml of 0.5 M in THF, 0.102 g, 0.25 mmol) and stirred at r.t. over the course of 72 h. $LiN[Si(CH_3)_3]_2$ (1.67 g, 0.01 mol) was then weighed in the glove box at r.t., dissolved in 40 mL anhydrous CH_2Cl_2, sealed with a septum and transferred out alongside the chlorinated TMSE-triphenylphosphine. As described above, PCl_3 (1.37 g, 0.01 mol) was added dropwise via a syringe over the course of 10 min at 0 °C followed by stirring at 0 °C for 30 min and at r.t. for 1 h. Subsequently, SO_2Cl_2 (1.35 g, 0.001 mol) was added at 0 °C over the course of 10 min via a syringe and stirred for 1 h at 0 °C. Finally, the solution of the chlorinated TMSE-triphenylphosphine mediator was added to the reaction mixture which was then stirred at r.t. overnight.

Yield: quantitatively; ^{31}P NMR (121 MHz, $CDCl_3$, δ): -18.17 ppm.

The work up of both procedures was carried out in identical fashion by filtering the reaction mixture through Celite (dried at 110 °C for >48 h prior to use) and rinsed twice with 10 mL toluene, after which the solution was evaporated to dryness. However, the filtering step may be omitted to increase the overall yield without observed loss of purity in the NMR, as was proven in a different experiment and can, therefore, be employed here. The polymer was taken without any intermediate steps for macrosubstitution.

2.2.4. Synthesis and deprotection of Boc-glycine allyl ester

The macrosubstituent was prepared according to the literature with slight modifications.[12,112] Boc-Gly-OH (9.00 g, 51.38 mmol) and K_2CO_3 (7.10 g, 51.38 mmol) were dissolved in 120 mL dimethylformamide (DMF) and the resulting suspension of K_2CO_3 cooled to 0 °C. Allyl bromide (6.22 g, 51.38 mmol) was added under stirring, the mixture was allowed to warm up to r.t. and was stirred overnight. DMF was removed at reduced pressure at a water bath temperature of 55 °C, the residue was dissolved in ethyl acetate, washed three and four times with H_2O and brine, respectively, and dried over $MgSO_4$. The solvent was removed under reduced pressure, and the Boc-glycine allyl ester was obtained as a slightly yellow viscous liquid.

Yield: 9.05 g (82%); ^{1}H NMR (300 MHz, $CDCl_3$, δ): 1.42 ppm (s, 9H), 3.90 ppm (d, 2H), 4.61 ppm (d, 2H), 5.12 ppm (br, 1H), 5.21-5.33 ppm (m, 2H), 5.82-5.95 ppm (m, 1H).

For the deprotection of the amino group, the Boc-glycine allyl ester was dissolved in a 2:1 mixture of CH_2Cl_2 and trifluoroacetic acid (TFA) and stirred for 1.5 h. The solvent was evaporated under reduced pressure and 100 mL toluene was repeatedly added to the glycine allyl ester (allyl-Gly) to remove residual CF_3COOH. The toluene was each time evaporated under reduced pressure until fine white crystals were obtained.

Yield: quantitative; ^{1}H NMR (300 MHz, DMSO-d_6, δ): 3.87 ppm (s, 2.1H), 4.68 ppm (d, 2.1H), 5.23-5.40 ppm (m, 2H), 5.87-5.97 ppm (m, 1H), 8.5 ppm (s, 3H).

2.2.5. Synthesis of poly(organo)phosphazene

The macrosubstitution was adapted from the literature and was performed slightly different for the one pot synthesis than for the poly(dichloro)phosphazenes synthesized from $Cl_3PNSi(CH_3)_3$.[12] Briefly, for the poly(dichloro)phosphazenes synthesized from $Cl_3PNSi(CH_3)_3$ and 100 mg phosphine mediator Ph_3PCl_2, Boc-glycine allyl ester (3.84 g, 0.0178 mol) was deprotected with a 2:1 (12:6 mL) mixture of CH_2Cl_2:TFA, as described. The deprotected macrosubstituent was transferred into the glove box and gradually dissolved in tetrahydrofuran (THF). Et_3N (2.5 mL, 0.0178 mol) was added in a twofold excess to avoid the formation of polytetrahydrofuran, and the poly(dichloro)phosphazene dissolved in CH_2Cl_2 was added dropwise under stirring. Additional THF was added when necessary to gain a cloudy, low viscous solution instead of a pasty one and the reaction was stirred in the glove box at r.t. for 24 h.

For the One-Pot approach, the macrosubstitution was performed the same for both synthesis pathways. Boc-glycine allyl ester (5.38 g, 0.025 mol) was deprotected in a 2:1 (20:10 mL) mixture of CH_2Cl_2:TFA, as described, K_2CO_3 (1.38 g, 0.010 mol) was added to the dried glycine allyl ester to prevent formation of polytetrahydrofuran, and transferred into the glove box along with the poly(dichloro)phosphazene. The mixture was suspended in THF, and Et_3N (3.5 mL, 0.025 mol) was added in excess. The poly(dichloro)phosphazene was dissolved in little CH_2Cl_2 (~5 mL) and the solution was added dropwise to the allyl-glycinate. Additional THF was added when necessary to gain a cloudy, low viscous solution, and the reaction was stirred in the glove box at r.t. for 24 h.

In general, the poly(organo)phosphazene solution was transferred out of the glove box and filtered through filter paper, THF was evaporated and the polymer subsequently re-dissolved in ethanol. The poly(organo)phosphazene was purified by dialysis over 24 h, with 30 min against water and the remaining time against EtOH.

Yield:

Synthesized via 2.2.2. : 1.17 g (60%); ^{1}H NMR (300 MHz, CDCl$_3$, δ): 3.76 ppm (br, 85H), 4.55 ppm (s, 86H), 5.17-5.31 ppm (m, 80H), 5.85-5.89 ppm (m, 40H), 7.50-7.67 ppm (m, 15H), (2:2:2:1); ^{31}P NMR (121 MHz, CDCl$_3$, δ): -9.98 ppm, 2.14 ppm, 14.53 ppm.

Synthesized via 2.2.3. : 0.80 g (29%); ^{1}H NMR (300 MHz, CDCl$_3$, δ): 3.73 ppm (br, 2H), 4.53 ppm (s, 2H), 5.13-5.28 ppm (m, 2H), 5.81-5.90 ppm (m, 1H);
^{31}P NMR (121 MHz, CDCl$_3$, δ): -9.08 ppm, 1.60 ppm, 8.70-10.52 ppm,14.37 ppm.

Synthesized via 2.2.3. and TMSE-phosphine mediator: 1.98 g (72%) (NB. The yield was achieved by omitting the filtration step between the poly(dichloro)phosphazene synthesis and the macrosubstitution);
^{1}H NMR (300 MHz, CDCl$_3$, δ): 0.08 ppm (s, 9H), 3.73 ppm (br, 124H), 4.54 ppm (br, 132H), 5.15-5.30 ppm (m, 134H), 5.83-5.92 ppm (m, 61H), (2:2:2:1);
^{31}P NMR (121 MHz, CDCl$_3$, δ): -9.56 ppm, 1.60 ppm, 8.62-12.09 ppm, 14.32 ppm.

2.2.6. Functionalization of poly(organo)phosphazene

The functionalization of the poly(organo)phosphazene polymer was performed by a simple "click-reaction" followed by the cross-linking and imprinting described in chapter 2.3. in a one vial reaction.[82,83,113] The mass percentages of the polymer and the cross-linkers were calculated to achieve a 1:1 ratio of double bond-functionalities and thiol-functionalities. The corresponding amounts were calculated to synthesize a 500 mg pellet. From the necessary amount of polymer, the needed mass of the allyl-Gly substituted poly(organo)phosphazene was calculated. The different methods are summarized in Table 4.

Table 4: Summary of methods to functionalize and cross-link the polymer during the imprinting process.

Method 1		wt%	mass / mg
	poly(organo)phosphazene		41.13
	TGA-PPz	11	55
	adipic acid divinyl ester	34	170
	trimethylpropane tris(3-mercaptopropionate)	55	275
	DMPA	1	5
Method 2	poly(organo)phosphazene		52.35
	TGA-PPz	14	70
	pentaerythritol tetraacrylate	34	170
	trimethylpropane tris(3-mercaptopropionate)	52	260
	DMPA	1	5
Method 3	poly(organo)phosphazene		41.13
	TGA-PPz	11	55
	adipic acid divinyl ester	39.5	197.5
	pentaerythritol tetrakis(3-mercaptopropionate)	49.5	247.5
	DMPA	1	5
Method 4	poly(organo)phosphazene		41.13
	TGA-PPz	11	55
	pentaerythritol tetraacrylate	37	185
	pentaerythritol tetrakis(3-mercaptopropionate)	52	260
	DMPA	1	5
Method 5	poly(organo)phosphazene		
	TGA-PPz		
	pentaerythritol tetraacrylate	42	210
	pentaerythritol tetrakis(3-mercaptopropionate)	58	290
	DMPA	1	5
Method 6	poly(organo)phosphazene		
	TGA-PPz		
	adipic acid divinyl ester	43	215
	trimethylpropane tris(3-mercaptopropionate)	57	285
	DMPA	1	5

The poly(organo)phosphazene was dissolved in 0.5 mL DMF and mixed with 1 wt% of the photo initiator 2,2-dimethoxy-2-phenylacetophenone (DMPA) and 1 eq. thioglycolic acid (TGA), providing the functional group for the imprinting process resulting in one functional monomer per repeating unit, in a non-UV-reflecting glass vial. Ar was bubbled through the reaction solution for 20 min and the mixture was subsequently exposed to UV light in the UV reactor for 3 h. The TGA-poly(allyl glycine)phosphazene (TGA-PPz) was reacted further according to chapter 2.3. without any intermediate steps.

Yield: quantitative; ^{1}H NMR (300 MHz, DMSO-d_6, δ): 1.85 ppm (br, 2.43H), 2.63 ppm (br, 2.46H), 3.22 ppm (br, 1.74H), 3.51-3.66 ppm (br. m, 4H), 4.09 ppm (br, 2.78H),4.54 ppm (br, 1.93H), 5.17-5.31 ppm (m, 1.73H), 5.88 ppm (br, 0.85H);
^{31}P NMR (121 MHz, DMSO, δ): -10.48 ppm, 0.66 ppm, 1.34 ppm, 3.79 ppm, 10.79 ppm, 13.91 ppm.

2.2.7. Deprotonation of propranolol hydrochloride

Propranolol was purchased as the racemic hydrochloride and was basified according to an adapted literature procedure.[114] Briefly, propranolol HCl (0.5 g, 1.69 mmol) was dissolved in 20 mL distilled water and extracted three times with each 10 mL CH_2Cl_2. The organic phase was dried over $MgSO_4$, the dichloromethane solution was evaporated, and the obtained propranolol was dried and stored in the fridge at 4 °C.

Yield: 0.32g (74.23%); ^{1}H NMR (300 MHz, MeOD, δ): 1.14 ppm (dd, 6H), 2.8 ppm (dd, 1H), 2.9 ppm (qin, 1H), 3 ppm (dd, 1H), 4.16-4.17 ppm (m, 2H), 4.20-4.28 ppm (m, 1H) 6.91-6.94 ppm (m, 1H), 7.35-7.51 ppm (m, 4.1H), 7.79-7.82 ppm (m, 1H), 8.28-8.32 ppm (m, 1H);

2.3. Molecular imprinting of propranolol

The imprinting process was adapted from the literature[12,83,113–118] in accordance with the requirements and properties of polyphosphazenes as the polymer backbone.

The TGA-PPz synthesized in chapter 2.2.6. was mixed with two cross-linkers, as described in Table 4, and additional 1 wt% DMPA was added. The solution was mixed with propranolol as the template in a 1:3 ratio corresponding to the functional monomer to synthesize the MIP, this step was omitted for the synthesis of the non-imprinted polymers serving as the control. According to Table 5, chloroform, toluene and/or salt were added as additional porogens. Afterwards, the reaction mixture was exposed to UV light in the UV reactor for 3 h, the pellet in the vial was washed top-down in a water filled beaker overnight and the pellet was subsequently obtained upon destruction of the glass vial. Finally, the pellet was dried on air overnight and stored under argon until further used.

Table 5: Summary of different methods for MIP/NIP pair synthesis.

MIP/NIP pair	Method	Crosslinker		PPz	Salt	Porogenous solvent
1	1	adipic acid divinyl ester	trimethylpropane tris(3-mercaptopropionate)	Yes	No	No
2	1	adipic acid divinyl ester	trimethylpropane tris(3-mercaptopropionate)	Yes	Yes	No
3	1	adipic acid divinyl ester	trimethylpropane tris(3-mercaptopropionate)	Yes	No	chloroform
4	1	adipic acid divinyl ester	trimethylpropane tris(3-mercaptopropionate)	Yes	Yes	chloroform
5	1	adipic acid divinyl ester	trimethylpropane tris(3-mercaptopropionate)	Yes	No	toluene
6	1	adipic acid divinyl ester	trimethylpropane tris(3-mercaptopropionate)	Yes	Yes	toluene
7	2	pentaerythritol tetraacrylate	trimethylpropane tris(3-mercaptopropionate)	Yes	No	No
8	2	pentaerythritol tetraacrylate	trimethylpropane tris(3-mercaptopropionate)	Yes	Yes	No
9	3	adipic acid divinyl ester	pentaerythritol tetrakis(3-mercaptopropionate)	Yes	No	No
10	3	adipic acid divinyl ester	pentaerythritol tetrakis(3-mercaptopropionate)	Yes	Yes	No
11	4	pentaerythritol tetraacrylate	pentaerythritol tetrakis(3-mercaptopropionate)	Yes	No	No
12	4	pentaerythritol tetraacrylate	pentaerythritol tetrakis(3-mercaptopropionate)	Yes	Yes	No
13	5	pentaerythritol tetraacrylate	pentaerythritol tetrakis(3-mercaptopropionate)	No	No	No
14	6	adipic acid divinyl ester	trimethylpropane tris(3-mercaptopropionate)	No	No	No

2.4. Rebinding assay

The propranolol used as template was removed from the dried pellets by a Soxhlet extraction with methanol for 24 h and again dried in the open air and stored under argon. To test the effectivity of the imprinting process, a rebinding assay was performed. For this purpose, a 2 mg/mL propranolol solution in methanol was prepared and the pellets were incubated on a shaking plate for 48 h each in 10 mL resulting in 20 mg propranolol per pellet, equaling 200% of the imprinted amount. The rebinding solution was filtered off through a filter paper, evaporated, and the remaining propranolol was resuspended in the mobile phase, as described in Table 6, for subsequent quantification by HPLC measurement.

2.5. HPLC analysis

The quantification of propranolol was adapted from the literature[119,120] to fit the available instrument and column specifications and was optimized according to the requirements. The method is summarized in Table 6. The propranolol resuspended in the mobile phase was filtered through a nylon filter into a HPLC-vial and injected subsequently for each MIP/NIP pair to correct for any accumulating systematic errors. Furthermore, regular washing steps were used to avoid any propranolol carryover between vials. Every measurement was performed in triplets. For quantification, a calibration curve of pure propranolol in the mobile phase was used.

Table 6: HPLC method for propranolol quantification.

Mobile Phase:	80% 20 mM KH_2PO_4 (pH 3)
	20% MeOH/ACN (1:1)
Column:	Rapid Resolution HD Eclipse Plus C18; 2.1 mm x 50 mm, particle size 1.8 μm
Flow:	0.3 ml/min
Injection Volume:	1 μl
Column Temperature:	25°C
Detection:	UV at 266nm

2.6. Degradation study

The degradation study was performed on three MIP/NIP pairs as representatives of the differently synthesized pellets. MIP/NIP pairs synthesized with adipic acid divinyl ester and trimethylpropane tris(3-mercaptopropionate) were used, according to pair 1 and 2. One pair was synthesized with salt as an additional porogen, pair 2, the second one was without any additional porogen, pair 1, and the third one was also synthesized without additional porogen and solely used for the degradation study without a previous rebinding assay, fresh pair 1.

The degradation study was performed analogue to the literature with slight adaptions.[12]

The pellets were cut in pieces of 20 mg and of approximate equal size and incubated at 37 °C in 2 mL of pure MilliQ water for one series (pH 7) and in MilliQ with pH 2, adjusted with 1N HCl, for a second series. The progress of degradation was analyzed after regular time intervals over 4 months for pure MilliQ water and 2 months for MilliQ water at pH 2. The samples were filtered through pre-weighed sintered glass crucibles and dried in a vacuum drying oven up to 80 °C and the mass loss was determined gravimetrically.

3. Results and discussion

3.1. Poly(organo)phosphazene synthesis

3.1.1. Substituent selection and synthesis

To allow for a proper imprint, as well as a rebinding, and still enable an observable degradation of the polymer in an appropriate time interval, a glycine substituent was chosen based on the outcomes of the research by Wilfert et al. on different spacers.[29] Since thiol-ene chemistry was chosen as method for functionalization and cross-linking, glycine was reacted with allyl-bromide to obtain the necessary double bond functionality for further syntheses. To specifically allow reaction of the N-terminus of the amino acid with the polymer backbone and functionalization of the C-terminus with the double bond entity, commercially available N-(tert-butoxycarbonyl)glycine (Boc-Gly-OH) was used, and the Boc-glycine allyl ester was deprotected immediately before the macrosubstitution onto the poly(dichloro)phosphazene.

The synthesis of the ester itself was scaled up 1.5 times from around 6 g of the starting material Boc-Gly-OH up to 9 g, and the purification procedure was adapted to preserve purity. This was carried out to allow a more efficient production of the substituent, and was only limited by the purification method, which comprised several washing steps in a separatory funnel, and therefore, was limited by available volume of the funnel and adequate solvent amounts. A decrease in yield was not observed, instead it could be increased in the end. Nevertheless, this may be accounted to increased skill in the synthesis of the glycine allyl ester over time, since the scale up was tackled at the beginning of the work on this subject. All in all, the yield of around 80% was satisfactory, even with no suitable comparison to a smaller synthesis approach.

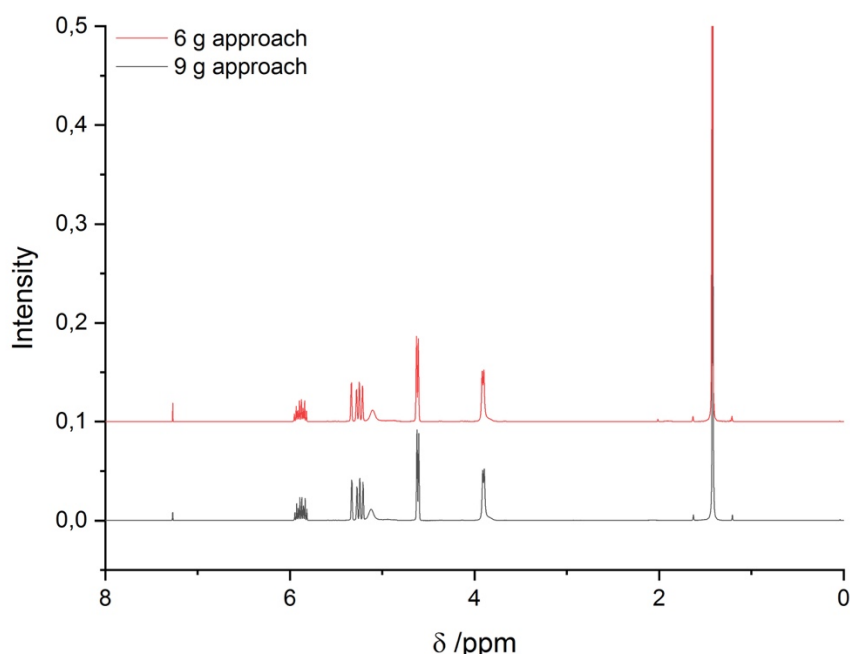Proton NMR measurements of both approaches are compared in Figure 13 and show no difference in quality.

Figure 13: Comparison of ^{1}H NMR spectra of Boc-glycine allyl ester before and after scale up.

3.1.2. Synthesis methods of polyphosphazenes

For the synthesis of the polyphosphazenes providing the backbone for the molecular imprinting a separate synthesis of the monomer, with storage in the glove box for later polymerization, was used. This approach allows a distinct control of the chain length by an exact monomer:initiator ratio, achieving polymers with a very low polydispersity up to a chain length of 50 repeating units. Although, for the scale of monomer synthesis feasible with this method, several small-scale experiments can be performed with one batch of monomer, large-scale experiments are hampered, especially due to the purification of the monomer via vacuum-distillation and, overall, the sensitive synthesis of the monomer.[2]

To allow scale up and a simpler way towards obtaining polyphosphazenes, and in this, an easier and faster way towards molecular imprinting, a one pot approach, circumventing an isolation of the monomer and directly polymerizing $Cl_3PNSi(CH_3)_3$ to poly(dichloro)phosphazene via a multi-step synthesis according to Wang,[26] was performed. This approach promises still reasonable, yet increased, polydispersities and higher molecular weights, another limitation for the approach with an isolated and purified monomer. Nevertheless, the polydispersity increases further as the molecular weight increases. In addition, the certainty in assumed chain length was diminished due to no direct influence on the monomer:initiator ratio and dependence on presumed quantitative reactions towards the monomer. Although, for the application of molecular imprinting these drawbacks posed no significant disadvantage, time restrictions hindered the adaption of the one pot approach for molecular imprinting and polyphosphazenes synthesized from a distinct monomer were used in the end. Still, the method itself was further improved over the course of this thesis in parallel to the molecular imprinting experiments.

The synthesized polymers are of the same quality as the polyphosphazenes produced from separately synthesized monomer according to their ^{1}H and ^{31}P NMR spectra. ^{31}P NMR spectra of the poly(dichloro)phosphazenes are compared, top graph in Figure 14, and both show the characteristic sharp peak at around -18 ppm. Regarding the macrosubstituted poly(allyl glycine)phosphazene, on the bottom left graph in Figure 14, a slight difference of the peak shape can be seen in the ^{31}P NMR spectra of the two methods, with a sharper peak for the one pot approach, indicating a polymer with higher purity, whereas a broader peak hints at a certain onset of degradation. Nevertheless, both peaks, again with a characteristic signal at around 0 ppm, are a proof of a successful macrosubstitution. Subsequent experiments suggest however, an increase in reaction time to avoid a small peak at around -10 ppm, stemming from incompletely substituted Cl-atoms. The ^{1}H NMR spectra of the polymerization from a separately synthesized monomer, on the bottom right in Figure 14, is dominated by the distinct solvent peak of chloroform at 7.26 ppm, and therefore, also the intensities of the normalized proton signals differ between the two methods. Still, the signals of the two methods overlap, and the ratios between the signals in each spectrum are identical. In conclusion, all three spectra comparisons are

evidence of a successful synthesis of poly(organo)phosphazene via the one pot synthesis, analogous to Wang,[26] with comparable qualities to polymers synthesized from separately polymerized monomer,
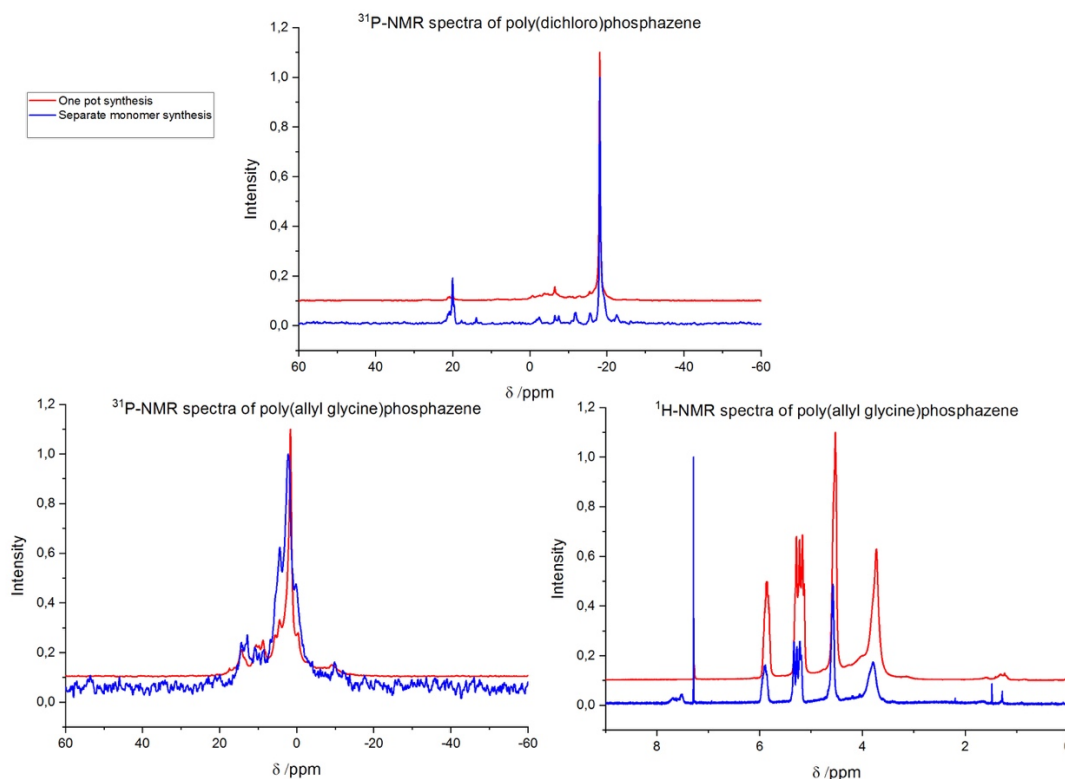

Figure 14: NMR spectra comparison of polymers synthesized via the one pot synthesis and separately synthesized monomer.

Yields of the poly(dichloro)phosphazene synthesis are assumed to be quantitative and following macrosubstitution an overall yield of 29% has been achieved, lower than the yield of poly(organo)phosphazenes stemming from a separately synthesized monomer with an overall yield of 39%, 65% for the monomer synthesis and 60% for the macrosubstitution. What should be noted again, is the problematic synthesis of the monomer, for which an exceptional high yield of 65% was accomplished for this thesis, which is most often not reached.

Analysis of the polymers synthesized via the one pot process has been carried out via dynamic light scanning (DLS), also, but not only, due to problems during the characterization of the polymers via gel permeation chromatography (GPC), mostly due to the GPC instrumentation. The polymers have been analyzed in EtOH as solvent, due to the insolubility of poly(allyl glycine)phosphazene in water. Additionally to the polymers synthesized via the one pot approach, polymers produced via the phosphine mediated one pot synthesis, as described below, have been analyzed and compared. First, polymers synthesized using the same approach but of different batches have been compared. This was performed for the one pot synthesis as well as for the phosphine mediated one pot synthesis. Then, the different synthesis methods, these are separately synthesized monomer and subsequent polymerization, one pot synthesis, one pot synthesis in CH_2Cl_2 and phosphine mediated one pot synthesis, have been analyzed.

Figure 15: DLS measurements with volume distribution (top) and intensity distribution (bottom) of poly(allyl glycine)phosphazenes synthesized via a one pot approach.

The main peak of the volume distribution of the different batches for the one pot synthesis overlap nicely at around 6 to 8 nm, Figure 15, despite smaller peaks below and above the main peak for the individual measurements. In the intensity distribution, a broader distribution of the peaks along the x-axis can be seen. Furthermore, it is noticeable that some peaks disappear after transformation from the intensity to the volume distribution, indicating that these signals correspond only to a low number of particles. The peak in the range from 100 to 1000 nm for polymer 3 stems, most likely, from aggregation products, indicated by its disappearance during the second run in the volume distribution due to dissociation of the accumulate.

The peaks in the intensity distribution, being the most exact representation, with the highest related content in the volume distribution, meaning the highest number of particles of a certain size, are taken for the determination of the hydrodynamic diameter. This gives a distribution of particle size between 7 to 11 nm for the one pot synthesis.
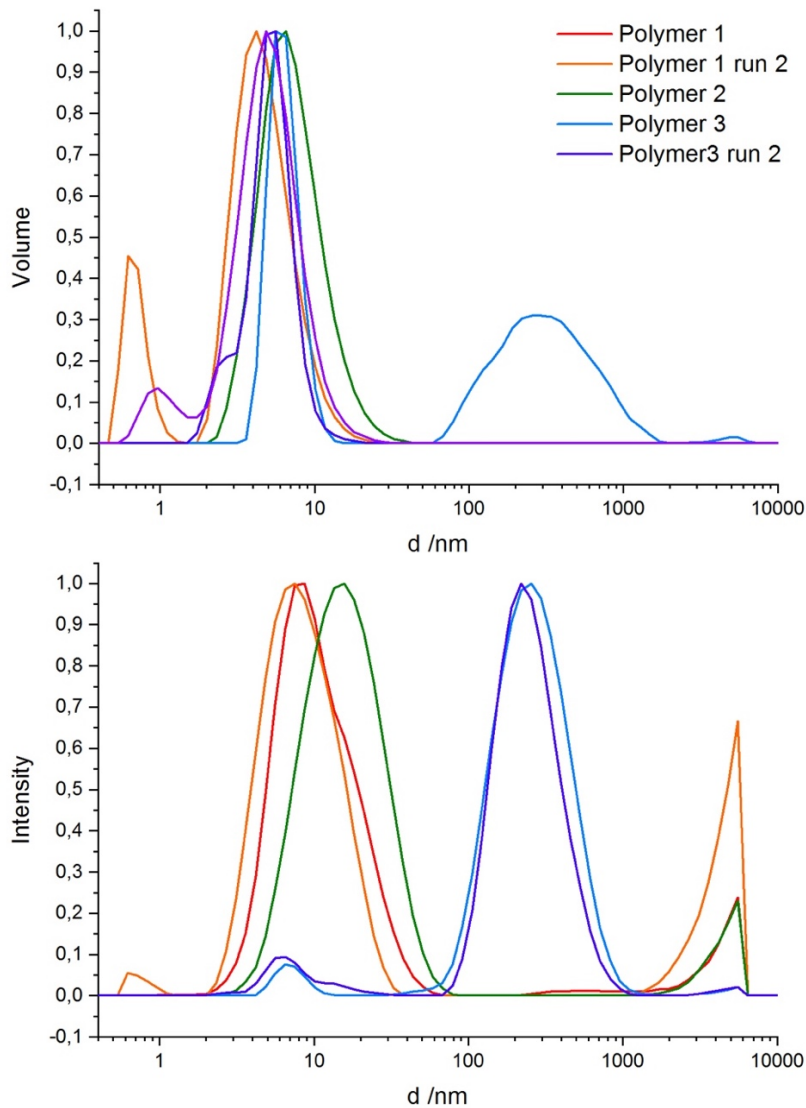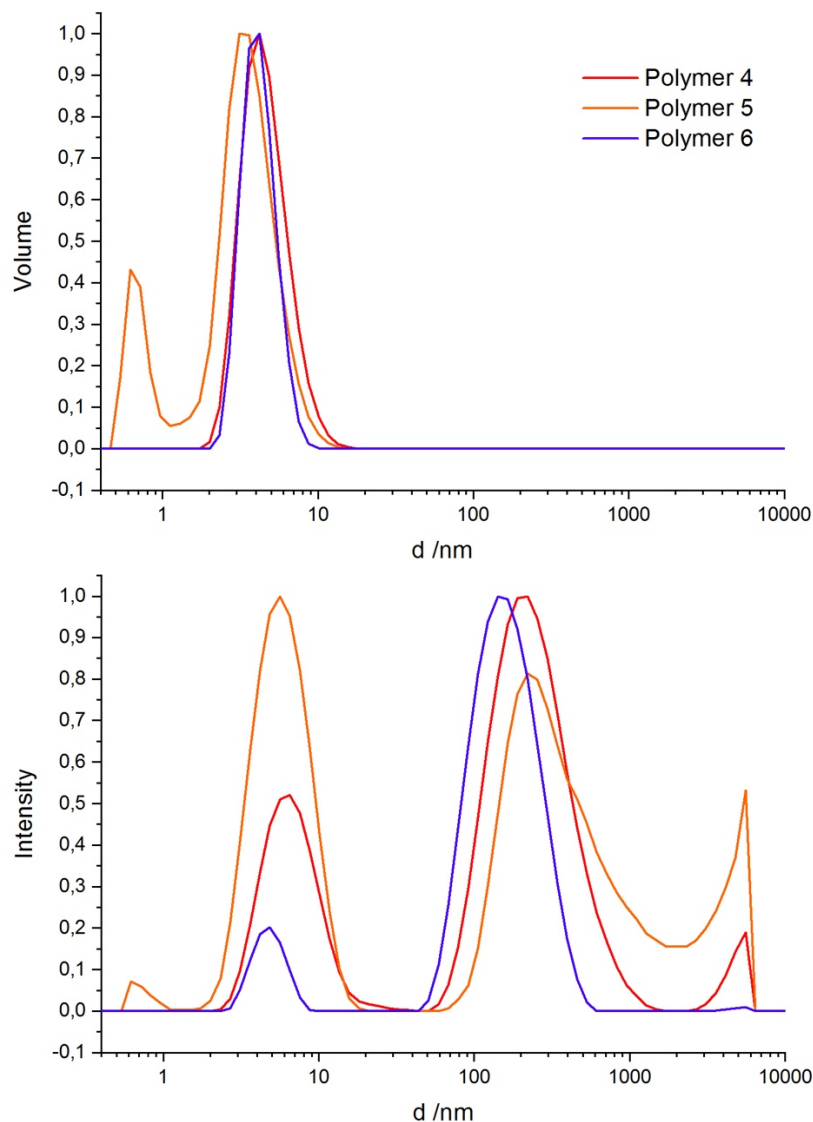
Figure 16: DLS measurements with volume distribution (top) and intensity distribution (bottom) of poly(allyl glycine)phosphazenes synthesized via a phosphine mediated one pot approach.

For the phosphine mediated one pot approach, depicted in Figure 16, the intensity distribution shows an even higher signal for a hydrodynamic diameter of around 200 nm, but again, these peaks disappear upon transformation to the volume distribution, indicating just a small percentage of these large, supposed aggregates in the sample. In the volume distribution, the size of the polymers appears similar again at a diameter of around 4 to 6 nm. For the most exact estimation of the hydrodynamic diameter, the peaks in the intensity distribution with the highest related peak in the volume distribution are taken again. This gives a particles size between 5 to 8 nm for the phosphine mediated one pot approach, lower than for the one pot synthesis without a phosphine mediator.

Whilst the intensity distribution of the different synthesis methods for poly(organo)phosphazenes, depicted at the bottom in Figure 17, shows again a rather diffuse dispersion of the peaks, the volume distribution, in the top graph in Figure 17, gives a clearer picture of the major particle size of the different synthesis approaches. For the one pot synthesis, as well as for the phosphine mediated one pot synthesis, averaged values of the measurements depicted in Figure 15 and Figure 16 are taken, therefore, again the peak for the one pot synthesis in the range from 100 to 1000 nm from polymer 3 can be seen, as described above.

Since a different monomer:initiator ratio has been used for the one pot reactions compared to the separately synthesized monomer, an expected increase in particle size from around 2-3 nm for the polyphosphazenes produced from separately synthesized monomer to a particle size between 5-8 nm for the different one pot approaches can be determined, proving to be of similar size. A clear trend for the different approaches of the one pot synthesis has not been determined, the data indicate a decrease in size from the one pot synthesis to the phosphine mediated one pot, nevertheless, as can be seen in Figure 15 and Figure 16, the particle size between different batches of the same synthesis method also vary slightly, not allowing an unambiguous statement.
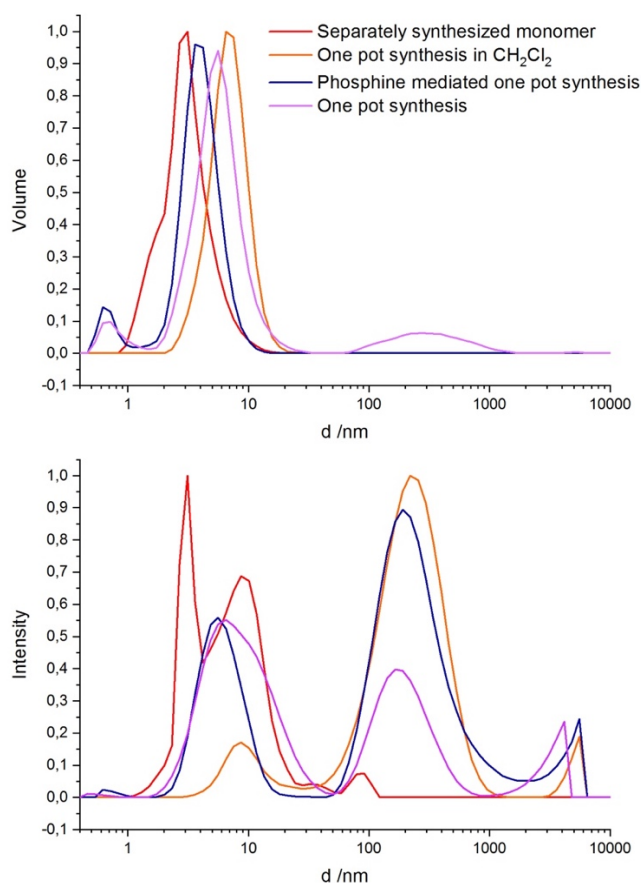

Figure 17: Comparison of DLS data, volume distribution (top) and intensity distribution (bottom), between the different synthesis methods for poly(organo)phosphazenes.

Nonetheless, the one pot synthesis is more straight forward than the procedure with isolated monomer and produced polymers were of satisfactory quality for the applications described in this thesis.

The problems mentioned for the characterization of the polymer synthesized via the one pot synthesis have called for a simpler and more reliable way to determine the number of repeating units per polymer chain, characterizing the polymer sufficiently for the purpose presented in this thesis. The use of commercially available tertiary phosphines, an already established method[23] and described in chapter 1.1.2.2. , utilized for the method of a separately synthesized monomer and subsequent polymerization, can be applied. This allows for a straight forward determination of the average number of repeat units via the ratio of substituent proton signals to the proton signal stemming from the end-group.

For the monomer synthesis, non-polar solvents are used, such as diethyl ether or toluene, as are for the one-pot synthesis,[25,26] whereas for tertiary phosphines a polar solvent is necessary to yield their ionized form $[R_3PCl]^+Cl$,[22] complicating the adaption of the method of utilizing tertiary phosphines. Thus, the one-pot synthesis itself was performed in CH_2Cl_2 first, to proof its practicability in polar solvents.

The change in solvent for the one pot synthesis has no detectable influence on the method according to its NMR spectra, as becomes apparent from the graphs in Figure 18.

The ^{31}P NMR spectra of the poly(dichloro)phosphazenes, depicted in the top graph in Figure 18, shows no difference, with the identical characteristic peak in both spectra. This persists for the signal of the ^{31}P NMR spectra of the poly(allyl glycine)phosphazene at the bottom left corner in Figure 18, showing a sharp, characteristic peak at around 0 ppm. An overlap of the signals in the ^{1}H NMR spectra can be seen at the bottom right, again the ratios between the signals in each spectrum are the same.

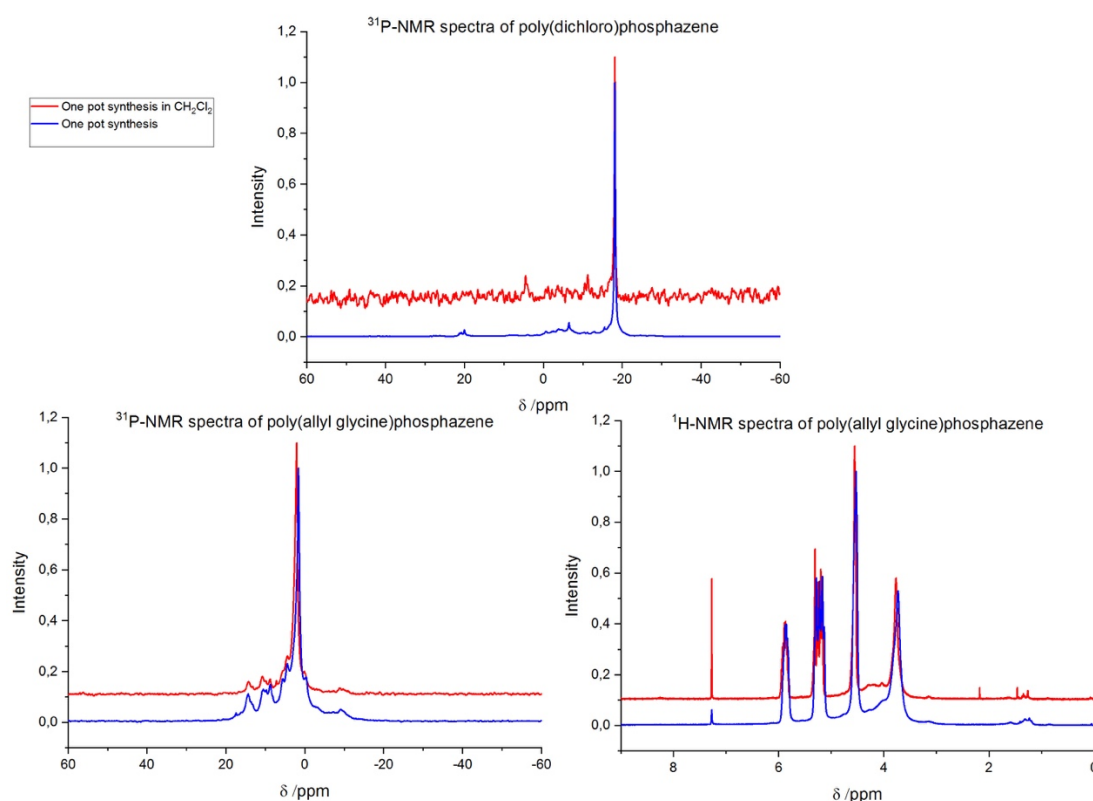
Figure 18: Comparison of NMR spectra of polymers synthesized via the one pot approach and the one pot synthesis in CH_2Cl_2.

Since the results have shown a proof of concept, the one-pot synthesis has been further adapted towards the phosphine mediated one-pot synthesis, as described in the second half of chapter 2.2.3.

Again, NMR analysis was used to compare the quality of the polymer with the one pot synthesis, Figure 19. Despite an increased noise for the phosphine mediated one pot synthesis, the ^{31}P NMR spectra of poly(dichloro)phosphazene, depicted in the top graph, show the usual characteristic peak at -18 ppm. Furthermore, the signal for the poly(allyl glycine)phosphazene at around 0 ppm, shown in the bottom left graph in Figure 19, is evidence of a successful macrosubstitution for the phosphine mediated one pot synthesis. Finally, comparing the ^{1}H NMR spectra, which can be seen at the bottom right corner in Figure 19, the great advantage of the phosphine mediation can be seen at one glance, with the peak of the end group at 0 ppm for the trimethyl silyl residue of the used phosphine now available for chain length determination.
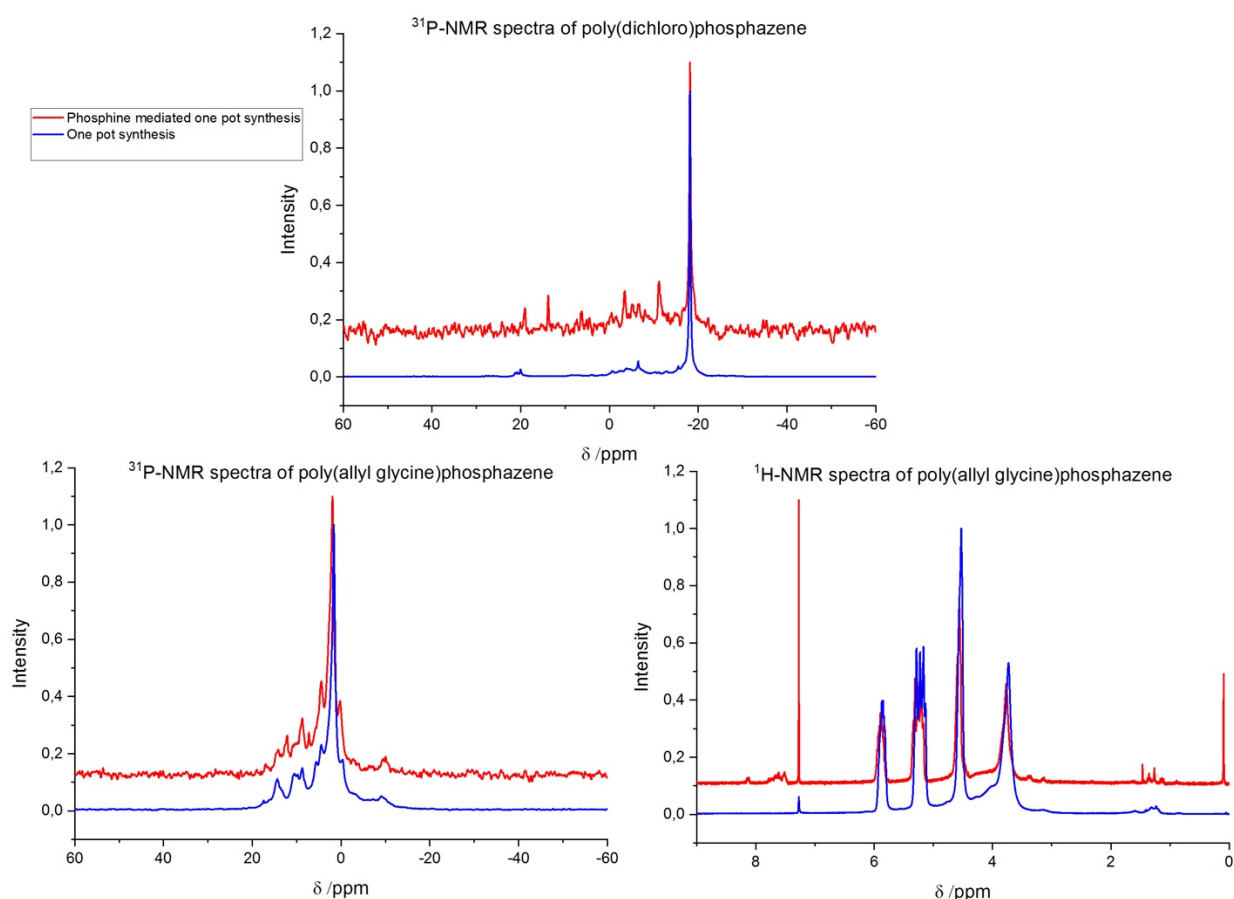

Figure 19: Comparison of NMR spectra of polymers synthesized via a one pot synthesis and a phosphine mediated one pot synthesis.

Highlighting this advantage, a ^{1}H NMR spectrum of both the phosphine mediated one pot synthesis, on the top, as well as of a polyphosphazene produced from a separately synthesized monomer, on the bottom, can be seen in Figure 20.

Integrating the signals from the substituent and the end group and assigning correct values for either one of them, allows the simple calculation of the chain length via the ratio of these two.
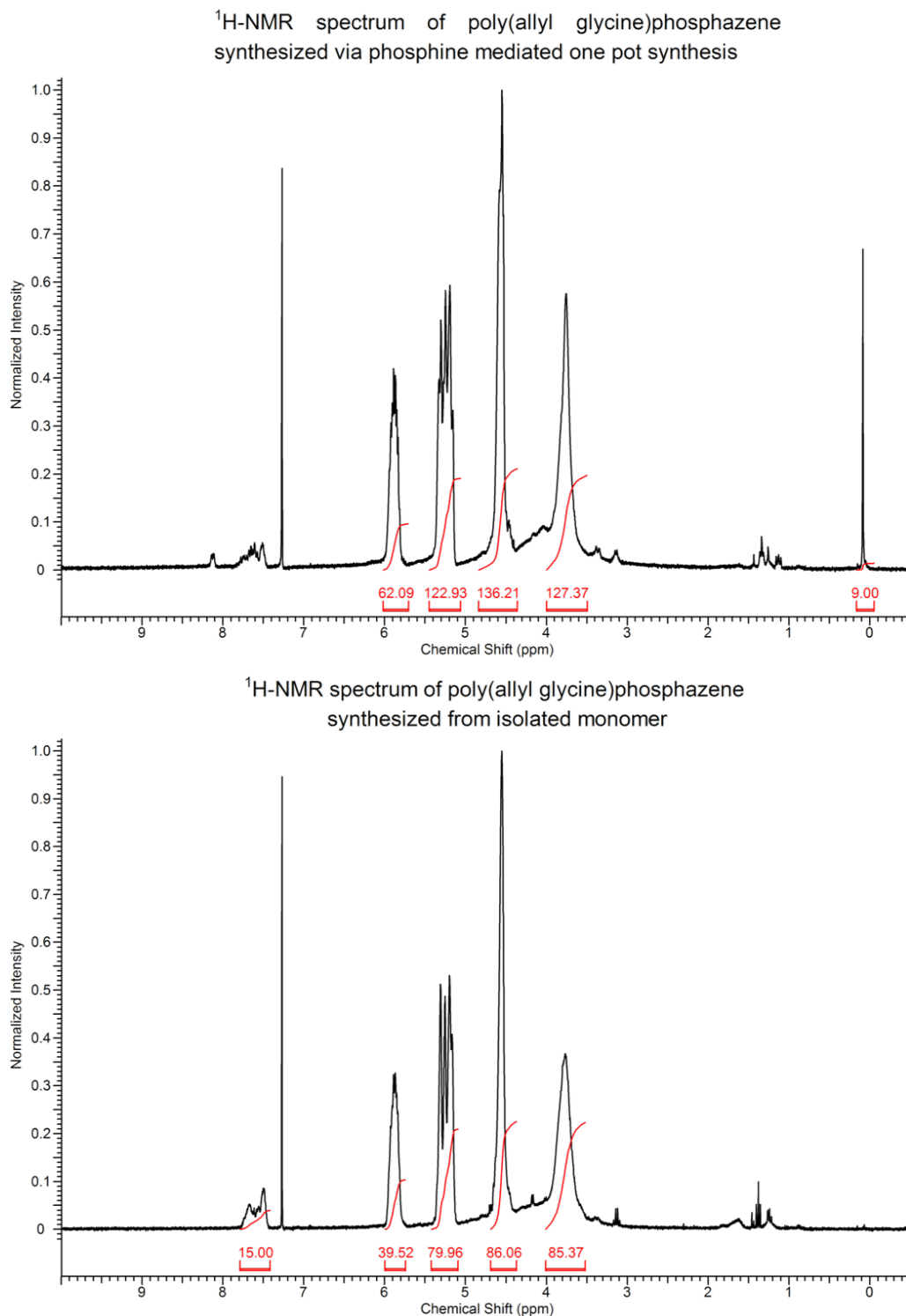

Figure 20: Determination of the chain length of poly(organo)phosphazenes, synthesized by different methods, via ^{1}H NMR spectroscopy and the ratios between substituent and end group proton signals.
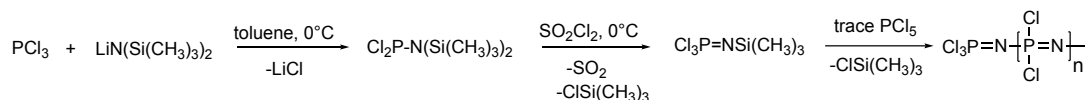
For the phosphine mediated one pot synthesis, an average chain length of 31 repeat units can be determined. When setting the integral for the signal of the trimethylsilyl group to its correct value of 9 protons, an integral of 62 for the signal around 6 ppm, corresponding to one proton of the substituent, and two substituents per repeat unit give a ratio 31:9 and hence a chain length of 31 repeat units. In the same fashion, a chain length of 20 repeat units can be derived for the polyphosphazene synthesized from the isolated monomer, again two substituents per repeat unit result in a ratio of 20:15 for a triphenylphosphine mediator with a correct integral of 15.

A schematic summary of the different synthesis approaches is depicted in Figure 21.

Monomer synthesis with subsequent polymerization to [NPCl₂]ₙ:
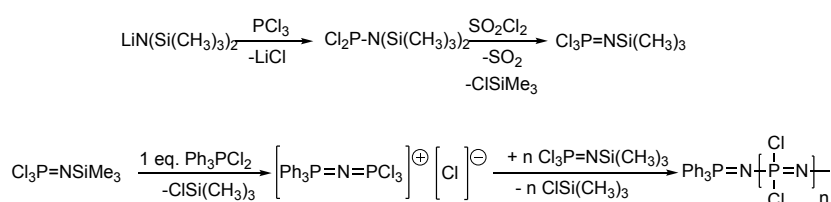
One pot synthesis:

Phosphine mediated one pot synthesis:
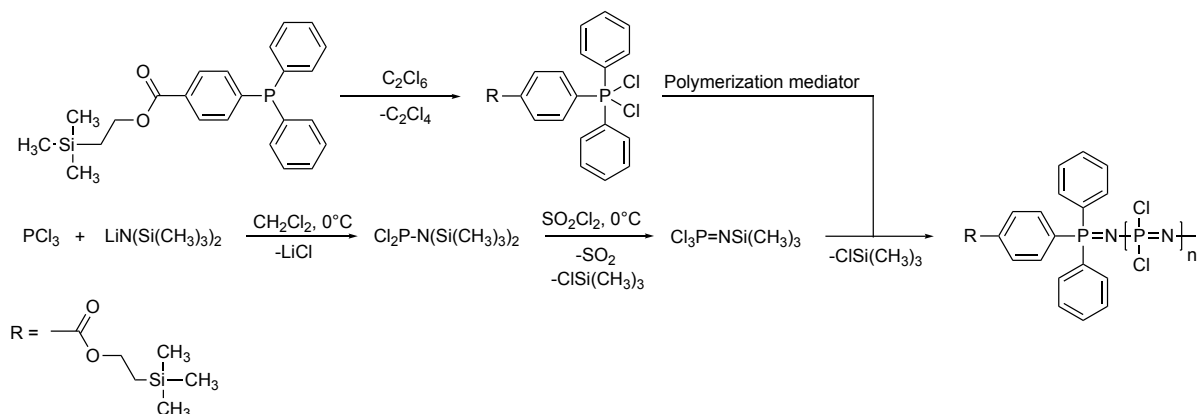
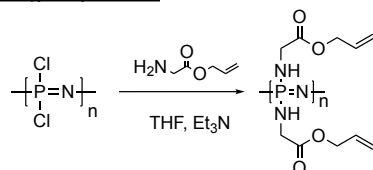**Macrosubstitution of poly(dichloro)phosphazene:**

Figure 21: Schematic summary of the different syntheses approaches for poly(dichloro)phosphazene and the macrosubstitution to poly(organo)phosphazene; n designates the number of repeating units as targeted by the monomer:initiator ratio.

To further improve the yield of the described phosphine mediated one pot synthesis, the method has been further adapted as described at the end in chapter 2.2.3. The filtration step between the poly(dichloro)phosphazene synthesis and the subsequent macrosubstitution was omitted and instead, the solvent from the one pot synthesis was directly removed under reduced pressure and the poly(dichloro)phosphazene was further reacted with the macrosubstituents. Comparison of the ^{1}H NMR as well as the ^{31}P NMR spectra indicate no decrease in quality, depicted in Figure 22. The chain lengths of both polymers deviate only minimal, with approximately 35 and 34 repeat units for the filtered and the non-filtered approach, respectively, and the proton spectra show a successful macrosubstitution, without any adverse effect of the omitted filtration step. The ^{31}P NMR spectra show nearly identical peaks with no sign of an influence of the filtration step on the purity of the polymer or an onset of degradation. Overall, the yield of the method was increased to astounding 79% from 29% for the one pot synthesis.
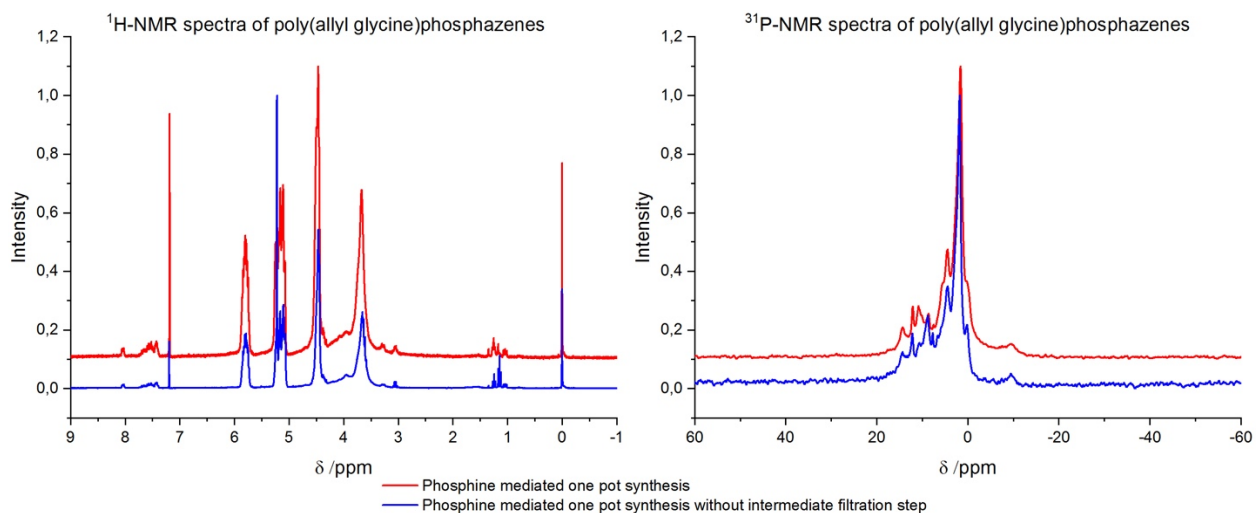

Figure 22: Comparison of poly(allyl glycine)phosphazenes synthesized via a phosphine mediated one pot synthesis, once with an intermediate filtration step between poly(dichloro)phosphazene and the macrosubstitution and once without.

3.1.3. Improvement of polymer purification method

Dialysis of the polymer, to optimize the purification of the poly(organo)phosphazene, is carried out, since an alternative to the laborious and time-consuming purification by precipitation has been sought. To achieve successful removal of the $Et_3N \cdot HCl$ impurities and excess of macrosubstituent, but still ensure no degradation of the polymer backbone, dialysis, first in water followed by EtOH, is used. Water ensures an effective purification from the $Et_3N \cdot HCl$ impurities, yet only a short time interval is chosen to prevent unwanted degradation. For the excess of macrosubstituent, EtOH is best suited, circumventing the problem of degradation due to higher stability of the polymer in this solvent. Accomplished purification has been determined by NMR spectroscopy with an overall disappearance of impurity peaks. Furthermore, the dialyzed polymer has been compared with a polymer purified by precipitation to ensure the same qualities of the polymer in regard to purity and stability and showed no decrease in neither of them, with no increase in intensity of impurity or degradation peaks. All in all, this makes dialysis an applicable purification method for poly(allyl glycine)phosphazenes. Every polymer described in this thesis was purified by dialysis.

3.1.4. Poly(dichloro)phosphazene stability in diglyme

The stability of poly(dichloro)phosphazenes synthesized via the one pot approach has been tested. For this purpose, one part of the polymer has been stored under argon at r.t., while a second part of the same batch has been dissolved in diglyme under air and likewise stored at r.t.. NMR measurements have been performed to determine any degradation of the polymer backbone over time, depicted in Figure 23 and Figure 24.
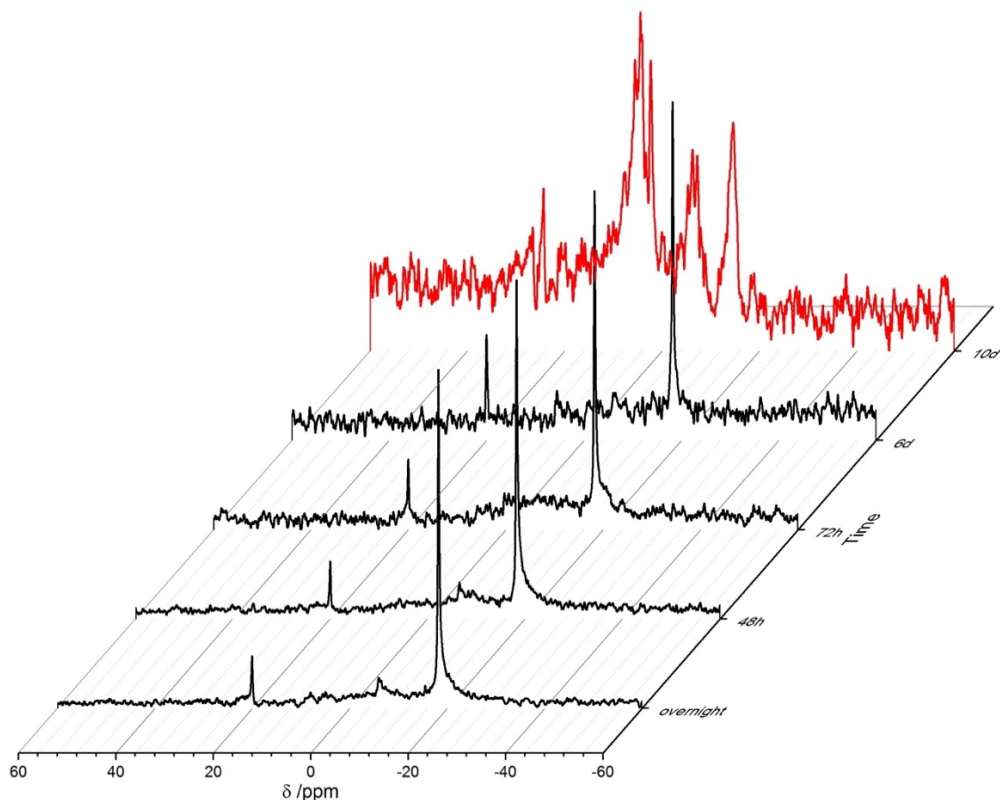
Figure 23: ^{31}P NMR spectra of poly(dichloro)phosphazene, stored under argon, over a time interval of ten days. Degraded polymer depicted in red.

The poly(dichloro)phosphazene stored under argon without solvent shows no sign of degradation up to six days, indicated by the sharp peak at -18 ppm, characteristic for poly(dichloro)phosphazenes, depicted in Figure 23. After ten days however, a clear degradation of the polymer can be seen, highlighted in red. The sharp peak at -18 ppm diminishes and a shift of the signal towards 0 ppm occurs. Nevertheless, storability of the polymer over the course of a week was demonstrated.
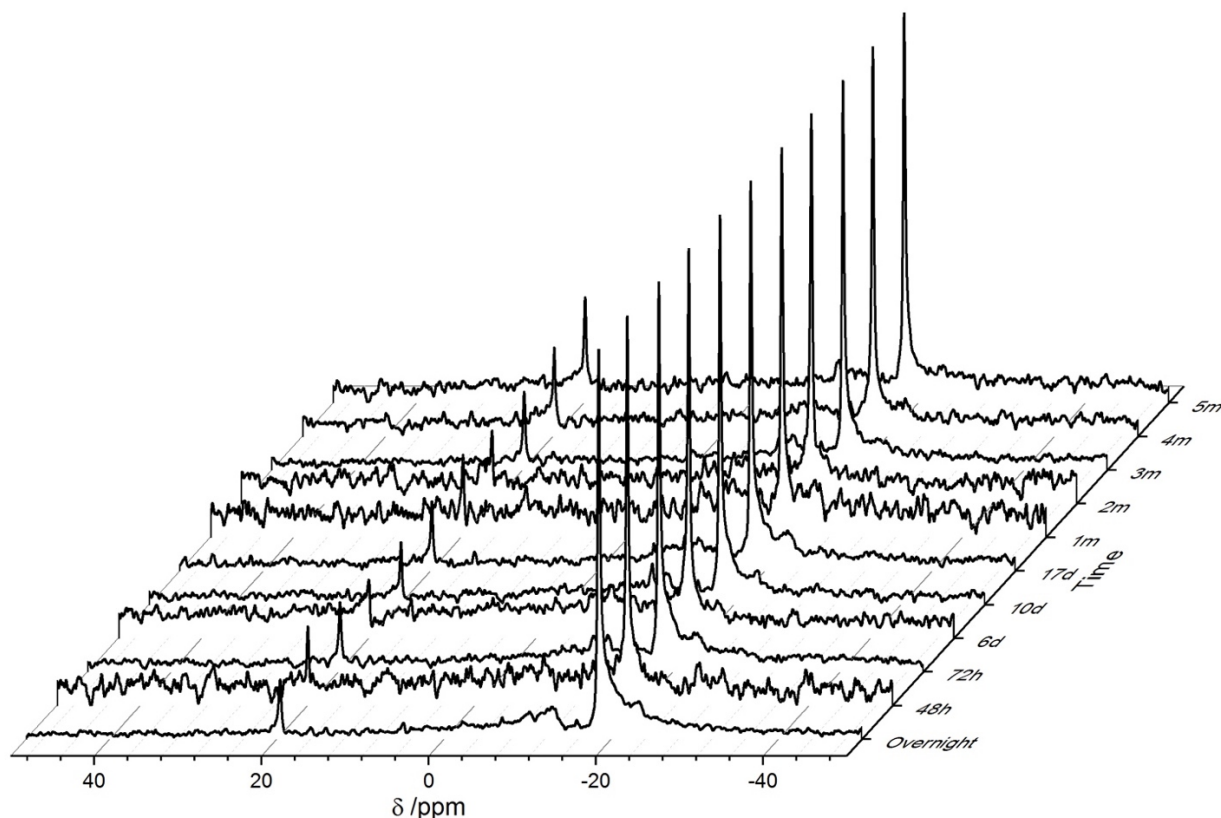
Figure 24: 31P NMR spectra of poly(dichloro)phosphazene, stored in diglyme, over a time interval of 5 months.

In diglyme, no degradation over the whole course of the experiment is observed for the poly(dichloro)phosphazene. The NMR measurements were stopped after five months. The characteristic peak at -18 ppm persists over the measured time interval, as depicted in Figure 24, proving a storability of the poly(dichloro)phosphazene well up to five months in accordance with Andrianov et al., reporting storage time of more than four years.[15] In combination with the easier scale up of the one pot synthesis, the storability of the poly(dichloro)phosphazene, either short-term in argon or long-term in diglyme, both at r.t., enables large-scale experiments from one batch of polymer, with polyphosphazenes of different properties gained after specific post-polymerization modifications.

3.2. Thiol-ene reactions: functionalization and cross-linking

Thiol-ene chemistry is the reaction chosen in this work for the functionalization and cross-linking of the poly(organo)phosphazenes, due to its compelling properties of a rapid reaction process, supposed air and moisture tolerant reaction conditions, and vast versatility. Therefore, the functional monomer and the cross-linkers have been selected to incorporate a thiol group as one selection criteria next to others discussed below.

3.2.1. Functional monomer selection and reaction

The functional monomer, at the heart of the imprinting process, has been selected not only for its thiol group, but more importantly for the functional group interacting with the template propranolol. With methacrylic acid (MAA) being the most prominent functional monomer for molecular imprinting, according to the literature, [12,83,113–118] a thiol containing carboxylic acid has been sought. Taking into consideration the aim of biocompatible MIPs, biological compounds, namely glutathione or cysteine, have been investigated in more detail. The presence of two carboxylic acid residues, as well as additional carbonyl and amine functionalities for the structure of glutathione, see Figure 25, raises concerns about the number of functionalities and unforeseeable influences on the imprinting process, stemming from the hydrogen bond forming groups. Since the aim of this thesis is a proof of concept of a novel molecular imprinting system, a simple and more understandable approach, meaning a clearer template-functional monomer interaction, is wanted. Therefore, glutathione has been discarded as a possible functional monomer, and a more straightforward functional monomer to template relation has been searched for. In this way, cysteine has also been reviewed, Figure 25. Despite a considerable smaller size and lower number of functional groups, cysteine still contains a primary amine as an amino acid, enabling further influence on the imprinting process due to hydrogen bonding, and therefore, adding another factor to the system. Thus, to simplify the functional monomer even more, and gain more and more similarity with the established functional monomer MAA, thioglycolic acid (TGA) has been chosen, Figure 25. Thioglycolic acid, also known as mercaptoacetic acid, satisfies the need of both, a carboxylic functional group for template binding, along with a thiol group for cross-linking. Besides these functionalities no further reactive groups are present, rendering thioglycolic acid a suitable and simple functional monomer to start with molecular imprinting experiments and developments towards the working system presented here.
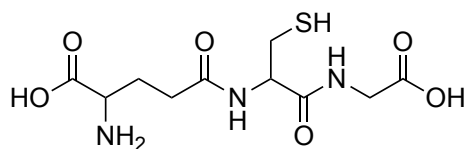
glutathione
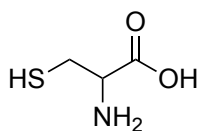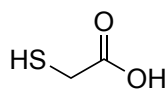
cysteine   mercaptoacetic acid

Figure 25: Chemical structures of possible functional monomers for the molecular imprinting process.

For the synthesis of the TGA-functionalized polyphosphazenes, as described in chapter 2.2.6. the reaction process has been optimized due to problems regarding the insolubility of the product in most solvents, complicating isolation and purification, and reactivity, despite the reported properties of the thiol-ene chemistry as a rapid, quantitative reaction, even in the presence of oxygen and moisture. Since thiol-ene chemistry is described as tolerant towards oxygen and air, no further precautions have been taken in this regard, however, as the reaction did not yield satisfying results, the synthesis was therefore adapted to bubbling argon through the reaction solution for 20 minutes prior to the reaction in the UV-reactor. In addition, certain glass vials proved incompatible with a UV-reaction. This became apparent after different experiments on varying scales, utilizing different glass vials, have resulted in differing outcomes, even though the packaging and description of the vials indicated no difference. To eliminate this problem, vials have been checked under UV light, and only non-reflecting, transparent ones have been taken for reactions.

Finally, the produced thioglycolic acid polymer is hardly soluble in standard solvents such as dichloromethane, tetrahydrofuran or others, and solubility in high boiling solvents such as dimethyl sulfoxide or dimethylformamide complicates further isolation. Thus, to circumvent the isolation step and therefore enabling the use of high boiling solvents, a one vial reaction in DMF, in resemblance to the one pot reaction, has been developed. The thioglycolic acid is reacted with the poly(allyl glycine)phosphazene and subsequently cross-linked, according to chapter 2.3.

To ensure a quantitative reaction of the thioglycolic acid under the set reaction conditions, the ratio of proton signals stemming from the thioglycolic acid and the allyl-glycine have been calculated, as applied for the determination of the number of repeat units of the polymer, proving the presence of the desired polymer.

3.2.2. Cross-linker selection and cross-linking

A trithiol (3TH), namely trimethylolpropane tris(3-mercaptopropionate), and a divinyl ester (VE), divinyl adipate, depicted in Figure 26, have been chosen as cross-linkers for initial experiments, since both have been used successfully in previous research.[12] Nevertheless, after preliminary investigations of MIPs based on these cross-linkers, the selection has been adapted by addition of two other functional molecules, namely pentaerythritol tetrakis(3-mercaptopropionate) (4TH) and pentaerythritol tetraacrylate (4Acr), depicted in Figure 26, to gain pellets with a higher rigidity due to a higher cross-linking, which has been considered to be the problem with the use of 3TH and VE. All in all, different combinations of these cross-linkers have been tested, listed in Table 4. Their effect is discussed in chapter 3.4. The absence of any double bond peaks, indicating complete cross-linking, has been determined via FT-IR.

trimethylolpropane tris(3-mercaptopropionate)
3TH

divinyl adipate
VE

pentaerythritol tetrakis(3 mercaptopropionate)
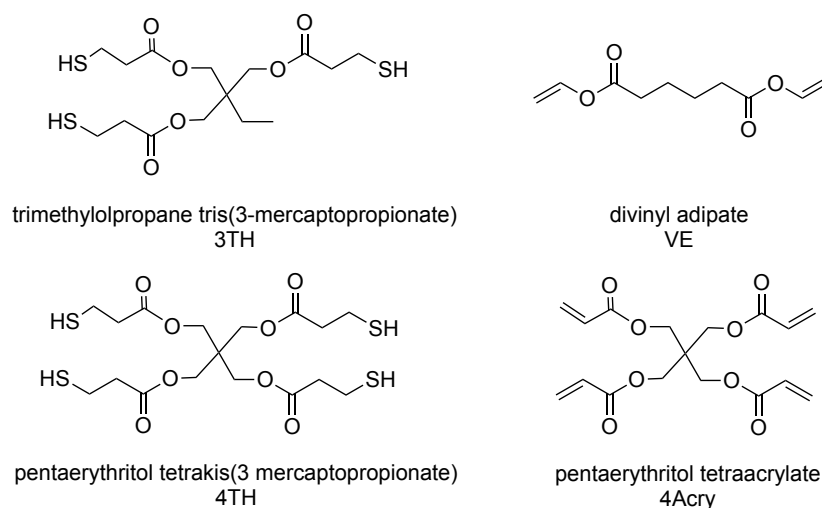4TH

pentaerythritol tetraacrylate
4Acry

Figure 26: Chemical structure of the different cross-linkers applied for the molecular imprinting process.

The cross-linking reaction itself is performed in a similar fashion as the functionalization with TGA. Since it is designed as a one vial reaction, the cross-linkers, as well as the porogens and the template, depending on the method, are added, and the reaction solution is placed in the UV-reactor. Argon is not bubbled through the solution again.

Sodium chloride, toluene and chloroform are used as porogens and their influence on the molecular imprinting process is investigated. Toluene and chloroform have been chosen to test the influence of the molecular size of the porogenous solvents, and salt as a straight forward approach to a porous material.

All in all, the adaption of thiol-ene chemistry for molecular imprinting opens up a different path towards MIPs. No pre-polymerization complex of the template and the functional monomer is formed, instead, the complex is composed of the template and the functionalized polymer which is cross-linked subsequently. Furthermore, the highlighted versatility of the thiol-ene reactions enables a quick adaption of the system towards different prerequisites, as has been shown above by the change in cross-linkers to gain rigidity.

A schematic of the functionalized and cross-linked polymer matrix is depicted in Figure 27.
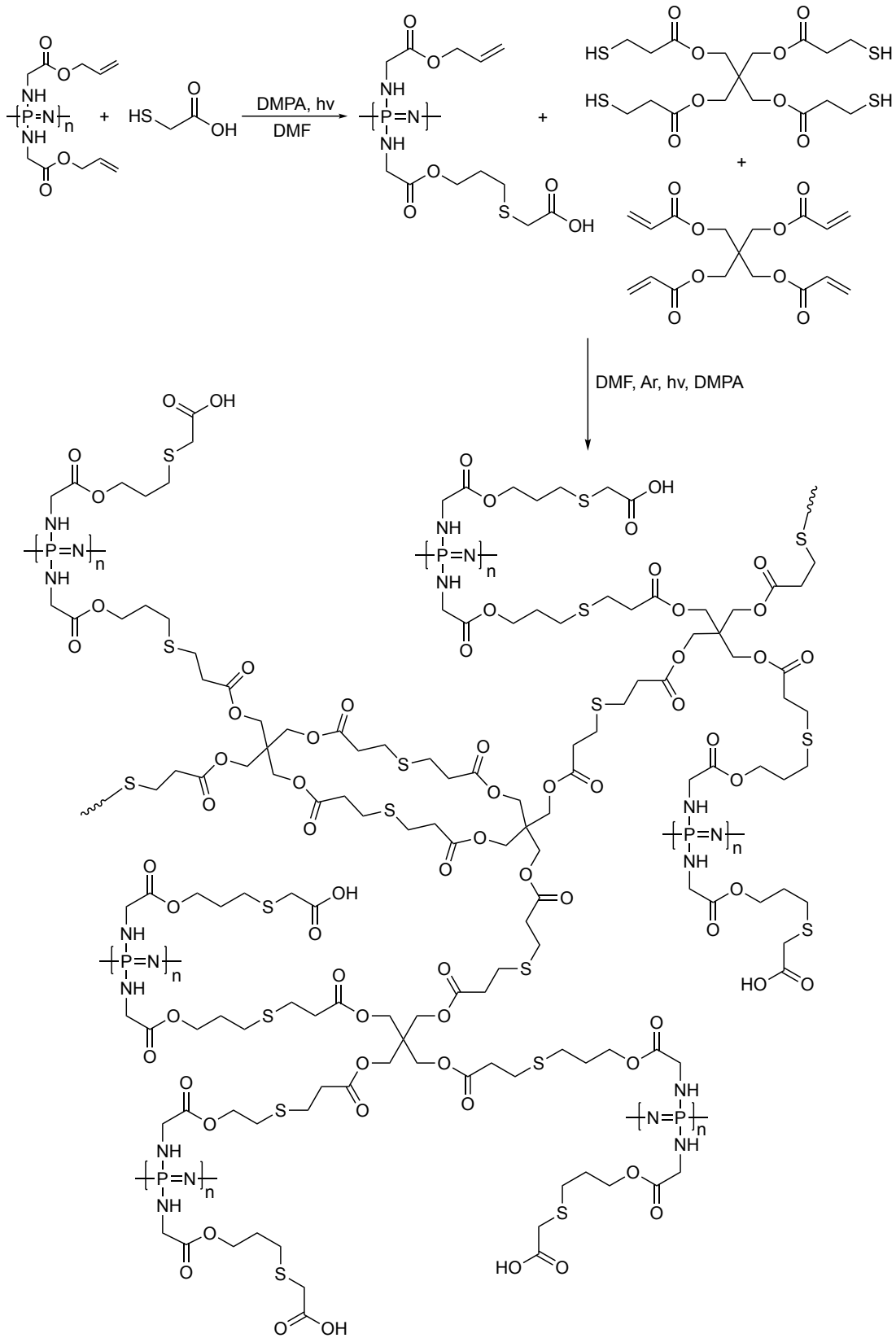
Figure 27: Schematic of the functionalized and 4TH/4Acry cross-linked poly(allyl glycine)phosphazene.

3.3. Propranolol

3.3.1. Deprotonation

Propranolol, allowing for a comparison with recent literature, was used as the template for molecular imprinting. Successful deprotonation of the commercially available hydrochloride was determined by the shift change of the proton signals stemming from the protons in vicinity of the secondary amine. A comparison of the ^{1}H NMR spectra can be seen in Figure 28.
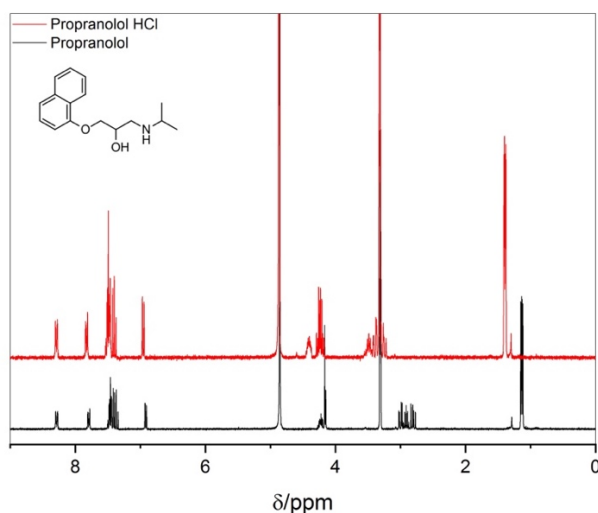
Figure 28: Comparison on ^{1}H NMR spectra of propranolol hydrochloride and propranolol in chloroform.

3.3.2. Propranolol stability in methanol

Propranolol was stored as a powder in the fridge at 4°C, and no changes were observed over the course of one month, Figure 29. However, the stability was also tested in methanol, i.e. the rebinding solution, allowing to estimate a suitable time scale of the rebinding experiment and to identify any influence of the solvent on the template during the procedure.
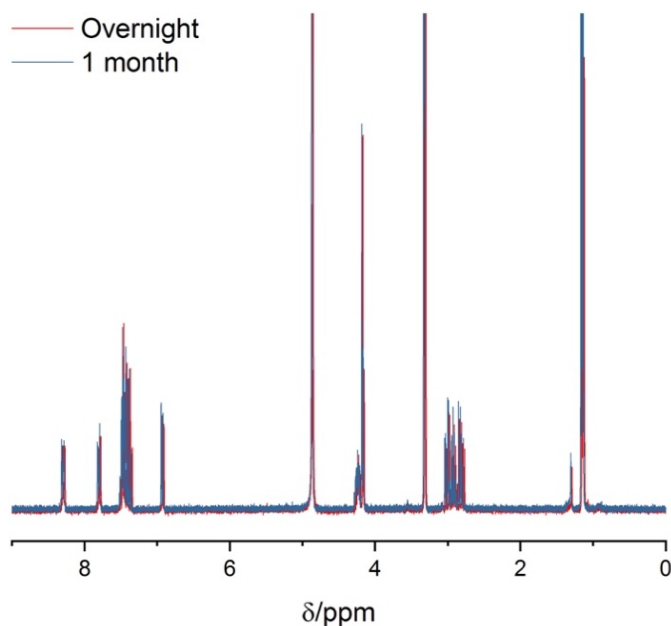
Figure 29: Stability of dry deprotonated propranolol stored in the fridge at 4°C over the course of one month.
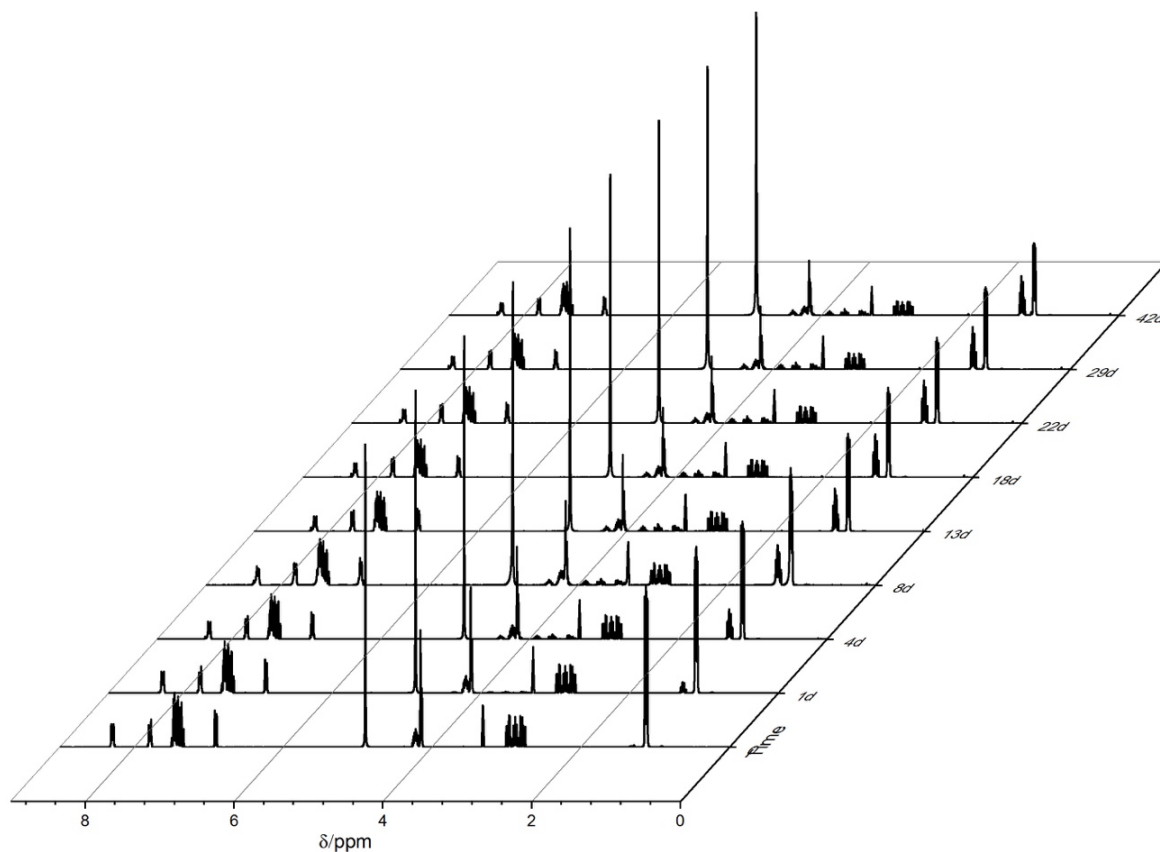
Figure 30: Comparison of ^{1}H NMR spectra of propranolol over the course of 42 days.

As can be seen in Figure 30, a change in the NMR spectra of propranolol can be already seen after one day. The signal at around 1 ppm steadily decreases, whereas a signal around 1.3 ppm appears and increases simultaneously with it. It is thought that this is possibly due to a combination of protonation, since the signal appearing at 1.3 ppm strongly resembles the respective peak for propranolol hydrochloride, and photo degradation, resulting in different degradation products like N-formylpropranolol.[121] A time scale of 48h for the rebinding essay was chosen, despite slight changes in the proton NMR. This was selected to allow sufficient, complete adsorption of propranolol by the polymers, whilst ensuring acceptable stability of the template at the same time.

3.4. Molecular imprinting

The molecular imprinting effect of the different molecularly imprinted polymer and non-imprinted polymer pairs, listed as MIP/NIP pairs in Table 7, has been tested via a rebinding essay and subsequent HPLC analysis, described in chapters 2.4. and 2.5.

Table 7: Summary of different methods for MIP/NIP pair synthesis.

MIP/NIP pair	Method	Crosslinker / wt%		PPz / wt%	Salt	Porogenous solvent / µL
1	1	VE /34%	3TH /55%	11%	-	-
2	1	VE /34%	3TH /55%	11%	Yes	-
3	1	VE /34%	3TH /55%	11%	-	chloroform /100µL
4	1	VE /34%	3TH /55%	11%	Yes	chloroform /100µL
5	1	VE /34%	3TH /55%	11%	-	toluene /100µL
6	1	VE /34%	3TH /55%	11%	Yes	toluene /100µL
7	2	4Acry /34%	3TH /52%	14%	-	-
8	2	4Acry /34%	3TH /52%	14%	Yes	-
9	3	VE /39.5%	4TH /49.5%	11%	-	-
10	3	VE /39.5%	4TH /49.5%	11%	Yes	-
11	4	4Acry /37%	4TH /52%	11%	-	-
12	4	4Acry /37%	4TH /52%	11%	Yes	-
13	5	4Acry /42%	4TH /58%	-	-	-
14	6	VE /43%	3TH /57%	-	-	-

The chromatographic peak corresponding to propranolol is integrated, and the mass determined via a calibration curve. From this value, the amount of template adsorbed by the pellet can be determined by subtraction from the concentration of propranolol in the rebinding solution. The adsorption values are normalized to the amount of polyphosphazenes used for the synthesis of the pellets and hence the amount of functional monomer, and, to analyze the corresponding MIP and NIP, the adsorption of the NIP is set to 100% and the MIP compared to it. The results are summarized in Table 8 and visualized in Figure 31. MIP/NIP pairs 1 and 2, corresponding to pellets cross-linked with 3TH and VE, once in the presence of salt and once without, are not listed, as they proved to not be working during preliminary tests, pairs 3 to 6 were synthesized using the same method as 1 and 2, but with the addition of chloroform and toluene, respectively, and are reported below to investigate the influence of the porogens.
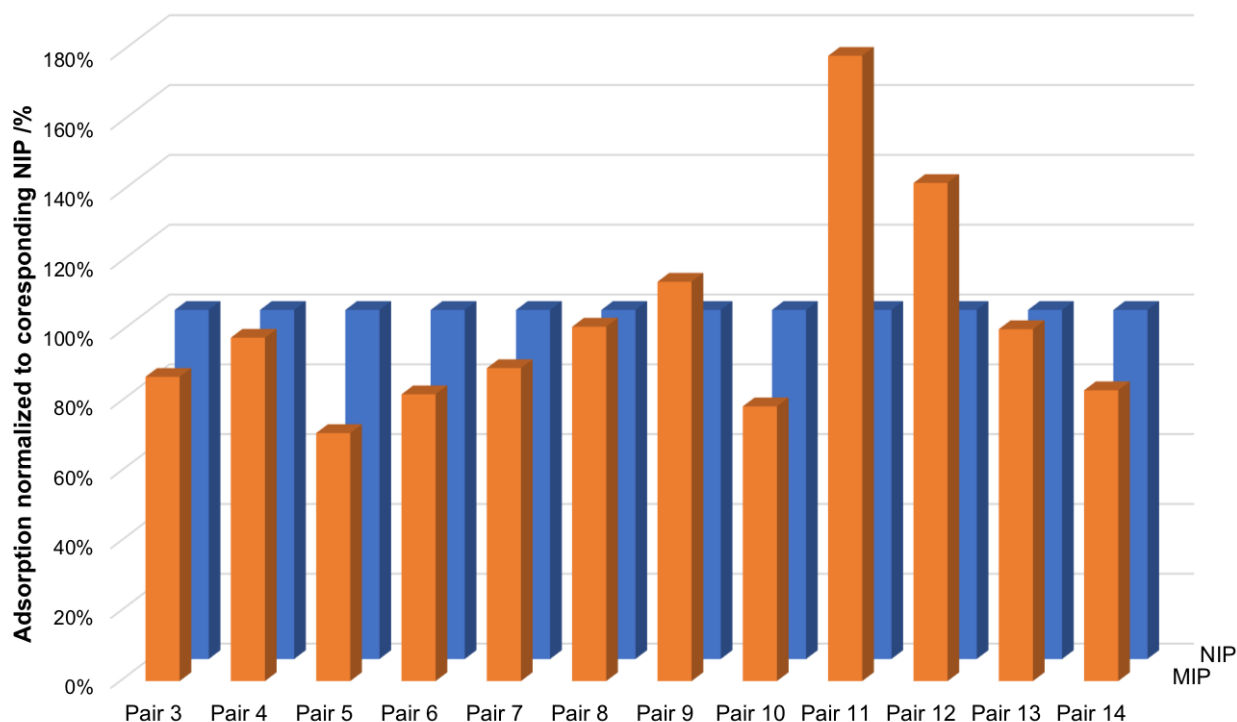
Figure 31: Rebinding results for the different tested MIP/NIP pairs.

As becomes apparent from Figure 31, all pairs, except 11 and 12, based on 4TH and 4Acry, do not reveal an imprinting effect, on the contrary, most of them show a higher adsorption of the template by the non-imprinted polymer. Furthermore, no clear effect of the use of sodium chloride as porogen can be determined by the results above, as the adsorption difference between MIP and NIP of the different pairs using NaCl as porogen are inconsistent. Pairs 4, 6 and 8, with salt, show a higher adsorption of the MIP than the pairs 3, 5 and 7, without salt, suggesting a positive influence of the salt as a porogen for the imprinting process, whereas pairs 9 to 14 indicate the opposite. For toluene and chloroform, no effect can be determined either, both porogens result in pellets with a higher adsorption for the non-imprinted polymer, with greater differences for chloroform than for toluene, and are, as pair 1 and 2 on which they are based, non-working systems.

Nevertheless, a successful imprint of propranolol has been achieved with pair 11 and pair 12 showing an adsorption of 179.12% and 142.69% compared to the NIP for pair 11 and 12, respectively. This shows, first and foremost, the importance of a rigid pellet, as has been suggested from the preliminary tests of the pellets cross-linked with 3TH and VE, since both pairs are cross-linked with 4TH and 4Acry and hence, display a higher stiffness. And furthermore, it hints on a negative effect of sodium chloride on the imprinting process as described above, yet a clear statement cannot be made. The necessity of the polyphosphazenes and the functional monomer for the imprinting effect becomes clear when looking at pair 13 in comparison with pair 12, since pair 13 is identical to pair 12 except no polyphosphazenes has been used during the synthesis of the pellets, and hence, also no functional monomer was present. It should be noted

that the adsorption values reported for pairs 13 and 14 are therefore also not normalized to the amount of polyphosphazenes used and the comparison between MIP and NIP is hampered by a slight difference in the mass of polyphosphazene used for the respective synthesis.

All in all, a working system for molecularly imprinted polymers on the basis of polyphosphazenes is reported with the MIP/NIP pair 11, synthesized with 4TH and 4Acry as cross-linkers and no porogens.

BET analysis has been performed for all MIP/NIP pairs and the results are reported in the attachments in Table 9. Briefly, the values for the specific surface of the polymers lie below the threshold to allow for a valid analysis and are therefore not interpreted, yet, for the purpose of completeness, attached at the end of the thesis.

Table 8: Result summary of adsorption values for the different tested MIP/NIP pairs. Values reported for pairs 13 and 14 correspond to the total amount of propranolol adsorbed by the pellet without normalization.

Method	MIP/NIP pair	MIP/NIP	m(Propranolol)/m(PPZ) / $\mu g*mg^{-1}$ (266nm)	Adsorption normalized to corresponding NIP / %
1	3	NIP	179.6	100%
		MIP	156.5	87%
1	4	NIP	283.3	100%
		MIP	278.7	98%
1	5	NIP	276.2	100%
		MIP	196.3	71%
1	6	NIP	296.9	100%
		MIP	244.0	82%
2	7	NIP	60.5	100%
		MIP	54.3	90%
2	8	NIP	259.3	100%
		MIP	263.2	102%
3	9	NIP	139.9	100%
		MIP	160.0	114%
3	10	NIP	321.7	100%
		MIP	253.2	79%
4	11	NIP	92.0	100%
		MIP	164.9	179%
4	12	NIP	245.4	100%
		MIP	350.2	143%
5	13	NIP	2.2	100%
		MIP	2.3	101%
6	14	NIP	3.9	100%
		MIP	3.3	83%

3.5. Degradation study

With the aim of degradable molecularly imprinted polymers, three MIP/NIP pairs have been chosen as representatives for the different pairs to a degradation study, according to chapter 2.6. The polymers were tested at pH 2 and pH 7 over two and four months, respectively, allowing a confirmation on the influence of the pH on the degradation, and an estimation of the necessary time interval for the pH 7 series. This was determined according to the degradation rate of the pH 2 series which was supposed to be faster than the one for pH 7.

The results are visualized in Figure 32 to Figure 35 and are attached in tabular form at the end of the thesis, Table 10.

To test the reproducibility and systemic error of the method itself, triplicates of each a MIP and NIP, synthesized according to MIP/NIP pair 1, were tested for the pH 2 series since a faster degradation of the polymer was expected for this series and therefore, an earlier interpretation of the results.
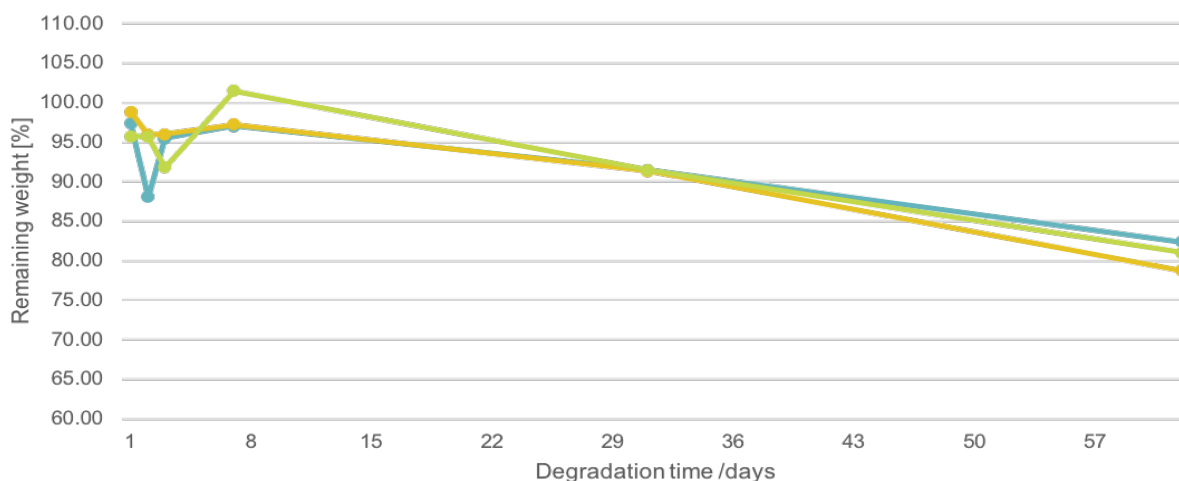

Figure 32: Degradation of triplicates of a MIP, synthesized according to MIP/NIP pair 1, at pH 2.
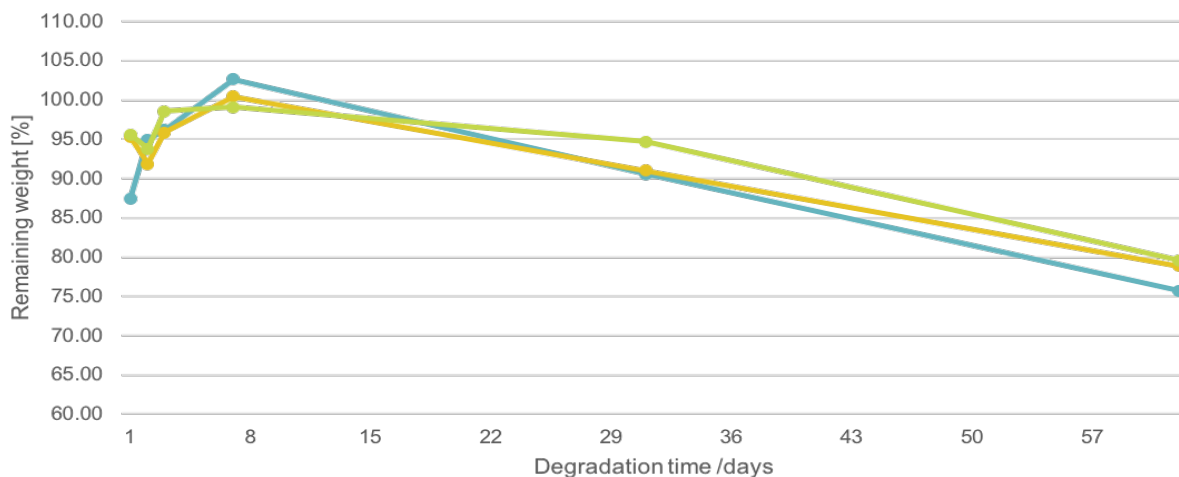

Figure 33: Degradation of triplicates of a NIP, synthesized according to MIP/NIP pair 1, at pH 2.

Both, the MIP and the NIP, show a high fluctuation for the first 3 values, even overshooting 100% of remaining weight, as depicted in Figure 32 and Figure 33. This may result from the low initial weight of just around 20 mg of polymer and the, in comparison, enormous weight of the sintered glass crucibles and the resulting error of the balance and the weighing process. In addition, for the first 3 data points especially, despite all efforts to secure complete dryness, some residual solvent may have falsified the measurement, explaining the rapid decrease in remaining weight after one day and a subsequent, relative increase of remaining weight for the next two data points compared to the first. Nonetheless, for the overall timescale, the method shows variations between the triplicates of only roughly 5% and no difference between the MIP and NIP.

Comparison of the three MIP/NIP pairs, one synthesized according to MIP/NIP pair 2, based on 3TH and VE with salt as a porogen, and the other two according to MIP/NIP pair 1, based on 3TH and VE without any additional porogen, once after rebinding and once without any previous testing, shows no difference in degradation between the different pairs, depicted in Figure 34. Fluctuations between the results can be seen, however all in a range of 10% and therefore, in accordance with the findings from Figure 32 and Figure 33, in the range of ±5%. Furthermore, all pellets show the same fluctuations in remaining weight for the first three to four data points, emphasizing the above proposed systemic error of the method in this time frame.

Figure 34: Degradation of MIP/NIP pairs at pH 2. A fresh MIP/NIP pair corresponds to normally synthesized pellets without a rebinding assay previous to the degradation study.

On the whole, a clear degradation down to approximately 80% to 85% of their initial weight can be seen for all pellets over a time interval of two month at pH 2.
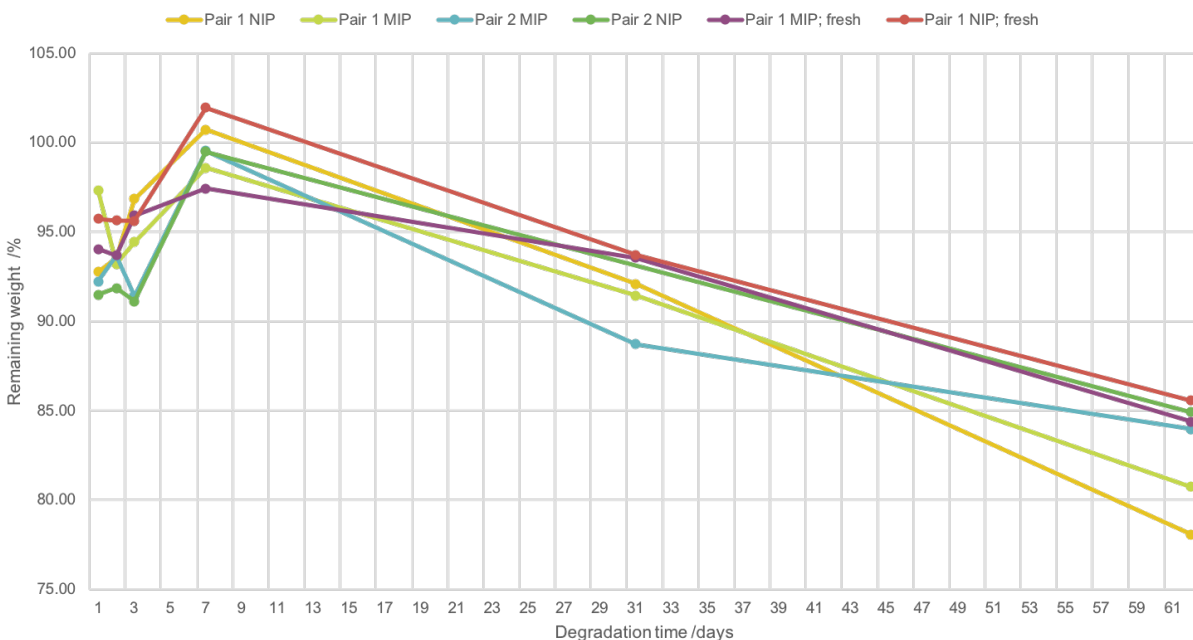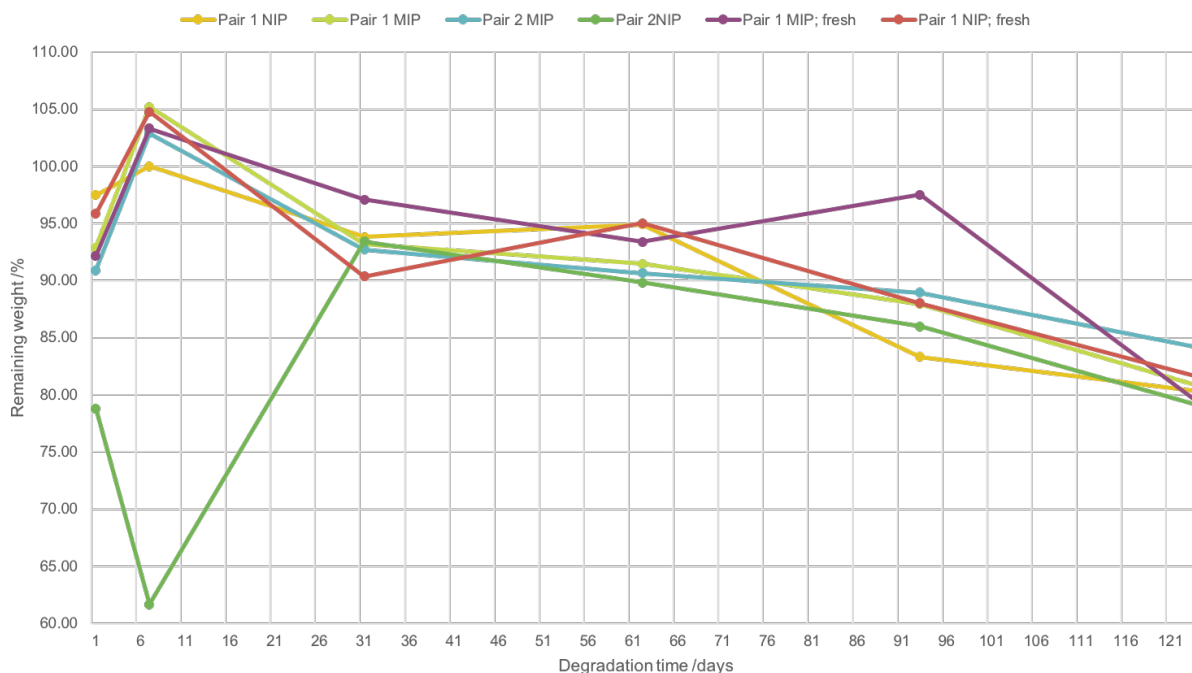
Figure 35: Degradation of MIP/NIP pairs at pH 7. A fresh MIP/NIP pair corresponds to normally synthesized pellets without a rebinding assay previous to the degradation study.

Comparing the degradation of the pellets at pH 7 depicted in Figure 35, the pellets show an even broader fluctuation for the first two data points, especially the values for the pair 2 NIP seem out of place with a degradation down to 78% and 61% after 1 and 7 days, respectively, compared to degradation rates for pH 2 at these time intervals, however a clear explanation for this could not be found. Despite these, again a clear trend can be seen for all 6 pellets alike, resulting in degradation down to around 80% to 85% over a time interval of 4 month at pH 7.

All in all, both degradation series, at pH 2 and pH 7, indicate a degradable polymer and degradation rates for the two, with a higher rate at the lower pH, are consistent with the hydrolytic degradation mechanism described in chapter 1.1.3.

4. Conclusion and outlook

In conclusion, the work presented herein reports substantial improvements in regard to polyphosphazene synthesis in the form of the one pot synthesis, synthesizing poly(organo)phosphazene from $LiN[Si(CH_3)_3]_2$ without any intermediate isolation step, and its amendments towards a phosphine mediate one pot synthesis. This gives a combination of advantages. On the one hand, the easier scale-up of the one-pot synthesis, and on the other hand, a simple characterization of the polymers, via NMR-specroscopy, from the isolated monomer approach. The latter is achieved using the functional end group of the polymer to determine the number of repeat units by comparing the ratio of the proton signals from the end group to the signals of the substituents. This was accomplished by the modification of the one pot synthesis described by Wang,[26] by means of an alteration of the solvent towards higher polarity, specifically dichloromethane, and the adoption of 4-diphenylphosphanyl benzoic acid-2-(trimethylsilyl) ethyl ester as a phosphine, the polymerization mediator, instead of PCl_5 as the polymerization initiator.[23] Furthermore, the overall yield of the synthesis of the poly(organo)phosphazene, comprised of monomer synthesis, polymerization of poly(dichloro)phosphazene $[NPCl_2]_n$ and subsequent post-polymerization modification (macrosubstitution), via the one pot approach was increased from 29% to 79% without any negative influence on purity. This was accomplished by omitting the intermediate filtration step between the polymerization of poly(dichloro)phosphazene and the necessary macrosubstitution to avoid the hydrolysis of the polymer backbone. Nevertheless, the stability of poly(dichloro)phosphazene under argon and in solution (diglyme) was tested, investigating the possible storage period of $[NPCl_2]_n$, since the one pot synthesis promises a simpler scale up and hence large-scale experiments from one batch of polymer, and stored $[NPCl_2]_n$ would allow for further variation during post-polymerization modification of the same poly(dichloro)phosphazene. Further, a scale up in the synthesis of the utilized substituent, a glycine allyl ester, was achieved as well as a simpler purification method of the synthesized poly(allyl glycine)phosphazene in form of a split dialysis in water and EtOH, tested and verified by NMR-spectroscopy.

Additionally, it was shown that poly(organo)phosphazenes are a suitable polymer backbone for the synthesis of, and further developments towards, biocompatible degradable molecularly imprinted polymers, enabling a tailored degradation rate by adjusting the substituent substituents as well as customized chemical and mechanical properties. This was demonstrated by rebinding essays with subsequent evaluation via HPLC of molecularly imprinted polymers specific for propranolol, based on poly(allyl glycine)phosphazenes modified with thioglycolic acid as the functional monomer, and subsequent cross-linking via thiol-ene chemistry. The influence of different cross-linkers, namely trimethylolpropane tris(3-mercaptopropionate) (3TH), divinyl adipate (VE), pentaerythritol tetrakis(3-mercaptopropionate) (4TH) and pentaerythritol tetraacrylate (4Acry), as well as of different porogens, such as chloroform, toluene and sodium chloride, on a successful imprint were investigated. Whilst a clear preference for a pellet of higher

rigidity, cross-linked with 4TH and 4Acry, was proven to gain a specific imprint, results regarding the influence of the different porogens were inconclusive. Degradation studies of representative polymer pellets in MilliQ water with a pH of 7 and 2 showed a degradation of the pellets down to around 80% to 85% over time intervals of four months (pH 7) and two months (pH 2), respectively, with the expected influence of a lower pH resulting in a faster degradation rate. The application of thiol-ene chemistry to functionalize and cross-link the polymer backbone opens up the door towards easily adaptable molecular imprinting systems due to the great versatility of thiol-ene reactions, allowing for almost any thiol or double bond functionality to be used. Thus, a modular construction kit for biocompatible, degradable molecularly imprinted polymers has been established.

In the future, the phosphine mediated one pot synthesis may be investigated in more detail in regard to the set reaction conditions, namely temperature and reaction times, to achieve the higher molecular weights and chain lengths reported for the one pot synthesis by Wang.[26] Even more, the potential of the one pot synthesis in regard to a scale up should be explored, and, in combination with the storability of the poly(dichloro)phosphazenes, the chance of the construction of a library of poly(organo)phosphazenes differing in substituent and functional monomer allowing for a fast screening of possible candidates for molecular imprinting. This may also pose a significant improvement in polyphosphazene synthesis for other research fields employing these polymers. In addition, the prospect of a possible scale-up raises interesting opportunities for the industry.

Likewise, with regard to the molecular imprinting, the rebinding analysis of the imprinted polymers should be extended not only to investigate the total adsorption capacity of the MIPs and NIPs, respectively, but also to study the difference in adsorption kinetics to disclose possible unobserved differences between molecularly imprinted polymers and their non-imprinted counterparts. This may be achieved by real-time nuclear magnetic resonance (RT-NMR) analysis or the use of equilibrium dialysis and subsequent or direct injection of the spiked dialysis solvent into a HPLC system, allowing for almost continuous examination of the adsorption of propranolol by the polymers. Furthermore, different rebinding conditions, namely the template concentration, could be tested to verify any further differences between the imprinted and non-imprinted polymers. In addition, a distinct analysis of the binding properties of the polymers analyzed via an AFM as a force meter may give further insight into the imprinting effect, directly observing the template-binding pocket interactions.

To examine the adaptability of the modular construction kit, different functional monomers, for example the discarded glutathione or cysteine, as well as a combination of cross-linker and functional monomer in the form of e.g. dimercaptosuccinic acid, simplifying the imprinting process by directly forming the template-functional monomer complex with the cross-linker itself, may be targeted. In combination with additional, more exact degradation studies to deduce possible

differences between the polymers, or also their behavior in other solvents and an evaluation of the biocompatibility of the molecularly imprinted polymers, the herein presented method alongside the proposed further experiments set forth a novel approach to molecular imprinting.

5. Abbreviations

Abbreviation	Description
3TH	trimethylolpropane tris(3-mercaptopropionate)
4Acry	pentaerythritol tetraacrylate
4TH	pentaerythritol tetrakis(3-mercaptopropionate)
ACN	acetonitrile
AFM	atomic force microscopy
allyl-Gly	glycine allyl ester
ATP	adenosine triphosphate
BET	Brunauer-Emmett-Teller
BJH	Barrett-Joyner-Halenda
Boc-Gly-OH	N-(tert-butoxycarbonyl)glycine
cAMP	cyclic adenosine monophosphate
DLS	dynamic light scattering
DMF	dimethylformamide
DMPA	2,2-dimethoxy-2-phenylacetophenone
DMSO	dimethyl sulfoxide
Et_3N	triethylamine
EtOH	ethanol
FT-IR	Fourier-transform infrared spectroscopy
GPC	gel permeation chromatography
HPLC	high performance liquid chromatography
JAK	Janus kinase
JAK/STAT	Janus kinase / signaling transducer and activator of transcritpion protein
MAA	methacrylic acid
MAPK	mitogen-activated protein kinase
MeOH	methanol
MIP	molecularly imprinted polymers
NIP	non-imprinted polymers
NMR	nuclear magnetic resonance
PPz	polyphosphazene
PTSD	post-traumatic stress disorder
RT-NMR	real-time nuclear magnetic resonance
SBSE	stir bar sorption extraction
SERS	surface enhanced Raman spectroscopy
SPE	solid phase extraction
SPME	solid phase micro extraction
SPR/FT-IR	surface plasmon resonance / Fourier-transform infrared spectroscopy
ss-NMR	solid-state nuclear magnetic resonance
TFA	trifluoroacetic acid
TGA	thioglycolic acid
TGA-PPz	thioglycolic acid poly(allyl glycine)phosphazene
THF	tetrahydrofuran
TMSE-triphenylphosphine	4-diphenylphosphanyl benzoic acid-2-(trimethylsilyl) ethyl ester
VE	divinyl adipate

6. Attachments

Table 9: Summary of BET-analysis results of the different MIP/NIP pairs.

Method	MIP/NIP pair	MIP/NIP	BET surface area / m²g⁻¹	Langmuir surface area / m²g⁻¹	Surface area BJH adsorption cumulative surface area of pores between 1.7000nm and 300.000nm diameter / m²g⁻¹	BJH desorption cumulative surface area of pores between 1.7000nm and 300.000nm diameter / m²g⁻¹	Pore Volume BJH adsorption cumulative volume of pores between 1.7000nm and 300.000nm diameter / cm³g⁻¹	BJH desorption cumulative volume of pores between 1.7000nm and 300.000nm diameter / cm³g⁻¹	Pore size BJH adsorption averge pore diameter (4V/A) / nm	BJH desorption averge pore diameter (4V/A) / nm
1	1	NIP	0.0558	0.0807	0.017		0.000036		8.3611	
1	1	MIP	0.1042	0.1903	0.083	0.019	0.000122	0.000111	5.8935	23.3047
1	1	NIP	0.1573	0.2372	0.103	0.0562	0.000173	0.00014	6.7103	9.9404
1	1	MIP	0.1891	0.3257	0.176	0.0715	0.000194	0.000109	4.4179	6.0781
1	2	NIP	0.3	0.5523	0.35	0.2472	0.000483	0.000996	5.5154	16.1204
1	2	MIP	0.1593	0.3003	0.144	0.0732	0.000243	0.000215	6.7316	11.769
1	3	NIP	0.3325	0.6943	0.268	0.0618	0.000228	0.000139	3.3944	9.0209
1	3	MIP	0.3055	0.5359	0.337	0.213	0.000411	0.000352	4.8809	6.6146
1	4	NIP	0.638	1.1495	0.615	0.3303	0.002329	0.000578	15.5466	7.004
1	4	MIP	0.3587	0.6982	0.338	0.2921	0.000479	0.00065	5.6744	8.9011
1	5	NIP	0.5471	1.1767	0.448	0.2874	0.000333	0.000278	2.9711	3.8727
1	5	MIP	0.132	0.2166	0.085	0.0104	0.000487	0.00006	22.8784	22.9873
1	6	NIP	0.1195	0.1783	0.055	0.0355	0.000194	0.000173	14.1314	19.5243
1	6	MIP	0.0904	0.1303	0.003		0.000044		52.9439	
2	7	NIP	0.3008	0.5013	0.227	0.061	0.000217	0.000209	3.8307	13.6659
2	7	MIP	0.3573	0.7046	0.289	0.164	0.000317	0.000509	4.3883	12.5191
2	8	NIP	0.5679	0.9209	0.402	0.1708	0.000412	0.000288	4.1056	6.7454
2	8	MIP	0.5722	0.8692	0.385	0.2265	0.000379	0.004432	3.9539	78.2781
3	9	NIP	0.0072	0.0087						
3	9	MIP	0.1656	0.325	0.141	0.0377	0.000178	0.000133	5.0453	14.0684
3	10	NIP	0.1241	0.2139	0.111	0.0117	0.000148	0.000115	5.3268	39.3261
3	10	MIP	0.1923	0.2774	0.073	0.0462	0.000166	0.000214	9.1505	18.5195
4	11	NIP	0.1524	0.2636	0.133	0.0504	0.000171	0.000996	5.1186	78.9727
4	11	MIP	-0.0106	-0.008	0.013	0.0187	0.000141	0.000128	44.3228	27.2859
4	11	NIP	0.1291	0.2454	0.114	0.1051	0.000209	0.000187	7.3368	7.1059
4	11	MIP	4.6613	6.7674	4.613	4.804	0.019963	0.044547	17.311	37.0922
4	11	NIP	4.7366	6.8945	4.743	4.8816	0.016514	0.061795	13.928	50.6346
4	11	MIP	4.3729	6.3357	4.329	4.5284	0.016732	0.040542	15.4589	35.811
4	12	NIP	0.2583	0.4247	0.247	0.1409	0.000501	0.000471	8.0995	13.3878
4	12	MIP	0.2497	0.4243	0.232	0.1072	0.000347	0.001458	5.998	54.4215
5	13	NIP	0.1627	0.3623	0.135	0.0422	0.000579	0.000114	17.11	10.8092
5	13	MIP	0.0766	0.1348	0.065	0.0164	0.000098	0.000081	6.0968	19.7985
5	13	NIP	59.243	80.3623	32.517	31.3606	0.039525	0.054507	4.8621	6.9523
6	14	MIP	0.249	0.4256	0.26	0.1604	0.000284	0.000186	4.3783	5.6437
6	14	NIP	0.3147	0.5704	0.29	0.0523	0.000313	0.000234	4.3208	17.8578

Table 10: Results of the degradation study of the representative MIP/NIP pairs.

pH 2

MIP/NIP pair	MIP/NIP	Initial weight / mg 1d	2d	3d	7d	31d	62d	weight after timescale / g 1d	2d	3d	7d	31d	62d	weight after timescale / % 1d	2d	3d	7d	31d	62d
1	MIP	15.5	20.1	15.6	20.2	17.6	19.9	12.7404	18.7142	19.8659	12.7600	12.7761	12.7925	97.42	88.06	95.51	97.03	91.48	82.41
1	MIP	17	17.1	17.4	17.9	19.7	16.5	13.3230	19.5654	12.6538	13.3404	13.3584	13.3714	98.82	95.91	95.98	97.21	91.37	78.79
1	MIP	18.8	20.7	19.5	13.3	18.8	21.1	12.4049	12.2864	19.2171	12.4184	12.4356	12.4527	95.74	95.65	91.79	101.50	91.49	81.04
1	NIP	15.1	25.8	23.4	15.2	22.3	16.9	12.5853	19.4122	19.6378	12.6009	12.6211	12.6339	87.42	94.96	96.15	102.63	90.58	75.74
1	NIP	17.1	18.4	14.4	22.3	20	19.4	13.4588	12.4811	12.5771	13.4812	13.4994	13.5147	95.32	91.85	95.83	100.45	91.00	78.87
1	NIP	15.8	22.4	27.4	21.9	24.4	14.2	13.4897	13.4692	19.7126	13.5114	13.5345	13.5458	95.57	93.75	98.54	99.09	94.67	79.58
2	MIP	19.3	20.5	19.8	21.9	21.3	21.2	13.5283	19.8600	19.6174	13.5501	13.569	13.5868	92.23	93.66	91.41	99.54	88.73	83.96
2	NIP	17.6	20.9	18	19.9	19	19.9	13.4845	20.1443	18.8603	13.5043		18.8772	91.48	91.87	91.11	99.50		84.92
1; fresh	MIP	16.8	20.6	22	19.4	21.7	20.5	13.4813	19.4546	13.5047	13.5002	13.5205	13.5378	94.05	93.69	95.91	97.42	93.55	84.39
1; fresh	NIP	21.1	18.3	20.5	20.5	20.7	20.8	13.3316	19.7355	12.7901	13.3525	13.3719	13.3897	95.73	95.63	95.61	101.95	93.72	85.58

pH 7

Pellet Nr.	Classification	Initial weight / mg 1d	7d	31d	62d	93d	124d	weight after timescale / g 1d	7d	31d	62d	93d	124d	weight after timescale / % 1d	7d	31d	62d	93d	124d
1	MIP	21.1	17.3	20.6	21.1	19.1	19.3	20.0431	20.0805	20.0613	20.0998	20.1166	20.1322	92.89	105.20	93.20	91.47	87.96	80.83
1	NIP	19.8	18.4	21	17.7	18	18.3	19.7486	19.7867	19.7670	19.8035	19.8185	19.8332	97.47	100.00	93.81	94.92	83.33	80.33
2	MIP	22	20.6	22	21.4	21.7	19.6	19.5570	19.5986	19.5782	19.618	19.6373	19.6538	90.91	102.91	92.73	90.65	88.94	84.18
2	NIP	17	36	19.8	17.7	20.7	19.6	18.8936	18.9343	18.9158	18.9502	18.968	18.9835	78.82	61.67	93.43	89.83	85.99	79.08
1; fresh	MIP	20.4	18	20.6	19.7	20.3	20.9	19.8058	19.8444	19.8244	19.8628	19.8826	19.8992	92.16	103.33	97.09	93.40	97.54	79.43
1; fresh	NIP	21.7	20.9	21.8	20.2	21.7	21.2	19.7602	19.7821	19.821	19.821	19.8401	19.8574	95.85	104.78	90.37	95.05	88.02	81.60

8. List of tables

9. References

1. Chaplin AB, Harrison JA, Dyson PJ. Revisiting the Electronic Structure of Phosphazenes. *Inorg Chem*. 2005;44(23):8407-8417. doi:10.1021/ic0511266

2. Rothemund S, Teasdale I. Preparation of polyphosphazenes: a tutorial review. *Chem Soc Rev*. 2016;5200(45):5200-5215. doi:10.1039/c6cs00340k

3. Allcock HR. *Phosphorus-Nitrogen Compounds; Cyclic, Linear, and High Polymeric Systems*. Academic Press; 1972.

4. Allcock HR. Recent advances in phosphazene (phosphonitrilic) chemistry. *Chem Rev*. 1972;72(4):315-356. doi:10.1021/cr60278a002

5. Magnusson E. The role of d functions in correlated wave functions: main group molecules. *J Am Chem Soc*. 1993;115(3):1051-1061. doi:10.1021/ja00056a033

6. Korkin AA. Stereoelectronic effects in silicon, phosphorus, and sulfur molecules. Quantum-chemical calculations and qualitative orbital models. *Russ Chem Rev*. 1992;61(5):473-483. doi:10.1070/RC1992v061n05ABEH000957

7. Gilheany DG. No d Orbitals but Walsh Diagrams and Maybe Banana Bonds: Chemical Bonding in Phosphines, Phosphine Oxides, and Phosphonium Ylides. *Chem Rev*. 1994;94(5):1339-1374. doi:10.1021/cr00029a008

8. Reed AE, Schleyer P v. R. Chemical bonding in hypervalent molecules. The dominance of ionic bonding and negative hyperconjugation over d-orbital participation. *J Am Chem Soc*. 1990;112(4):1434-1445. doi:10.1021/ja00160a022

9. Reed AE, Schleyer P v. R. The anomeric effect with central atoms other than carbon. 2. Strong interactions between nonbonded substituents in mono- and polyfluorinated first- and second-row amines, FnAHmNH2. *Inorg Chem*. 1988;27(22):3969-3987. doi:10.1021/ic00295a018

10. Andrianov AK, DeCollibus DP, Gillis HA, et al. Poly[di(carboxylatophenoxy)phosphazene] is a potent adjuvant for intradermal immunization. *Proc Natl Acad Sci U S A*. 2009;106(45):18936-18941. doi:10.1073/pnas.0908842106

11. Jankowsky S, Hiller MM, Wiemhöfer H-D. Preparation and electrochemical performance of polyphosphazene based salt-in-polymer electrolyte membranes for lithium ion batteries. *J Power Sources*. 2014;253:256-262. doi:10.1016/J.JPOWSOUR.2013.11.120

12. Rothemund S, Aigner TB, Iturmendi A, et al. Degradable Glycine-Based Photo-Polymerizable Polyphosphazenes for Use as Scaffolds for Tissue Regeneration. *Macromol Biosci*. 2015;15(3):351-363. doi:10.1002/mabi.201400390

13. Henke H, Brüggemann O, Teasdale I. Branched Macromolecular Architectures for Degradable, Multifunctional Phosphorus-Based Polymers. *Macromol Rapid Commun*. 2017;38(4):1600644. doi:10.1002/marc.201600644

14. Henke H, Wilfert S, Iturmendi A, Brüggemann O, Teasdale I. Branched polyphosphazenes with controlled dimensions. *J Polym Sci Part A Polym Chem*. 2013;51(20):4467-4473. doi:10.1002/pola.26865

15. Andrianov AK, Chen J, LeGolvan MP. Poly(dichlorophosphazene) as a precursor for

biologically active polyphosphazenes: Synthesis, characterization, and stabilization. *Macromolecules*. 2004;37(2):414-420. doi:10.1021/ma0355655

16. Allcock HR. *Chemistry and Applications of Polyphosphazenes*. Wiley-Interscience; 2003.

17. Blackstone V, Soto AP, Manners I. Polymeric materials based on main group elements: the recent development of ambient temperature and controlled routes to polyphosphazenes. *Dalt Trans*. 2008;0(33):4363. doi:10.1039/b719361k

18. Suárez-Suárez S, Carriedo GA, Tarazona MP, Presa Soto A. Twisted Morphologies and Novel Chiral Macroporous Films from the Self-Assembly of Optically Active Helical Polyphosphazene Block Copolymers. *Chem - A Eur J.* 2013;19(18):5644-5653. doi:10.1002/chem.201203458

19. Blackstone V, Pfirrmann S, Helten H, et al. A Cooperative Role for the Counteranion in the PCl 5 -Initiated Living, Cationic Chain Growth Polycondensation of the Phosphoranimine Cl 3 P═NSiMe 3. *J Am Chem Soc*. 2012;134(37):15293-15296. doi:10.1021/ja307703h

20. Blackstone V, Lough AJ, Murray M, Manners I. Probing the Mechanism of the PCl 5 −Initiated Living Cationic Polymerization of the Phosphoranimine Cl 3 P═NSiMe 3 using Model Compound Chemistry. *J Am Chem Soc*. 2009;131(10):3658-3667. doi:10.1021/ja808517d

21. Suárez Suárez S, Presa Soto D, Carriedo GA, Presa Soto A, Staubitz A. Experimental and Theoretical Study of the Living Polymerization of N -Silylphosphoranimines. Synthesis of New Block Copolyphosphazenes. *Organometallics*. 2012;31(7):2571-2581. doi:10.1021/om201012g

22. Godfrey SM, McAuliffe CA, Sheffield JM. Structural dependence of the reagent Ph3PCl2 on the nature of the solvent, both in the solid state and in solution; X-ray crystal structure of trigonal bipyramidal Ph3PCl2, the first structurally characterised five-coordinate R3PCl2 compound. *Chem Commun*. 1998;4(8):921-922. doi:10.1039/a800820e

23. Wilfert S, Henke H, Schoefberger W, Brüggemann O, Teasdale I. Chain-End-Functionalized Polyphosphazenes via a One-Pot Phosphine-Mediated Living Polymerization. *Macromol Rapid Commun*. 2014;35(12):1135-1141. doi:10.1002/marc.201400114

24. Soto AP, Manners I. Poly(ferrocenylsilane -b- polyphosphazene) (PFS -b- PP): A New Class of Organometallic−Inorganic Block Copolymers. *Macromolecules*. 2009;42(1):40-42. doi:10.1021/ma8016713

25. Bin Wang, Eric Rivard A, Manners I. A New High-Yield Synthesis of Cl3PNSiMe3, a Monomeric Precursor for the Controlled Preparation of High Molecular Weight Polyphosphazenes. 2002. doi:10.1021/IC011125N

26. Wang B. Development of a one-pot in situ synthesis of poly(dichlorophosphazene) from PCl 3. *Macromolecules*. 2005;38(2):643-645. doi:10.1021/ma0489772

27. Tian Z, Hess A, Fellin CR, Nulwala H, Allcock HR. Phosphazene High Polymers and Models with Cyclic Aliphatic Side Groups: New Structure–Property Relationships. *Macromolecules*. 2015;48(13):4301-4311. doi:10.1021/acs.macromol.5b00946

28. Liu X, Breon JP, Chen C, Allcock HR. Substituent Exchange Reactions with High Polymeric Organophosphazenes. *Macromolecules*. 2012;45(22):9100-9109. doi:10.1021/ma302087a

29. Wilfert S, Iturmendi A, Schoefberger W, et al. Water-soluble, biocompatible

polyphosphazenes with controllable and pH-promoted degradation behavior. *J Polym Sci Part A Polym Chem*. 2014;52(2):287-294. doi:10.1002/pola.27002

30. Allcock HR, Morozowich NL. Bioerodible polyphosphazenes and their medical potential. *Polym Chem*. 2012;3(3):578-590. doi:10.1039/C1PY00468A

31. Henke H, Kryeziu K, Banfić J, et al. Macromolecular Pt(IV) Prodrugs from Poly(organo)phosphazenes. *Macromol Biosci*. 2016;16(8):1239-1249. doi:10.1002/mabi.201600035

32. Hackl CM, Schoenhacker-Alte B, Klose MHM, et al. Synthesis and in vivo anticancer evaluation of poly(organo)phosphazene-based metallodrug conjugates. *Dalt Trans*. 2017;46(36):12114-12124. doi:10.1039/C7DT01767G

33. Teasdale I, Brüggemann O. Polyphosphazenes: Multifunctional, biodegradable vehicles for drug and gene delivery. *Polymers (Basel)*. 2013;5(1):161-187. doi:10.3390/polym5010161

34. Chen K, Huang X, Wan C, Liu H. Heteroatom–doped hollow carbon microspheres based on amphiphilic supramolecular vesicles and highly crosslinked polyphosphazene for high performance supercapacitor electrode materials. *Electrochim Acta*. 2016;222:543-550. doi:10.1016/J.ELECTACTA.2016.11.007

35. Allcock HR. Chapter 3. Structural Diversity in Fluorinated Polyphosphazenes: Exploring the Change from Crystalline Thermoplastics to High-performance Elastomers and Other New Materials. In: ; 2016:54-79. doi:10.1039/9781782629368-00054

36. Lee SC, Chang JY. Preparation of molecularly imprinted polymers using photocross-linkable polyphosphazene and selective rebinding of amino acids. *Macromol Res*. 2009;17(7):522-527. doi:10.1007/BF03218901

37. Chen L, Wang X, Lu W, Wu X, Li J. Molecular imprinting: perspectives and applications. *Chem Soc Rev*. 2016;45(8):2137-2211. doi:10.1039/C6CS00061D

38. Alexander C, Andersson HS, Andersson LI, et al. Molecular imprinting science and technology: a survey of the literature for the years up to and including 2003. *J Mol Recognit*. 2006;19(2):106-180. doi:10.1002/jmr.760

39. Whitcombe MJ, Kirsch N, Nicholls IA. Molecular imprinting science and technology: a survey of the literature for the years 2004-2011. *J Mol Recognit*. 2014;27(6):297-401. doi:10.1002/jmr.2347

40. Lofgreen JE, Ozin GA. Controlling morphology and porosity to improve performance of molecularly imprinted sol–gel silica. *Chem Soc Rev*. 2014;43(3):911-933. doi:10.1039/C3CS60276A

41. Komiyama M, Takeuchi T, Mukawa T, Asanuma H. *Molecular Imprinting: From Fundamentals to Applications*. Wiley-VCH; 2003.

42. Vasapollo G, Sole R Del, Mergola L, et al. Molecularly imprinted polymers: Present and future prospective. *Int J Mol Sci*. 2011;12(9):5908-5945. doi:10.3390/ijms12095908

43. Yan H, Row K. Characteristic and Synthetic Approach of Molecularly Imprinted Polymer. *Int J Mol Sci*. 2006;7(5):155-178. doi:10.3390/i7050155

44. El Kirat K, Bartkowski M, Haupt K. Probing the recognition specificity of a protein molecularly imprinted polymer using force spectroscopy. *Biosens Bioelectron*.

2009;24(8):2618-2624. doi:10.1016/j.bios.2009.01.018

45.   Bergmann NM, Peppas NA. Molecularly imprinted polymers with specific recognition for macromolecules and proteins. *Prog Polym Sci*. 2008;33(3):271-288. doi:10.1016/j.progpolymsci.2007.09.004

46.   Zhang Y, Song D, Lanni LM, Shimizu KD. Importance of Functional Monomer Dimerization in the Molecular Imprinting Process. *Macromolecules*. 2010;43(15):6284-6294. doi:10.1021/ma101013c

47.   Golker K, Karlsson BCG, Olsson GD, Rosengren AM, Nicholls IA. Influence of Composition and Morphology on Template Recognition in Molecularly Imprinted Polymers. *Macromolecules*. 2013;46(4):1408-1414. doi:10.1021/ma3024238

48.   Silvestri D, Borrelli C, Giusti P, Cristallini C, Ciardelli G. Polymeric devices containing imprinted nanospheres: a novel approach to improve recognition in water for clinical uses. *Anal Chim Acta*. 2005;542(1):3-13. doi:10.1016/J.ACA.2004.12.005

49.   Baggiani C, Anfossi L, Baravalle P, Giovannoli C, Tozzi C. Selectivity features of molecularly imprinted polymers recognising the carbamate group. *Anal Chim Acta*. 2005;531(2):199-207. doi:10.1016/J.ACA.2004.10.025

50.   O'Mahony J, Molinelli A, Nolan K, Smyth MR, Mizaikoff B. Anatomy of a successful imprint: Analysing the recognition mechanisms of a molecularly imprinted polymer for quercetin. *Biosens Bioelectron*. 2006;21(7):1383-1392. doi:10.1016/J.BIOS.2005.05.015

51.   Walsh R, Osmani Q, Hughes H, Duggan P, McLoughlin P. Synthesis of imprinted beads by aqueous suspension polymerisation for chiral recognition of antihistamines. *J Chromatogr B*. 2011;879(30):3523-3530. doi:10.1016/J.JCHROMB.2011.09.036

52.   He J, Lv R, Cheng J, et al. Preparation and characterization of molecularly imprinted microspheres for dibutyl phthalate recognition in aqueous environment. *J Sep Sci*. 2010;33(21):3409-3414. doi:10.1002/jssc.201000301

53.   Wang B, Wang Y, Yang H, Wang J, Deng A. Preparation and characterization of molecularly imprinted microspheres for selective extraction of trace melamine from milk samples. *Microchim Acta*. 2011;174(1-2):191-199. doi:10.1007/s00604-011-0613-4

54.   G. Mayes A, Mosbach K. Molecularly Imprinted Polymer Beads: Suspension Polymerization Using a Liquid Perfluorocarbon as the Dispersing Phase. 1996. doi:10.1021/AC960363A

55.   Zhang L, Cheng G, Fu C. Synthesis and characteristics of tyrosine imprinted beads via suspension polymerization. *React Funct Polym*. 2003;56(3):167-173. doi:10.1016/S1381-5148(03)00054-3

56.   Pang X, Cheng G, Li R, Lu S, Zhang Y. Bovine serum albumin-imprinted polyacrylamide gel beads prepared via inverse-phase seed suspension polymerization. *Anal Chim Acta*. 2005;550(1-2):13-17. doi:10.1016/J.ACA.2005.06.067

57.   Kawaguchi M, Hayatsu Y, Nakata H, et al. Molecularly imprinted solid phase extraction using stable isotope labeled compounds as template and liquid chromatography–mass spectrometry for trace analysis of bisphenol A in water sample. *Anal Chim Acta*. 2005;539(1-2):83-89. doi:10.1016/J.ACA.2005.03.005

58.   Haginaka J, Tabo H, Matsunaga H. Preparation of molecularly imprinted polymers for organophosphates and their application to the recognition of organophosphorus compounds and phosphopeptides. *Anal Chim Acta*. 2012;748:1-8.

doi:10.1016/J.ACA.2012.08.022

59.   Hiratsuka Y, Funaya N, Matsunaga H, Haginaka J. Preparation of magnetic molecularly imprinted polymers for bisphenol A and its analogues and their application to the assay of bisphenol A in river water. *J Pharm Biomed Anal*. 2013;75:180-185. doi:10.1016/J.JPBA.2012.11.030

60.   Wang X, Mao H, Huang W, et al. Preparation of magnetic imprinted polymer particles via microwave heating initiated polymerization for selective enrichment of 2-amino-4-nitrophenol from aqueous solution. *Chem Eng J*. 2011;178:85-92. doi:10.1016/J.CEJ.2011.10.015

61.   Haginaka J, Kagawa C. Uniformly sized molecularly imprinted polymer for d-chlorpheniramine: Evaluation of retention and molecular recognition properties in an aqueous mobile phase. *J Chromatogr A*. 2002;948(1-2):77-84. doi:10.1016/S0021-9673(01)01262-6

62.   Hosoya K, Yoshizako K, Shirasu Y, et al. Molecularly imprinted uniform-size polymer-based stationary phase for high-performance liquid chromatography structural contribution of cross-linked polymer network on specific molecular recognition. *J Chromatogr A*. 1996;728(1-2):139-147. doi:10.1016/0021-9673(95)01165-X

63.   Haginaka J, Sakai Y. Uniform-sized molecularly imprinted polymer material for (S)-propranolol. *J Pharm Biomed Anal*. 2000;22(6):899-907. doi:10.1016/S0731-7085(00)00293-4

64.   Nakamura M, Ono M, Nakajima T, Ito Y, Aketo T, Haginaka J. Uniformly sized molecularly imprinted polymer for atropine and its application to the determination of atropine and scopolamine in pharmaceutical preparations containing Scopolia extract. *J Pharm Biomed Anal*. 2005;37(2):231-237. doi:10.1016/J.JPBA.2004.10.017

65.   Beltran A, Marcé RM, Cormack PAG, Borrull F. Synthesis by precipitation polymerisation of molecularly imprinted polymer microspheres for the selective extraction of carbamazepine and oxcarbazepine from human urine. *J Chromatogr A*. 2009;1216(12):2248-2253. doi:10.1016/j.chroma.2009.01.024

66.   Liu Y, Hoshina K, Haginaka J. Monodispersed, molecularly imprinted polymers for cinchonidine by precipitation polymerization. *Talanta*. 2010;80(5):1713-1718. doi:10.1016/J.TALANTA.2009.10.011

67.   Alizadeh T. Preparation of molecularly imprinted polymer containing selective cavities for urea molecule and its application for urea extraction. *Anal Chim Acta*. 2010;669(1-2):94-101. doi:10.1016/J.ACA.2010.04.044

68.   Wen-Hui L, Stöver HDH. Monodisperse Cross-Linked Core−Shell Polymer Microspheres by Precipitation Polymerization. 2000. doi:10.1021/MA9920691

69.   Ye L, Cormack PA., Mosbach K. Molecular imprinting on microgel spheres. *Anal Chim Acta*. 2001;435(1):187-196. doi:10.1016/S0003-2670(00)01248-4

70.   Ye L, Weiss R, Mosbach K. Synthesis and Characterization of Molecularly Imprinted Microspheres. 2000. doi:10.1021/MA000825T

71.   Puoci F, Iemma F, Muzzalupo R, et al. Spherical Molecularly Imprinted Polymers(SMIPs) via a Novel Precipitation Polymerization in the Controlled Delivery of Sulfasalazine. *Macromol Biosci*. 2004;4(1):22-26. doi:10.1002/mabi.200300035

72. Ho K-C, Yeh W-M, Tung T-S, Liao J-Y. Amperometric detection of morphine based on poly(3,4-ethylenedioxythiophene) immobilized molecularly imprinted polymer particles prepared by precipitation polymerization. *Anal Chim Acta*. 2005;542(1):90-96. doi:10.1016/J.ACA.2005.02.036

73. Zhang H, Dramou P, He H, Tan S, Pham-Huy C, Pan H. Molecularly Imprinted Stationary Phase Prepared by Reverse Micro-Emulsion Polymerization for Selective Recognition of Gatifloxacin in Aqueous Media. *J Chromatogr Sci*. 2012;50(6):499-508. doi:10.1093/chromsci/bms028

74. Dvorakova G, Haschick R, Chiad K, Klapper M, Müllen K, Biffis A. Molecularly Imprinted Nanospheres by Nonaqueous Emulsion Polymerization. *Macromol Rapid Commun*. 2010;31(23):2035-2040. doi:10.1002/marc.201000406

75. Ramström O, Mosbach K. Synthesis and catalysis by molecularly imprinted materials. *Curr Opin Chem Biol*. 1999;3(6):759-764. doi:10.1016/S1367-5931(99)00037-X

76. Lanza F, Sellergren B. Method for Synthesis and Screening of Large Groups of Molecularly Imprinted Polymers. 1999. doi:10.1021/AC981446P

77. Dirion B, Cobb Z, Schillinger E, Andersson LI, Sellergren B. Water-Compatible Molecularly Imprinted Polymers Obtained via High-Throughput Synthesis and Experimental Design. 2003. doi:10.1021/JA0355473

78. Martin-Esteban A, Tadeo JL. Selective Molecularly Imprinted Polymer Obtained from a Combinatorial Library for the Extraction of Bisphenol A. *Comb Chem High Throughput Screen*. 2006;9(10):747-751. doi:10.2174/138620706779026024

79. Verheyen E, Schillemans JP, van Wijk M, Demeniex M-A, Hennink WE, van Nostrum CF. Challenges for the effective molecular imprinting of proteins. *Biomaterials*. 2011;32(11):3008-3020. doi:10.1016/J.BIOMATERIALS.2011.01.007

80. Oh W-G, Kim BS. Novel Biodegradable Molecularly Imprinted Polymers Based on Poly(3-hydroxybutyrate). *Macromol Symp*. 2007;249-250(1):76-80. doi:10.1002/masy.200750313

81. Jang H-K, Kim BS. Molecular recognition properties of biodegradable photo-crosslinked network based on poly(lactic acid) and poly(ethylene glycol). *Macromol Res*. 2013;21(4):370-375. doi:10.1007/s13233-013-1025-6

82. Lowe AB. Thiol-ene "click" reactions and recent applications in polymer and materials synthesis. *Polym Chem*. 2010;1(1):17-36. doi:10.1039/B9PY00216B

83. Lowe AB. Thiol–ene "click" reactions and recent applications in polymer and materials synthesis: a first update. *Polym Chem*. 2014;5(17):4820. doi:10.1039/C4PY00339J

84. Allcock HR, Phelps MVB, Barrett EW, Pishko M V., Koh W-G. Ultraviolet Photolithographic Development of Polyphosphazene Hydrogel Microstructures for Potential Use in Microarray Biosensors. *Chem Mater*. 2006;18(3):609-613. doi:10.1021/cm050316b

85. Qian Y-C, Huang X-J, Chen C, Ren N, Huang X, Xu Z-K. A Versatile Approach to the Synthesis of Polyphosphazene Derivatives via the Thiol-Ene Reaction. *J Polym Sci Part A Polym Chem*. 2012;50:5170-5176. doi:10.1002/pola.26361

86. Allcock HR, Scopelianos AG. Synthesis of sugar-substituted cyclic and polymeric phosphazenes and their oxidation, reduction, and acetylation reactions. *Macromolecules*. 1983;16(5):715-719. doi:10.1021/ma00239a001

87. Krogman NR, Weikel AL, Nguyen NQ, Nair LS, Laurencin CT, Allcock HR. Synthesis and Characterization of New Biomedical Polymers: Serine- and Threonine-Containing Polyphosphazenes and Poly(l -lactic acid) Grafted Copolymers. *Macromolecules*. 2008;41(21):7824-7828. doi:10.1021/ma801961m

88. Morozowich NL, Weikel AL, Nichol JL, et al. Polyphosphazenes Containing Vitamin Substituents: Synthesis, Characterization, and Hydrolytic Sensitivity. *Macromolecules*. 2011;44(6):1355-1364. doi:10.1021/ma1027406

89. Wachter SB, Gilbert EM. Beta-adrenergic receptors, from their discovery and characterization through their manipulation to beneficial clinical application. *Cardiology*. 2012;122(2):104-112. doi:10.1159/000339271

90. Maehle A-H, Prüll C, Halliwell RF. The emergence ofthe drug receptor theory. *Nat Rev Drug Discov*. 2002;1(8):637-641.

91. Quirke V. Putting theory into practice: James Black, receptor theory and the development of the beta-blockers at ICI, 1958-1978. *Med Hist*. 2006;50(1):69-92. http://www.ncbi.nlm.nih.gov/pubmed/16502872. Accessed June 18, 2018.

92. Wallukat G. The β-adrenergic receptors. *Herz*. 2002;27(7):683-690. doi:10.1007/s00059-002-2434-z

93. Stapleton MP, Shakespeare -William, Andjuliet R, Stapleton MP. Historical Perspectives Sir James Black and Propranolol The Role of the Basic Sciences in the History of Cardiovascular Pharmacology. https://www.ncbi.nlm.nih.gov/pmc/articles/PMC325477/pdf/thij00027-0106.pdf. Accessed June 18, 2018.

94. Angina Pectoris - National Library of Medicine - PubMed Health. https://www.ncbi.nlm.nih.gov/pubmedhealth/PMHT0023182/. Accessed June 18, 2018.

95. FDA. Inderal (Propranolol Hydrochloride) - Label. https://www.accessdata.fda.gov/drugsatfda_docs/label/2011/016418s080,016762s017,017683s008lbl.pdf. Accessed June 18, 2018.

96. Propranolol - Drugbank. https://www.drugbank.ca/drugs/DB00571. Accessed June 18, 2018.

97. Al-Majed AA, Bakheit AHH, Abdel Aziz HA, Alajmi FM, AlRabiah H. Propranolol. In: *Profiles of Drug Substances, Excipients, and Related Methodology*. 42nd ed. ; 2017:287-338. doi:10.1016/bs.podrm.2017.02.006

98. Vatner SF, Young MA, Vatner DE. Large Coronary Artery Regulation by α- and β-Adrenergic Receptors in Conscious Calves. In: *Coronary Circulation in Physiological and Pathophysiological States*. Tokyo: Springer Japan; 1991:29-41. doi:10.1007/978-4-431-68108-3_3

99. Moreland RS, Bohr DF. Adrenergic control of coronary arteries. *Fed Proc*. 1984;43(14):2857-2861. http://www.ncbi.nlm.nih.gov/pubmed/6386528. Accessed June 19, 2018.

100. U.S. National Library of Medicine. Propranolol (Cardiovascular): MedlinePlus Drug Information. https://medlineplus.gov/druginfo/meds/a682607.html. Accessed June 19, 2018.

101. Brohée L, Peulen O, Nusgens B, et al. Propranolol sensitizes prostate cancer cells to

glucose metabolism inhibition and prevents cancer progression. *Sci Rep*. 2018;8(1):7050. doi:10.1038/s41598-018-25340-9

102. Pantziarka P, Bouche G, Sukhatme V, Meheus L, Rooman I, Sukhatme VP. Repurposing Drugs in Oncology (ReDO)-Propranolol as an anti-cancer agent. *Ecancermedicalscience*. 2016;10:680. doi:10.3332/ecancer.2016.680

103. Ashrafi S, Shapouri R, Shirkhani A, Mahdavi M. Anti-tumor effects of propranolol: Adjuvant activity on a transplanted murine breast cancer model. *Biomed Pharmacother*. 2018;104:45-51. doi:10.1016/J.BIOPHA.2018.05.002

104. Steimer T. The biology of fear- and anxiety-related behaviors. *Dialogues Clin Neurosci*. 2002;4(3):231-249. http://www.ncbi.nlm.nih.gov/pubmed/22033741. Accessed June 29, 2018.

105. Cannon WB. *Bodily Changes in Pain, Hunger, Fear and Rage: An Account of Recent Researches into the Function of Emotional Excitement.* New York: D Appleton & Company; 1915. doi:10.1037/10013-000

106. Sherin JE, Nemeroff CB. Post-traumatic stress disorder: the neurobiological impact of psychological trauma. *Dialogues Clin Neurosci*. 2011;13(3):263-278. http://www.ncbi.nlm.nih.gov/pubmed/22034143. Accessed June 28, 2018.

107. Murchison CF, Zhang X-Y, Zhang W-P, Ouyang M, Lee A, Thomas SA. A distinct role for norepinephrine in memory retrieval. *Cell*. 2004;117(1):131-143. http://www.ncbi.nlm.nih.gov/pubmed/15066288. Accessed June 28, 2018.

108. Tully K, Bolshakov VY. Emotional enhancement of memory: how norepinephrine enables synaptic plasticity. *Mol Brain*. 2010;3(1):15. doi:10.1186/1756-6606-3-15

109. Giustino TF, Fitzgerald PJ, Maren S. Revisiting propranolol and PTSD: Memory erasure or extinction enhancement? *Neurobiol Learn Mem*. 2016;130:26-33. doi:10.1016/j.nlm.2016.01.009

110. Gardner AJ, Griffiths J. Propranolol, post-traumatic stress disorder, and intensive care: incorporating new advances in psychiatry into the ICU. *Crit Care*. 2014;18(6):698. doi:10.1186/s13054-014-0698-3

111. Allcock HR, Reeves SD, Denus CR De, Crane CA. Influence of Reaction Parameters on the Living Cationic Polymerization of Phosphoranimines to Polyphosphazenes. 2001;3:748-754.

112. Hu M, Li L, Wu H, et al. Multicolor, One- and Two-Photon Imaging of Enzymatic Activities in Live Cells with Fluorescently Quenched Activity-Based Probes (qABPs). *J Am Chem Soc*. 2011;133(31):12009-12020. doi:10.1021/ja200808y

113. Mautner A, Qin X, Wutzel H, et al. Thiol-ene photopolymerization for efficient curing of vinyl esters. *J Polym Sci Part A Polym Chem*. 2013;51(1):203-212. doi:10.1002/pola.26365

114. Hunt CE, Ansell RJ, Alexander C, et al. Use of fluorescence shift and fluorescence anisotropy to evaluate the re-binding of template to (S)-propranolol imprinted polymers. *Analyst*. 2006;131(5):678. doi:10.1039/b518248d

115. Alizadeh T, Allahyari L. Highly-selective determination of carcinogenic derivative of propranolol by using a carbon paste electrode incorporated with nano-sized propranolol-imprinted polymer. *Electrochim Acta*. 2013;111:663-673. doi:10.1016/j.electacta.2013.08.075

116. Allender C., Richardson C, Woodhouse B, Heard C., Brain K. Pharmaceutical applications for molecularly imprinted polymers. *Int J Pharm*. 2000;195(1):39-43. doi:10.1016/S0378-5173(99)00355-5

117. Kempe H, Kempe M. Novel Method for the Synthesis of Molecularly Imprinted Polymer Bead Libraries. *Macromol Rapid Commun*. 2004;25(1):315-320. doi:10.1002/marc.200300189

118. Renkecz T, Ceolin G, Horváth V, et al. Selective solid phase extraction of propranolol on multiwell membrane filter plates modified with molecularly imprinted polymer. *Analyst*. 2011;136(10):2175. doi:10.1039/c0an00906g

119. Shalini Y, Sai Annapurneswari T, Sundari CBT, Jayathirtha Rao V, Ravinder Nath A. Method development and validation for simultaneous estimationf of Propranolol Hydrochloride and Flunarizine Dihydrochloride in bulk and pharmaceutical dosage form by RP-HPLC. *Int Res J Pharm Appl Sci*. 2012.

120. Annapurneswari TS, Shilpa S, Bala C, Sundari T, Rao VJ, Nath AR. Development and validation of a RP-HPLC method for simulatanious estimation of Propranolol HCl and Clonazepam in bulk and pharmaceutical doseage form. *Int Res J Pharm*. 2012;3(9). www.irjponline.com. Accessed March 28, 2017.

121. Uwai K, Tani M, Ohtake Y, et al. Photodegradation products of propranolol: The structures and pharmacological studies. *Life Sci*. 2005;78(4):357-365. doi:10.1016/j.lfs.2005.04.033

CURRICULUM VITAE

Paul Strasser

Personal Data

Date of Birth	22.03.1993
Place of Birth	Ried im Innkreis
Nationality	Austria
Address	Hofmark 20
	4742 Pram
	+43 699 11049734
	paul_strasser@gmx.at

Education

2016-2018	Joint Master Program "Biological Chemistry" at JKU Linz and JCU Budweis, Master thesis: *"Developments towards biocompatible degradable molecularly imprinted polymers based on polyphosphazenes"* at the Institute of Polymer Chemistry at the JKU Linz under Univ.-Prof. Dr. Oliver Brüggemann and Assoc. Univ.-Prof. Dr. Ian Teasdale
2013-2016	Bachelor's Program "Biological Chemistry" at JKU Linz and JCU Budweis, awarded degree Bachelor of Science (BSc) of the JKU Linz, Bachelor thesis: *"Determination of Gamma-Hydroxybutyric acid (GHB) in biological fluids"* at the Institute of Analytical Chemistry under Assoc. Univ.-Prof. DI Dr. Himmelsbach. and a Bachelor's degree (Bc) awarded by the University of South Bohemia in České Budějovice, Bachelor thesis: *"Warburg effect in lymph gland of Drosophila melanogaster upon parasitoid wasp infection"* at the Department of Molecular Biology and Genetics under doc. Mgr. Tomáš Doležal, Ph.D.
2007-2012	Höhere Technische Bundeslehranstalt Andorf; Werkstoffingenieurwesen und Umwelttechnik mit Schwerpunkt auf Kunststofftechnik

| 2003-2007 | Hauptschule Pram |
| 1999-2003 | Volksschule Pram |

Internships

6/2011	Pöttinger Landtechnik, Grieskirchen
6/2010	Agrotel, Neuhaus, DE
6/2009	Aspöck Systems, Peuerbach